AN ADSORPTION STUDY OF NICKEL AND COBALT
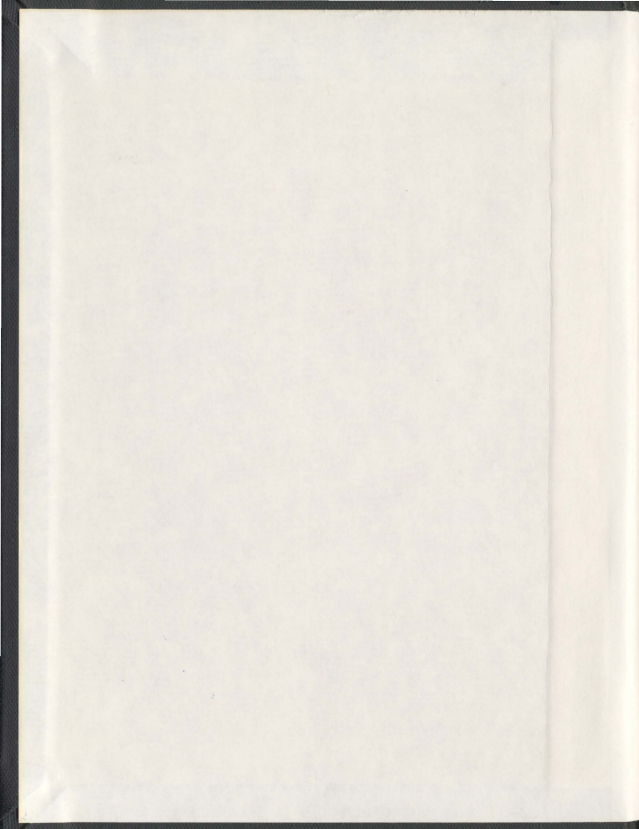## ON SAPRIST NEWFOUNDLAND PEAT

EMMANUEL SESOFIA ASAPO

AN ADSORPTION STUDY OF NICKEL AND COBALT ON SAPRIST

NEWFOUNDLAND PEAT

By

Emmanuel Sesofia Asapo

A Thesis submitted to the School of Graduate Studies

in Partial Fulfilment of the Requirements for the award of the degree of

Doctor of Philosophy

Faculty of Engineering and Applied Science,

Memorial University of Newfoundland,

June, 2011

St. John's, Newfoundland, Canada

ABSTRACT

Air dried saprist Newfoundland peat, harvested from a private peat bog owned by Traverse Nursery in Torbay, St. John's, was employed as the sole adsorbent in laboratory batch and column experiments for the removal of Nickel and Cobalt cations from stock solutions. The saprist peat type has not been widely investigated as an adsorbent, unlike the fibrist peat. Characterization using non-destructive methods showed the peat as being acidic, consisting of small, overlapped and collapsed cellular masses. The cation exchange capacity was 70 meq/100g, with a wet bulk density of 0.65 g/cm^3 and ~90 % organic content. The peat matrix was dominated by oxygenated functional groups and to a lesser extent amine/amide groups which are all capable of complexing / co-ordination with Ni^{2+} and Co^{2+}.

The response surface method of the Box-Behnken design showed that peat dose, concentration, solution pH and contact time were the significant factors that influenced the peat Ni^{2+} and Co^{2+} adsorption capacity with the interaction effect of the factors being metal specific. The batch test investigation showed that the metal uptake reaction was a pseudo-second order type and attainment of equilibrium was metal concentration and pH dependent. Kinetic equilibrium adsorption over 12 h gave a maximum adsorption capacity of 385 mg/g for Ni^{2+} at a peat dose of 21 g/L, pH of 5.5 and Ni^{2+} concentration of 125 mg/L while for Co^{2+} it was 33.44 mg/g at a peat dose of 2g/L, pH of 8 and Co^{2+} concentration of 200 mg/L with regression coefficients near unity.

Equilibrium adsorption data gave good fits with both the Langmuir and Freundlich isotherms from which corresponding adsorption parameters were determined. The percent metal removed was nearly 100% for the two metals at solution pH 3, especially at metal concentrations below 50 mg/L while, between 35 % and 75% removal were obtained at concentrations between 125 and 200 mg/L. Competitive sorption tests showed that at higher concentrations and peat doses, more Ni^{2+} and Co^{2+} were removed in the presence of Cd^{2+}, Pb^{2+}, and Zn^{2+} with the order of removal being $Pb^{2+} > Ni^{2+} > Cd^{2+} > Zn^{2+} > Co^{2+}$. Breakthrough was metal and flow rate dependent. The maximum adsorption capacity of the 12.5 cm long peat bed was 72 g/L and 24.7 g/L for Ni^{2+}, at a flow rate of 1.0 L/h and 2.0 L/h respectively. For Co^{2+}, 17 g/L and 6.7 g/L was the computed maximum adsorption capacity at a flow rate of 1.0 L/h and 2.0 L/h. The adsorbent exhaustion rate was metal and flow rate dependent with Ni^{2+}, at a flow rate of 1.0 L/h, 0.69 g/L was computed and for Co^{2+}, at a flow rate of 1.0 L/h, 2.16 g/L was computed.

The metal uptake mechanism on the saprist Newfoundland peat was strongly pH dependent and based on the experimental data; complexation was the dominant reaction at acidic conditions especially at pH ~3.0, while ion exchange was the main reaction at basic conditions. Kinetics and equilibrium sorption data especially desorption with 0.1 M to 2 M HCl, showed that the two reactions occurred simultaneously at the pH of 5.5 and 8 for Ni uptake while, Co uptake occurred predominantly by ion exchange at pH 10 and by complexation at pH of 5.5 and 8.

AKNOWLEDGEMENT

Table of Contents

List of Tables

List of Figures

List of Abbreviations and Acronyms

AER	Adsorbent exhaustion rate
Ag	Silver
Al	Aluminum
Al_2O_3	Aluminum oxide
As	Arsenic
ASTM	American Society for Testing and Materials
b	Langmuir constant
Ba	Barium
BDST	Bed depth service time
Be	Beryllium
Ca	Calcium
C_{acc}	Accumulated metal concentration along the column
$CaCl_2$	Calcium chloride
$CaCO_3$	Calcium carbonate
CaO	Calcium oxide
$Ca(OH)_2$	Calcium hydroxide
Cd	Cadmium
CDC	Canadian Disease Centre
$CdCO_3$	Cadmium carbonate
$Cd(OH)_2$	Cadmium hydroxide
CdS	Cadmium sulphide
C_e	Concentration at equilibrium in mg/L
CEC	Cation Exchange Capacity
$(CH_3CO_2)Ca$	Calcium acetate
C_o	Initial concentration in mg/L
^{13}C-NMR	Solid state carbon 13 nuclear magnetic resonance
Co	Cobalt
$Co(CO_3)_2$	Cobalt carbonate

Co(OH)$_2$	Cobalt hydroxide
CoS	Cobalt sulphide
Cr	Chromium
Cs	Caesium
Cu	Copper
CuCO$_3$	Copper carbonate
Cu(OH)$_2$	Copper hydroxide
EDTA	Ethylene diamine tetra acetic acid
FAAS	Flame Atomic Absorption Spectrophotometer
FAO	Food and Agriculture Organization
Fe	Iron
FeCO$_3$	Iron carbonate
Fe(OH)$_2$	Iron hydroxide
FTIR	Fourier transform infra red
Ga	Gallium
HCl	Hydrochloric acid
HF	Hydrogen fluoride
Hg	Mercury
HNO$_3$	Nitric acid
IARC	International Agency for Research on Cancer
ICP-MS	Inductively coupled plasma-mass spectrometer
In	Indium
K	Freundlich isotherm constant
k	column adsorption rate constant (L/mg min)
Ksp	Solubility product constant
La	Lanthanum
Li	Lithium
M	Mass of adsorbent in g
MCL	Maximum contaminant level
Mn	Manganese

$MnCO_3$	Manganese carbonate
$Mn(OH)_2$	Manganese hydroxide
$1/n$	Freundlich exponent
Na_2CO_3	Sodium bicarbonate
$NaHCO_3$	Soda ash
$NaOH$	Sodium hydroxide
Ni	Nickel
$NiCO_3$	Nickel carbonate
$Ni(OH)_2$	Nickel hydroxide
NL	Newfoundland and Labrador
N_o	Adsorption capacity in mg/L
Pb	Lead
$PbCO_3$	Lead carbonate
$Pb(OH)_2$	Lead hydroxide
q_e	adsorbed metal at equilibrium in mg/g
q_m	Langmuir monolayer saturation capacity
$R*$	Separation factor
SEM	Scanning electron microscope
SiO_2	Silicon oxide
Sn	Tin
Sr	Strontium
t	Time (h or min)
t_{50}	Time to attain breakthrough in h
T	Temperature in ^{o}C
TiO_2	Titanium oxide
TRI	Toxic Release Inventory
US	United States
USEPA	United States Environmental Pollution Agency
USGS	United States Geological Society
V	Volume in L, or mL or cm^3

v	Linear flow velocity (cm/min) of feed bed
WHO	World Health Organization
X	Bed depth of column in cm
XRD	X-ray diffractometer
Y	Yttrium
Zn	Zinc
$ZnCO_3$	Zinc carbonate
$Zn(OH)_2$	Zinc hydroxide

List of Appendices

CHAPTER ONE

INTRODUCTION

1.1 Preamble

Mining of high grade nickel (Ni) at Labrador, and the recovery of Ni and cobalt (Co) from the refining effluents at Long Harbour by Vale (formerly Voisey's Bay Nickel Company Limited) is one of the laudable initiatives of the Newfoundland and Labrador (NL) government to improve the provincial economy. This mine is one of the 235 major mines that constitute the Canadian mining industry which employs about 370,000 Canadians, accounting for over 4% of the national Gross Domestic Product. The estimated annual wage of the Canadian mining industry is $17.38 billion providing a market to 2,200 suppliers of goods and an investment of about $300 million in annual research and development (Canadian Mining, 2008). Canada is known to have the second largest deposit of mineral ores containing Ni and contributes about 16% of the total world Ni mine production (USGS, 2008).

In NL, mining employs ~2500 people, accounting for 8% of the Gross Domestic Product of the provincial goods. With the Vale Ni mining, NL has become the second largest supplier of Ni in Canada with ~34% of the total Canadian Ni production (Waddle, 2004). From an economic view point, a project like the Vale Inco nickel mining at Labrador is highly commendable. About 65% of the Ni consumed in developed countries is used in the manufacture of austenitic stainless steel, and 12% goes into superalloys

(e.g., inconel 600) or nonferrous alloys (e.g., cupronickel). Both families of alloys are valued for their corrosion resistance properties with the aerospace industry being a leading consumer. Ni super alloys are also used in land-based combustion turbines, e.g. electric power generation stations. The remaining 23% of Ni consumption is divided between alloy steels, rechargeable batteries, catalysts and other chemicals, coinage, foundry products, and plating (USGS, 2006a). There is therefore a large global Ni market.

Co is mainly consumed in super alloys productions such as Haynes alloys, MAR-M, and Airesist (~49%) aircraft gas turbine engines, 9% in cemented carbides for cutting and wear-resistant applications, 15% in various other metallic uses, and the remaining 26% in a variety of chemical productions. The total estimated value of Co consumed in the US in 2009 was $270 million (USGS, 2010). Identified world Co resources are about 15 million tons. Co-60 is an artificial isotope, an important gamma ray source extensively used as a tracer and radio therapeutic agent (CDC, 2008).

1.2 The Problem

Vale Ni refining through the hydromet process at Long Harbour, Newfoundland, uses the Ni concentrates from Ni Ore mined in Labrador (Voisey's Bay, 2007). The raw Ni ore is obtained via open pit mining and flotation. The hydromet process surpasses the conventional pyrometallurgical smelting process for the mining of high grade Ni in terms of metal recovery and energy use (Taylor, 2007). The hydromet process generates 381,000 t/yr residue that is mostly acidic and requires neutralization before disposal.

Treated effluent to be discharged is estimated at 7, 220, 000 m^3/yr. Lime is applied to neutralize the acidic hydromet effluents from the refining process and the products are deposited in a specially designed disposal facility for final discharge into the nearby Sandy pond which is the immediate receiving body (Vale Inco, 2007). With an estimated 50,000 tons per year Ni mining capacity (Stefan, 2008), large volumes of fresh water will be consumed during operations which will be contaminated with associated dissolved metals. This has constituted a challenge with regards to environmental protection and conservation.

Refining effluents after the lime treatment will still contain dissolved Ni and Co ions, and their complexes, and other minerals/metals at levels far higher than permitted values. For Ni, 0.5 mg/L is the concentration allowed (MMLERs, 2007) while no clear effluent limit is available in the current Canadian government regulations for Co. Consequently, adequate attention in terms of developing a proper treatment technology is required. It is anticipated that there will be a greater amount of Ni and Co contamination of the ground and surface water in the near future, through the discharge of treated and untreated wastewater to the receiving water bodies surrounding the treatment site.

Mining and refining wastewaters are generally complex and complicated with the presence of heavy metals and organic compounds and have been identified as one of the major contributors to soil and water contamination (Couillard et al., 2004). Higher concentrations of metals have been associated with soils from various mining sites in Canada (Parker and Dumaresq, 2002) and in water samples of closed mine sites (Couillard et al., 2004). Industrial discharge in 2002 of Ni along with cadmium (Cd), zinc

(Zn) and copper (Cu) in the US was reported to be approximately 0.5×10^6 t which was about 42% of the total metal discharged by industries reported under the 2002 Toxic Release Inventory (TRI) (Al-Faqih et al., 2008).

1.3 Ni and Co in the Environment

Ni at elevated concentrations can be a toxic element which is normally widely distributed in the environment (Çiftçi et al., 2007) and its complexes are known to be human carcinogens (IARC, 1990). Ni is also known to cause dermatitis, nausea, chronic asthma and coughing. Ni is emitted to the atmosphere from volcanoes and windblown dusts and from numerous man-made sources such as melting and blowing of solid Ni. The Ni content of soil may range widely from 2 to 50 mg/ kg of soil or more depending on the mineral composition of the soil. The metal is highly mobile in plants and is readily absorbed by plant roots (Çiftçi et al., 2007). The carcinogenicity of Ni compounds depends on their capacity to release ionic Ni, and on factors that promote localization of high concentrations of Ni ions at critical tissue sites such as the heart and lungs (IARC, 1990).

Intake of Ni varies depending on the source and level of contact. Average dietary intakes are known to be between 400-500 µg/day with a maximum of 2% of this value being inhaled, especially in urban locations (De Zuane, 1997). The recommended WHO limit for Ni in drinking water is 70µg/L (WHO, 2006) while 15µg/L is recommended by USEPA (USEPA, 1996).

Co and its complexes are listed by the International Agency for Research on Cancer (IARC) as agents with possible human carcinogenic effects. High human uptake of cobalt can cause heart problems, vomiting and nausea and vision problems (IARC, 1990). Exposure through eating and drinking is known to be small, although, Co at a concentration above 40 mg/L could be harmful to plants depending on species (Ontario Fact Sheet, 2001).

Contamination of the environment by toxic metals is a real and growing problem for today's society (Blais et al., 1976) and may not be fully controlled since society will still rely on the use of these metals. The relative toxicity of metals when ingested by mammals may follow the order: Ag, Hg, Ti, Cd > Cu, Pb, Co, Sn, Be > In, Ba > Mn, Zn, Ni, Fe, Cr > Y, La > Sr, Sc > Cs, Li and Al (Evans, 1989). Most of these metals are found in water around mines due essentially to the economic and technical challenges posed by the treatment of the metal contaminated water especially in meeting the stringent environmental regulations, where they exist. One major issue with these metals aside of their eco-toxicity is their inability to biodegrade, unlike organic contaminants (Qin and Wen, 2007).

1.4 Research Objective and Scope

Nowadays, increased attention is focused on the development of effective and inexpensive technologies capable of treating large quantities of wastewater. Adsorption process can use readily available and highly efficient raw materials such as peat, and

other waste materials such as rice husk, and saw dust to separate or remove heavy metals from waste effluents (Romão et al., 2007).

Poorly humified peats (fibric and hemic peat) have been widely investigated as effective heavy metal adsorbent materials in metal contaminated water and wastewater (Coupal and Lalancette, 1976; Bloom and McBride, 1979; Ho et al., 1995, Crist et al., 1996; Ringqvist et al., 2002). Peat is known to effectively adsorb about 30 metals (Dissanayake and Weerasooriya, 1981). However, highly humified/decomposed (saprist) peat has not been widely investigated as an adsorbent as it has mostly been used as an horticultural amendment, to enhance the water holding capacity of sandy soils (Li et al., 2004) due to its high adsorptive capacities (Kuziemska and Quant 1998). Highly decomposed peat is used in this study, as an adsorbent in the development of filter columns which can be incorporated into existing treatment processes or operated independently in the treatment of mining wastewater containing Co and/or Ni.

This study investigates through batch experiments, the adsorption capacity, rates, kinetics, and controlling parameters, and proposes the uptake chemistry involved in the Ni and or Co ions adsorption using the highly decomposed or saprist peat from a Newfoundland bog. The efficiency of Ni and Co uptakes on this peat type in a competitive sorption with other metals such as Cd, Pb and Zn was also investigated. The adsorbent exhaustion rate was determined via column experiment at the breakthrough of 50% of the metals influent concentrations.

1.5 Thesis Organization

Chapter 2 is the literature survey, which is divided into four major sections. The first section provides a background on the conventional and emerging techniques in heavy metals removal from associated wastewaters. Section two of the survey covers the metal adsorption process, adsorbent choice and its adsorption capacity. The third section is on peat as a metal adsorbent and the fourth section is an introduction to the statistical design of experiments.

In Chapter 3 of the thesis a detailed classification, characterization and comparison study of fibrist and saprist NL peats is presented.

Chapter 4 presents the methods and materials used in the kinetics, equilibrium adsorption, desorption and column experiments.

Chapter 5 presents the results and discussion of the Box-Behnken design and kinetic experiments.

In Chapter 6 of the thesis, results and discussions of the batch equilibrium adsorption and desorption, and competitive studies are presented.

In Chapter 7, the fixed bed leaching column results and discussion, and the metals uptake chemistry on the saprist NL peat are reported.

Chapter 8 presents the conclusions and recommendations from the study.

CHAPTER TWO

LITERATURE REVIEW

2.1 Overview

The adsorption process, using activated carbon (granular or powdered) is being substituted by low cost materials such as agricultural wastes, clay, saw dust and others. This approach has emerged over the years, as a cost - effective alternative for the treatment of metal contaminated water and wastewater. Peat is one of the abundant natural materials with a high metal adsorptive capacity that can be used at an industrial level. Information regarding the formation and distribution of peat, chemical composition, ease of application and metal uptake rate and capacity are needed for treatment design purposes. In addition, understanding of the chemistry of the metal uptake process, could aid in sustained application.

Many studies have been done in order to understand peat types, formation processes, uptake or removal efficiency and metal uptake chemistry for various metals in municipal, industrial and mining wastewaters. In order to understand the state of the art of peat as an adsorbent for metals removal in wastewater, a literature search and review have been carried out and the results reported in this chapter.

2.2 Heavy Metal Contamination and Removal

Metals whose densities are > 5 g/mL are referred to as heavy metals (Alloway, 1995). Some of these metals are excessively released into the environment through

industrial activities such as mining and metal finishing (Rubio and Tessele, 1997; Ngah and Hanafiah, 2008). Industrial wastewater treatment compared to domestic wastewater, poses a more complex challenge because it is a mixture of varying compositions of contaminants rather than a simple solution containing dilute concentration of contaminants (Huang et al., 1988).

The maximum contaminant level (MCL - levels above which there is a known risk to health) in mg/L of heavy metals is very low, for example the MCL levels are for Hg 0.00003, Cd - 0.005, Pb - 0.006, As - 0.01, Ni - 0.20, and Zn - 0.80 (USEPA, 2009). Above these values, severe health related issues have been reported. If heavy metals pass through the wastewater treatment process, they will be returned to the environment where they will persist and may follow various pathways in their dispersion which could be difficult to monitor or contain (Mulligan et al., 2001). Metals contaminated wastewaters are generally treated by conventional techniques or one of the various emerging techniques and, in some cases, a combination of treatment techniques is employed.

2.2.1 Conventional Metal Removal Technique

The conventional technique is based on the metal precipitation process (Higgins and Sater, 1984; Patterson, 1989; Zhou et al., 1999) which is accompanied by selected separation processes for the precipitated phase. At the industrial level, contaminant concentrations are high and methods such as precipitation, filtration and especially membrane filtration, and addition of chemicals such as coagulants are very common. In the conventional technique, metal decontamination involves pH adjustment (Pavlović et

al., 2007) with lime solution to convert soluble metal salts to insoluble hydroxide precipitates that can be removed by gravity settling (Benjamin et al., 1996) in a clarifier (USEPA, 1982). The precipitates are removed as sludge, dried and burn to ashes or, and added to soils (Blais et al., 1976). Precipitation techniques can be enhanced oxidation/reduction precipitation, or secondary / co-precipitation (Patterson, 1989).

The precipitation of dissolved heavy metals in wastewater is by directly adding precipitating agents containing carbonate such as soda ash (Na_2CO_3), sodium bicarbonate, ($Na(HCO_3)$) or calcium carbonate ($CaCO_3$). Hydroxides and sulphides are also being used as precipitants especially sodium hydroxide ($NaOH$) and calcium hydroxide ($Ca(OH)_2$) or slaked lime. Sulfide precipitation in an oxygen depleted solution is commonly employed in the precipitation of Ag, Cd and Hg but odour and toxicity are two environmental problems associated with this application (Wang et al., 2004) although sulphides exhibit high reactivity and low heavy metal solubility over a broad pH range (Bhattacharyya et al., 1979).

Precipitation is a fairly rapid process which tends to be close to its equilibrium as soon as it is initiated (Wang et al., 2004). Metal concentration in the wastewater and the solution pH are the two main factors that govern precipitation reactions (Pavlović et al., 2007). During precipitation, the remaining concentration of the ionic species in solution is controlled by the solubility of the solid phase present (Wang et al., 2004).

Most often, carbonate is preferred to hydroxide in the precipitation of some metals such as Cd and Pb (USEPA, 1982) because it is cheaper (Pavlović et al., 2007), and the products of the reaction settle and filter better than hydroxide sludge at higher pH (Wang

et al., 2004). Heavy metals do not precipitate at the same pH, but a range of 9.5 to 11 is adequate in treating most mine and metallurgical wastewaters (Typliski and Labarre, 1980). Studies have shown that the precipitation of copper initiates at around a pH of 6, while for other metals such as Ni, Zn, As, Pb and Sb, the pH range is between 7 and 10 (Zhou et al., 1999; Pavlović et al., 2007). When the pH of a solution is adjusted, the ionic equilibrium of the reaction involving a metallic compound is altered which could lead to the production of insoluble precipitates of the metal (Pavlović et al., 2007). For example, in the removal of a metal ion (M^{2+}) from a wastewater, hydroxide, carbonate and sulphide precipitation reactions can be represented by equations 2.1, 2.2 and 2.3.

Hydroxide precipitation: $M^{2+}_{(aq)} + 2OH^{-}_{(aq)} \Leftrightarrow M(OH)_{2(s)} \downarrow$ 　　　　　2.1

Carbonate precipitation: $M^{2+}_{(aq)} + CO_3^{2-}_{(aq)} \Leftrightarrow MCO_{3(s)} \downarrow$ 　　　　　2.2

Sulfide precipitation: 　$M^{2+}_{(aq)} + S^{2-}_{(aq)} \Leftrightarrow MS_{(s)} \downarrow$ 　　　　　2.3

The solubility product constant Ksp, which is the equilibrium constant for a saturated solution and solid formation (precipitate) for equation 2.2, for example, is given by equation 2.4.

$$Ksp = \left[M^{2+}\right]\left[CO_3^{2-}\right]$$ 　　　　　2.4

$\left[M(OH)_{2(s)}\right]$ is approximately 1 because it is a solid.

Table 2.1 is a summary of the solubility product constants of some selected metal salts at 25°C.

Table 2.1: Solubility product constants of selected hydroxides, carbonates and sulfides

Metal Salt	Solubility product constant Ksp	Metal Salt	Solubility product constant Ksp	Metal Salt	Solubility product constant Ksp
$Cd(OH)_2$	5.9×10^{-15}	$CdCO_3$	2.5×10^{-14}	CdS	2×10^{-28}
$Co(OH)_2$	5.92×10^{-15}	$CoCO_3$	1.0×10^{-10}	CoS	4×10^{-21}
$Cu(OH)_2$	1.6×10^{-19}	$CuCO_3$	2.5×10^{-10}	CuS	6×10^{-36}
$Fe(OH)_2$	8.7×10^{-38}	$FeCO_3$	3.1×10^{-11}	FeS	6×10^{-19}
$Mn(OH)_2$	2.0×10^{-13}	$MnCO_3$	2.24×10^{-11}	MnS	3×10^{-14}
$Ni(OH)_2$	5.8×10^{-15}	$NiCO_3$	1.3×10^{-7}	NiS	3×10^{-19}
$Pb(OH)_2$	1×10^{-17}	$PbCO_3$	6×10^{-14}	PbS	3×10^{-28}
$Zn(OH)_2$	4×10^{-17}	$ZnCO_3$	1.6×10^{-11}	ZnS	2×10^{-25}

Source: Meites, (1963)

When the Ksp of a particular compound in solution is exceeded (super saturated), precipitation of the compound is initiated. Carbonates generally have larger solubility products compared with hydroxides; thus it is easier to exceed the solubility product constant of hydroxides compared with carbonates in precipitating them out of solution. Although carbonate precipitation is preferred in the precipitation of some metals, hydroxide precipitation is mostly employed because of the ease of handling (Pavlović et al., 2007) and the solubility of the precipitated phase that facilitates separation (Baltpurvins et al., 1996). Metal hydroxides tend to be colloidal in nature hence coagulants may be added to facilitate settling (Wang et al., 2004).

Large quantities of lime are consumed when metals are removed from industrial wastewater (USEPA, 1982). The consumption depends on the solubility product constants of the metals products, and is also connected with the competing reactions and re-solubilisation of the precipitates if the pH is decreased or increased from the minimum solubility point. Table 2.2 summarizes the addition and consumption of lime per kg of metal removed and values are not based on the reaction stoichiometry of the metal precipitated.

Table 2.2: Lime addition/consumption for metal precipitation

Stream Parameter	Lime addition (kg/kg)	Stream Parameter	Lime addition (kg/kg)
Aluminum (Al)	0.81	Iron (dissolved) (Fe)	1.28
Antimony (Sb)	4.53	Lead (Pb)	2.19
Arsenic (Ar)	1.75	Manganese (Mn)	3.51
Cadmium (Cd)	2.84	Mercury (Hg)	1.48
Chromium (Cr)	2.73	**Nickel (Ni)**	0.42
Cobalt (Co)	2.35	Silver (Ag)	3.23
Copper (Cu)	1.38	Zinc (Zn)	1.25

Source: USEPA (1982)

According to Zamlow et al., (1990), while the lime precipitation method is simple and inexpensive compared with carbonate precipitation, it has inherently associated disadvantages. These include, generation of large volumes of sludge which are costly to

handle (Patterson, 1989) and hazardous to manage (Patterson, 1989 and Eccles, 1999). The precipitation layer in settling ponds is known to undergo inversion at about $4^{o}C$ requiring extra settling facilities during low temperatures; effluents generated are not sufficiently low in heavy metal content, and metals not directly recovered as precipitates are mostly wasted. Multiple basin configurations are needed for efficient operation and also a sludge dewatering facility is required (Huang et al., 1988). The chemistry of lime precipitation is such that skilled operators are needed. Studies have also shown that effluents containing low concentrations of heavy metal are not effectively treated by precipitation (Brown et al., 2000; Qdais and Moussa, 2004).

2.2.2 Alternate Techniques for Metal Removal from Wastewater

Due to the disadvantages associated with the use of the conventional metal treatment method (precipitation), and the usual drive for efficiency and simplification of operation, some techniques have emerged over the years, more capable of removing heavy metals from water and wastewater. One of these techniques is based on the metal adsorption process. Other technologies include filtration using different membranes such as ultrafiltration, nanofiltration and reverse osmosis (Kurniawan et al., 2005), sorptive flotation (Zouboulis and Matis, 1997; Matis et al., 2003), and photocatalysis (Papadama et al., 2007 and Wang et al., 2008). These groups of heavy metal treatments which are not related to precipitation are collectively referred to as emerging techniques (Patterson, 1989) or classified as alternate techniques.

The most common adsorbent material is activated carbon (McKay et al., 1999; Annadurai et al., 2002a; Babel and Kurniawan, 2003) which has limited application in heavy metal contamination treatment due to its exorbitant cost (Bailey et al., 1999).

2.2.2.1 Basics of the Adsorption Process

Adsorption is the binding of chemical species at a phase boundary such as the surface of suspended particles (Benjamin et al., 1996) or the process by which ions or molecules present in one phase (the adsorbate) tend to condense and concentrate on the surface of another phase (Sawyer et al., 1994) generally known as the adsorbent. It is a mass transfer process due to unbalanced surface forces or energy (Eckenfelder, 2000). Adsorption can only occur if there is an affinity between the contaminant molecules and the solid surface sites. This affinity can be through chemical mechanisms (chemisorption, defined on page 30) or physical van der Waals forces (physisorption) (McKay and Ng, 2002).

Physical adsorption is due to molecular condensation in the capillaries of the solid enhanced by the electrostatic forces. One of these forces is the London – van der Waals force which is due to the instantaneous dipoles that exist around atoms or molecules caused by small disturbances of electronic motions. The disturbances could create temporary charges on the solid surface leading to adsorption (Reinbold et al., 1979; Griffin and Roy, 1985).

Chemical adsorption on the other hand is due to the formation of chemical bonds between the adsorbate and the adsorbent or the formation of ion complexes (Voice and

Weber, 1983; Eckenfelder, 2000). In chemisorption, a molecule may lose its identity due to the formation of a new compound by re-arrangement of the bonds to meet unsatisfied valences of the solid surface (Voice and Weber, 1983). Adsorption is known to follow the sequence below (Ruthven, 1984; Cooney, 1999):

1. Transportation via advection and dispersion of adsorbate to the fixed boundary layer that surrounds the adsorbent (bulk solution).

2. Movement of the adsorbate across the fixed film boundary layer through diffusive transport.

3. Attachment of the adsorbate to the adsorbent surface by a bonding process.

Eckenfelder (2000), reported that the rate of diffusion of solute molecules controlled the overall adsorption within the pores of the adsorbent particles. This rate is adsorbate concentration, molecular weight, and temperature dependent.

Studies have shown that if the solid surface (adsorbent) is properly selected and the solution chemistry appropriately adjusted, adsorption-based processes are capable of removing metals over a wider pH range and to a much lower residual level than processes based on precipitation (Benjamin et al., 1996). Many materials with high metal-binding potentials have been investigated as possible and effective adsorbents applicable in wastewater treatment. From these studies, the best adsorbent is metal specific. A group of adsorbents popularly referred to as "low cost" adsorbents has become the focus of research in recent years.

2.2.2.2 Low Cost Adsorbents for Treating Metal Contaminated Wastewater

Chitosan, a polymeric compound with many functional groups obtained by the deacetylation of the shells of crabs and shrimps (Babel and Kurniawan, 2003), through chemisorption reaction, has successfully removed Cd^{2+}, Hg^{2+}, Zn^{2+} and Ni^{2+} in the presence of a strong chelating agent like ethylene diamine tetra acetic acid (EDTA) (Jha et al., 1988). Natural Zeolites (activated and non-activated), have effectively removed Pb^{2+}, Zn^{2+}, and Cd^{2+}, via ion exchange reaction; Ni^{2+} removal using natural zeolites were found not to be effective (Blanachard et al., 1984; Zamlow et al., 1990; Türkman et al., 2004). Smectite clays, through ion exchange and chemisorption reactions, have effectively removed Zn^{2+}, Pb^{2+}, Al^{2+}, and Cd^{2+}, but not as effectively as natural zeolites (Brigatti et al., 1996). Iron oxide coated sand and Al_2O_3 and SiO_2-TiO_2, have effectively removed by chemisorption uncomplexed and complexed metal cations of Cu, Cd, Pb, Ni and Zn and Cr^{6+} and Ni^{2+} and Cd^{2+} (Benjamin et al., 1996; Ismail et al., 2008).

Sawdust, banana and orange peels, and coconut fibers are some of the natural agricultural materials (wastes) that have been studied. Coconut husk fibers and palm pressed fibers have been used in removing Cr^{6+} (Tan et al., 1993), Zn^{2+}, and Cd^{2+} (Babarinde, 2002) from water solutions with some good results. Sawdust has effectively removed Cr^{6+} (Zarraa, 1995), and 63% Cu under various wastewater conditions (Ajmal et al., 1998). 95% Pb^{2+}, 93% Zn^{2+}, 80% Ni^{2+}, and 75% Cr^{6+}, were all removed from an industrial wastewater using chemically activated sawdust (Saravanane et al., 2001) and chemically modified sawdust from oak and black locust hardwood removed Cu^{2+} and Zn^{2+} from stock solutions (Sciban et al., 2006).

17

Apple wastes, in packed beds could remove Cu^{2+} (Marañón and Sastre, 1991 and, Lee and Yang, 1997), at various chemical treatment levels with promising results. Banana and orange peels, have effectively removed Cu^{2+}, Zn^{2+}, Ni^{2+}, Co^{2+} and Pb^{2+} ions. At high solution pH, about 7.97 mg/g of Pb^{2+} was adsorbed by banana and 7.75 mg/g by orange (Annadurai et al., 2002b). Chemically modified peanut hulls have also been used in the removal of Co^{2+} and Ni^{2+} from stock solutions (Hashem et al., 2005).

Fibrist peat over the years has emerged as one of the most effective metal adsorbents and has been used in the removal of Hg^{2+}, Cd^{2+}, Zn^{2+}, Cu^{2+}, Fe^{2+}, Ni^{2+}, Ag^+, Pb^{2+} (Coupal and Lalancette, 1976) and some organic matters such as dyes (Leslie, 1974), biological components and suspended solids in wastewater (Pérez et al ., 2005).

2. 3 Main Factors for Adsorbent Choice

The choice of an adsorbent is determined by the contaminant concentration (Türkman et al., 2004) and the overall cost of treatment (Babel and Kurniawan, 2003; Türkman et al., 2004) associated with the decontamination of the metal polluted wastewater. Where adsorption is applicable, availability and cost of adsorbents also determine the selection of materials. Cost is an important parameter for comparing adsorbent materials (Bailey et al., 1999), but cost information is seldom reported, and the cost of individual adsorbents varies depending on the degree of processing and local availability. While cost is scarcely consistent, the use of low-cost adsorbent materials has been growing due to the simplicity in engineering application, and technical feasibility (Babel and Kurniawan, 2003).

An adsorbent is "low cost'' if it requires little processing, is abundant, or is a by-product or waste material from another industry (Bailey et al., 1999). Agricultural wastes, though reported to be good adsorbents are not readily available all year. Where available, decomposition due to microbial activities makes handling difficult, thus they have limited applications. Table 2.3 is a summary of the cost per kg of some effective natural adsorbents. Sphagnum peat moss is a natural, low cost, readily available material, and an effective metal adsorbent.

Table 2.3: Prices of some selected natural adsorbents

Adsorbent	Cost (US $/kg)	Source
Chitosan[1]	15.43	Babel and Kurniawan 2003
Activated carbon	~2.54 (quality and production dependent)	Dansons Inc., 2008*
Coconut husks	0.32 – 0.5 (treatment level dependent)	L. Shawer, 2010*
Sawdust	~0.3 (wood type and packaging dependent)	L. Shawer, 2010*
Zeolites	0.05 - 0.14 (quality and end use dependent)	USGS, 2006a
Clay	0.022 - 0.375 (type and quality dependent)	USGS, 2006b
Peat	0.024 - 0.052 (peat type dependent)	USGS, 2006c

[1]Chitosan is generally classified as low cost adsorbent because the raw materials used in its production are low cost. *Personal Communication.

2.4 Adsorbent Capacity

The design of an adsorption process entails the evaluation of adsorption rates, mechanisms of adsorption and equilibrium studies (Kadlec and Keoleian, 1986). The time taken prior to the removal of a given amount of solute from solution is the rate of adsorption and is determined by the kinetic study of the system. The ability or capacity of an adsorbent for a solute, which determines the quantity of adsorbent to be used, is estimated via an equilibrium study (Al-Duri, 1995).

The chemical kinetics of a reaction provides information on how fast the rate of the chemical reaction occurs and the reaction conditions that can influence the outcome. Some kinetics models based on the sorbent concentration include the Lagergren pseudo-first order equation (Lagergren, 1898), the Ritchie second order equation (Ritchie, 1977), the Blanchard et al., second order equation (Blanchard et al., 1984) and the widely applied Ho et al., pseudo-second order kinetics equation (Ho et al., 1996). The Ho et al., equation is based on the chemisorption (defined on page 30) of the adsorbent and the monolayer coverage of the adsorbate. The linearized form is given by equation 2.5 and the detailed derivation is given in Appendix A1.

$$\frac{t}{q_t} = \frac{1}{K_{1,ads} q_e^2} + \frac{1}{q_e} t \qquad (2.5)$$

In equation 2.5, q_t and q_e are the adsorbed quantities at time t in h and at equilibrium, in mg/g, and $K_{1,ads}$ is the pseudo-second order rate constant in $g mg^{-1} h^{-1}$. A plot of t versus t/q_t is linear with the slope being the reciprocal of the adsorbed quantity at equilibrium and the intercept a combination of the pseudo-second order rate constant and adsorbed quantity at equilibrium.

Adsorbent capacity can be evaluated using the batch or fixed bed column experiments. Batch equilibrium tests are conducted on soil suspensions to study equilibrium adsorption with individual or combined contaminants (Yong et al., 1992). Most studies have relied on the batch experiments to evaluate the effects of control parameters such as solution pH, contaminant concentration and contact time of the contaminant solution with the adsorbent.

Batch experiments are conducted by adding a known concentration of contaminant to a known mass of adsorbent for a fixed time. They are less time - consuming and are thus attractive. These tests have been applied, in studying adsorption kinetics (Zhipei et al., 1984; Gosset et al., 1986; Viraraghavan and Dronamraju 1993; Crist et al., 1996) and adsorption thermodynamics (Gosset et al, 1986). Sparks (2003) however, reported that the batch test is not a panacea for kinetic analyses although it is widely applied. This might be due to the fact that, in wastewater flowing systems, the contact time between the adsorbent and adsorbate is not long enough for the attainment of equilibrium and consequently data obtained in batch experiments are not generally adequate (Zhou et al., 2004).

In addition to obtaining the adsorption kinetics, adsorption isotherms are developed using batch tests. According to Warith (1996), isotherms give the mathematical relationship between the equilibrium concentration of contaminant in solution, and the amount adsorbed. These isotherms are valuable predictive relationships that could be used in estimating the attenuation capacity of the contaminants. At equilibrium, there is a distribution of solute between the liquid and solid phase with the

distribution ratio (liquid to solid phases) being a measure of the position of the equilibrium in the adsorption process usually represented by isotherms (Allen, 1987).

Column experiments are highly promising in removing metallic impurities from wastewater (Naumova et al., 1995) and therefore are explored in large scale treatment techniques and in the evaluation of adsorbent potentials. There are two ways by which influent can enter into a column. One is by upflow and the other by downflow. The downflow method is most common as it has an added advantage of adsorbing contaminants in a single step and is easy to operate (Zhou et al., 2004).

In column experiments, adsorption occurs as soon as the contaminant solution flows through the column. With continuous flow in a downward column, the equilibrium adsorption zone will move down the column. At the exit, the contaminant concentration in the effluent increases with time and eventually equals the initial concentration. This is the adsorption breakthrough point (Zhou et al, 2004) and in geo-environmental engineering, it is the point where 50% of the influent concentration is detected at the column exit (Yong et al., 1992). The concentration is taken at 50% of the influent value because saturation of the adsorbent bed usually occurs at this point and the flow can be regarded as being in steady state (Shackelford, 1993). At the breakthrough, the column operation can be stopped for maintenance.

2.4.1 Adsorption Isotherms

The adsorption capacity can be calculated in terms of the equilibrium adsorbate capacity given by equation 2.6.

$$q_e = \frac{(C_o - C_e)V}{M} \qquad (2.6)$$

where, q_e is the adsorbent phase capacity for the adsorbate at equilibrium (mg adsorbate/g adsorbent), C_o and C_e are the initial and final equilibrium concentrations of adsorbate after adsorption has occurred (mg/L), V is the volume of the adsorbent (L) and M is the mass of the adsorbent (g). A general formula represented by equation 2.7 for the adsorption isotherm has been proposed by Jaeger and Erdös (1956).

$$q_s = \frac{KC_s}{A + BC_s^D} \qquad (2.7)$$

In this equation, q_s (mg/g) is the adsorbed quantity per unit mass of adsorbent and C_s (mg/L) is the solid phase solute equilibrium concentration and, K, A, B and D are the isotherm constants.

Among the most commonly used adsorption isotherms are the Langmuir and Freundlich isotherms. Each isotherm is developed on different assumptions such that the application to a batch study depends on the prevailing solution conditions. The Freundlich isotherm is a better model compared to the Langmuir isotherm when dealing with dilute metal solutions (Kalymkova et al., 2008).

The Langmuir isotherm is based on four main assumptions: adsorption occurs at specific local sites on the adsorbent surface, the adsorbing site can only bind one molecule at a given time, the energy of adsorption is approximately the same from site to site, and there is no attraction between adsorbed adjacent molecules. A complete monolayer of adsorbed species is obtained in this case. The isotherm is given by equation 2.8

$$q_e = \frac{q_m b \, C_e}{1 + bC_e} \qquad (2.8)$$

where q_m (mg/g) is the maximum value that q tends toward as C_e (concentration at equilibrium in mg/L) becomes large and is also referred to as Langmuir monolayer saturation capacity (Conney, 1999). Ho et al., (1995) reported that, this constant is a strong parameter for comparing adsorption because it is an indication of the maximum adsorption capacity. The other constant b is the Langmuir isotherm constant which represents the ratio of the rate of desorption to that of adsorption, during adsorption. The two constants (q_m and b) are determined from a linearized form of equation 2.8 given by equation 2.9.

$$\frac{1}{q_e} = \frac{1}{q_m} + \frac{1}{bq_m Ce} \qquad (2.9)$$

When $1/q_e$ is plotted against $1/C_e$ a straight line is obtained with slope $1/bq_m$ and intercepts $1/q_e$ on the $1/q_e$ axis.

One important parameter that is usually evaluated through the determination of the Langmuir constant is the separation factor R*. This factor was first developed by Poots et al., (1978), to predict the favourable nature of an adsorption. R* is given by equation 2.10.

$$R^* = \frac{1}{1 + bC_o} \qquad (2.10)$$

where, b is the Langmuir constant (L/mg), and C_o is the initial metal concentration (mg/L). Ni or Co adsorption is favourable if $0 < R^* < 1$, unfavourable if $R^* > 1$ (b is

negative when there is no site coverage in the adsorbent), irreversible if $R^* = 0$ and is of linear isotherm if $R^* = 1$

The Freundlich isotherm is an empirical relationship that predicts adsorption in the liquid phase (Cooney, 1999) on heterogeneous surfaces (Al-Duri, 1995) and is represented by equation 2.11 which is usually operated in the linearized form as given by equation 2.12.

$$q = KC_e^{\frac{1}{n}} \tag{2.11}$$

$$\log q = \log K + \frac{1}{n}\log C_e \tag{2.12}$$

where K is the Freundlich isotherm constant expressed in $mg^{(1-1/n)} kg^{-1} L^{1/n}$ when q is expressed in $mg\ kg^{-1}$ and C_e in mgL^{-1}(Chen et al., 1999). K is a measure of the adsorbent capacity and 1/n the Freundlich exponent a dimensionless parameter, is the heterogeneity factor ranging from 0 to 1 (Al-Duri, 1995), and C_e is the adsorbate concentration at equilibrium. Kumar and Bandyopadhyay (2006) referred to these two constants as a measure of relative adsorption capacity. Both constants are dependent on some ambient factors such as temperature and pH. A plot of log q vs log C_e gives a straight line with slope as 1/n and intercept as log K (Cooney, 1999). This isotherm is known to be mathematically correct and accurate but does not converge to Henry's law at low surface coverage and when q approaches zero, equilibrium cannot be described (Cooney, 1999; Chiou, 2002).

Other adsorption isotherms that have been employed include the Redlich-Peterson isotherm that requires extra manipulations to determine the isotherm constants (Al-Duri,

1995; Cooney, 1999), and the Dubinin-Radushkevich isotherm that can be used in the estimate of adsorbent porosity and the energy of adsorption (Kapoor et al., 1989) though these two particulars isotherms were not good fits for the data obtained in this study.

2.4.2 Breakthrough Curves in Column Experiments

The breakthrough curve is used in column experiments to determine the time of exhaustion of the adsorbent bed (Cooney, 1999). The time of adsorbent exhaustion is a linear relationship in which the adsorbent bed depth and contact time, generally referred to as service time, are monitored. The bed depth service time (BDST) model was developed by Bohart-Adams (1920) and is based on the surface reaction theory. This model can be used to investigate the performance of adsorbents in columns under various conditions (Walker and Weatherley, 1997).

The Bohart-Adams model has been widely modified by many researchers and one of the simplified forms is given by equation 2.13a (Hutchins, 1973; McKay and Bino, 1990; Goel et al., 2005; Sze et al., 2008). It is often applied in the estimation of the time taken to attain the breakthrough of a pre-determined exit concentration for a given initial solution concentration. For this research, breakthrough was the time (h) or volume (L) at which 50% of the initial metal concentration was detected at the column exit.

$$t = \frac{N_o}{C_o v} H - \frac{1}{C_o k} \ln\left(\frac{C_o}{C_t} - 1\right) \qquad (2.13a)$$

In equation 2.13a, C_o is the initial concentration of solute in mg/L, C_t is 50% of the initial concentration of solute at breakthrough in mg/L, k is the adsorption rate

constant in L/mg.h, and measures the rate of solute transfer from the fluid phase to the solid phase (Cooney, 1999), N_o is the adsorption capacity in mg/L, H is the bed depth of the column in m, v is the linear flow velocity of feed to bed in m/h, and t is the service time of the column in h. Equation 2.13a can be re-arranged as shown in equation 2.13b.

$$\ln\left(\frac{C_i}{C_o}\right) = kC_o t - N_o k \frac{H}{v} \qquad (2.13b)$$

For purely advective transport of a non-reactive contaminant, the breakthrough can be determined by a plot of relative concentration (C/C$_0$) versus the pore volume (Bowders et al., 1985; Marshall et al., 1996) (see Appendix A2 for details of this method).

2.5 Peat as a Metal Adsorbent

Peat possesses a unique combination of chemical and physical properties that enable it to filter, coalesce and adsorb contaminants making it a useful and suitable material in wastewater treatment (Pérez et al., 2005). Peat is a complex matrix of macromolecules that are easily dispersed in water, resulting in a negatively charged colloidal system. The extent of decomposition of peat influences the particle size distribution and its physico-chemical properties (Andreasson et al., 1988).

One of the earliest investigations in Canada in which peat was used for adsorbing heavy metals was that of Coupal and Lalancette (1976), which followed the work of Leslie (1974) in which peat was used in the treatment of dye house effluent. Because of the polar character of peat, the specific adsorption potential for dissolved solids, such as metals and polar organic molecules, is quite high (Brown et al., 2000). One study reported

27

that, about 30 metals from the periodic table could be absorbed by peat (Dissanayake and Weerasooriya, 1981).

Bloom and McBride (1979) investigated the removal of Mn^{2+}, Fe^{2+}, Co^{2+}, Ni^{2+}, Zn^{2+}, La^{3+}, Al^{3+} and Ca^{2+} using acid treated peat. A natural peat bog was used in treating effluent containing Cu^{2+}, Ni^{2+}, Co^{2+} and Zn^{2+} from a nearby mine (Egger et al., 1980). Zhipei et al., (1984) studied the removal of Pb^{2+}, Cd^{2+}, Zn^{2+}, Ni^{2+} and Cr^{2+} with finely divided Chinese peat. Ca-impregnated peat was used in the removal of Cu^{2+}, Cd^{2+}, Zn^{2+} and Ni^{2+}, and Pb^{2+} (Gossett et al., 1986). Viraraghavan and Dronamraju (1993) studied the removal of Cu^{2+}, Ni^{2+} and Zn^{2+} with horticultural peat.

These studies showed the high metal removal capacity of peat as a metal adsorbent in the treatment of metal contaminated water and wastewater. Removal efficiencies between 84% and 99% were obtained for Hg, Cd, Zn, Cu, Fe, Ni, Ag, Pb and some organic matter (Coupal and Lalancette, 1976). Untreated natural peat bog was reported to have removed 100% of Cu and 30% of Ni from a mining effluent (Egger et al., 1980). Chemically modified peat (to improve the sulfo content of a Russian peat by sulphate treatment) removed ~ 90% Pb from a mixture of municipal and storage-battery wastewater (Kertman et al., 1993). Metal removal efficiencies between 72% and 98% for a wastewater containing Pb, Ni, Ga, B, Zn, In, Fe, Cd, Co, Mn, V, Mo Cr and Cu have also been reported using peat from the Tomsk region in Russia (Naumova et al., 1993).

2.5.1 Peat- Metal Adsorption Chemistry

Most plant - derived materials like peat contain organic compounds such as lignin, cellulose and humic acids as major constituents of their decomposition products. Organic constituents are polar functional groups such as aldehydes, amines, carboxyls, hydroxyls, ketones, and phenolic acid groups with the hydrogen and carbon in their molecular structure and could be involved in heavy metal adsorption (Bloom and Mc Bride, 1979; Qin et al., 2006). The stronger the polar groups in an adsorbent, the higher the potential for metal and polar organic molecules adsorption (Qin et al., 2006). This is the case with peat.

The functional groups are usually involved in reactions leading to metal uptake by the adsorbent. The two most reported reaction mechanisms found in low cost adsorbents such as peats are: Ion exchange and Complexation (Brown et al., 2000). In some cases, the two reactions have been interchangeably used to explain the mechanism of peat metal uptake (Kadlec and Keoleian, 1986).

In ion exchange, a solid material, carrying exchangeable cations or anions, is used in an operation in which the ions can be exchanged for a stoichiometrically equivalent amount of other ions of the same sign when there is contact (Helfferich, 1962). Cation exchangers are carriers of exchangeable cations while anion exchangers are carriers of anions. When a material is capable of exchanging anions and cations it is known as an amphoteric ion exchanger (Helfferich, 1962).

According to Zagorodni (2007), the ion exchanger is a phase containing an osmotically inactive (carrier cannot migrate from the phase where it is located) and

insoluble carrier with the electrical charge (matrix). Ion exchange is most often a reversible process (Helfferich, 1962). Figure 2.1 shows a typical ion movement in an ion exchange process.
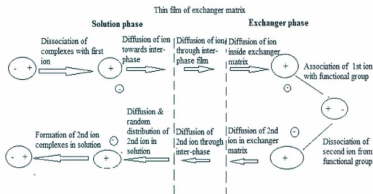
Fig. 2.1: Schematic steps of ion exchange (adapted from Zagorodni, 2007)

An ion exchange reaction is a competition between the resin (exchangeable ions carried by an ion exchanger) counterions and solution counterions for functional groups of the material (Zagorodni, 2007). Bel' kevich et al., (1980) reported that ion exchange in peat is due specifically to the presence of a group of compounds that contained carboxyl - COOH, phenolic hydroxyls - OH, heterocyclic amine - =NH, and thiol – SH. In compounds containing these groups, hydrogen of the functional groups are exchanged with metals and ~ 50 % of this exchange reaction occurred in the humus substances, while about 30 – 40% occurred in the readily hydrolysable substances and lignin.

Bloom and McBride (1979) showed that the carboxylic group in an acid treated peat was responsible for the binding of Cu, Mn and Ni in wastewater containing the

cations of these metals with the release of the H^{+} ion. This reaction was also confirmed in a Ca-impregnated peat study (Crist et al., 1996). The ion exchange reaction could be represented by equation 2.14 (Blais et al., 2003).

$$R - Ca^{2+}\left(Mg^{2+}\right) + Me^{2+} \rightarrow R - Me^{2+} + Ca^{2+}\left(Mg^{2+}\right) \qquad (2.14)$$

In equation 2.14, Me^{2+} is the metal cation and R is the matrix of the Ca or Mg cations-impregnated peat adsorbent.

In complexation reactions, inner-sphere (metal ions bind directly to the ligands without water molecules) or outer-sphere (metal ions bind to water molecules and both are bonded to the surface of the ligands) type complexes can be formed by bonding between metal ions due strictly to the electronic interactions between the metal ions and the ligand (Sposito, 1984; Sparks, 2003). In this form of bonding, the d-orbital electrons of the metal atom accept electron pairs (i.e. the metal acts as a Lewis acid) from a ligand (the Lewis base) to form a covalent bond and each ligand replaces one of the hydration shell water molecules in the reaction (Koretsky, 2000).

The complexation reaction, between a hydrated metal ($\left[M\left(H_2O\right)_x\right]^{n+}$) and a ligand ($L^{-1}$) to form an outer – sphere complex (Sparks, 2003), could be represented by equation 2.15 given below.

$$a\left[M\left(H_2O\right)_x\right]^{n+} + bL^{-1} \Leftrightarrow \left[M\left(H_2O\right)_x\right]_a L_b \qquad (2.15)$$
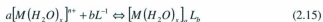
In the above equation, n^+ refers to the charge on the metal ion, x is the coordination number, and a and b are stoichiometric coefficients. In solutions, free metal ions are actually aqua complexes, with the water being a ligand that binds metals; hence, every

complexation reaction in water is effectively a ligand-exchange reaction (Morel and Hering, 1983).

Many studies (Egger et al., 1980; Ringqvist and Holmgren, 1998; Ringqvist et al., 2002) have supported the peat-metal ion complexation reaction. One study (Ringqvist et al., 2002), showed that monovalent cations are held primarily by simple cation exchange while multivalent cations have the potential to form co-ordinate linkages.

Other reactions that have been suggested but supported to a lesser extent as possible metal uptake routes on peat include chemisorption and surface adsorption. In chemisorption, ions are not specifically exchanged, but electrons are exchanged and this could result into metal-peat binding at the surface of the peat (Evangelou, 1998; Brown et al., 2000). Cooney (1999) reported that heat is usually involved in chemisorption.

Surface adsorption on the other hand is a physical process where positively charged ions are attached to a negatively charged surface without the exchange of electrons or ions (Brown et al, 2000). Cooney (1999) suggested that surface adsorption involves no heat.

2.5.2 Peat Formation

Peat with its natural constituents provides, a unique material for developing knowledge on the mechanisms and factors influencing metal binding onto organic matter (Twardowska and Kyziol, 2003). Peat is a spongy vegetable substance composed of mosses and aquatic plants in different stages of decomposition (Kerr, 1905), or partially fossilized plant matter (Pérez et al., 2005). It is a natural resource like wood or other

biomass and can be considered as a bio-fuel in the energy context (Smuts, 1996). It is formed in the poorly oxygenated water of marshes, bogs, and swamps. When the rate of plant matter production and accumulation in the water is greater than the rate of decomposition, the resulting vegetation is slowly and easily oxidized by microorganisms to form peat (Spedding, 1988; Pérez et al., 2005). Smuts (1996) reported this to be the pre-requisite for the formation of peat. Figure 2.2 summarizes the peat, lignite and coal formation stages.

$$Biomass \quad \overset{Slow\ microbial\ oxidation}{\Rightarrow} \quad Peat \quad \overset{High\ pressure\,/\,temperature}{\Rightarrow} \quad Lignite \rightarrow Coal$$
$(e.g.\ leaves,\ ferns,\ mosses,\ etc)$

| Time | $\leftrightarrow$ | 10, 000 years | $\leftrightarrow$ | ~ 40 million years | $\leftarrow$ |

Fig. 2.2: Schematic representation of peat, lignite and coal formation (adapted from Spedding, 1988; Smuts 1996).

Peat is accumulated, through the successive growth and decay of plants, and the replacement of one type of bog vegetation by another. The rate of growth and accumulation of peat is variable, but very slow (Dachnowski, 1912). The processes of formation and accumulation occur in the first few meters of the earth and several factors affect the characteristics of the peat, such as the nature of the vegetation, regional climate, water pH, and degree of metamorphosis (Brown, 2000; Pérez et al., 2005).

Sphagnum mosses, true mosses (Bryales), sedges and woody plants are the most important peat forming plants with Sphagnum mosses being regarded as the most versatile. Cells of sphagnum mosses are thin-walled with large cavities which assist the

absorption and transportation of water from the ground. These cells have lignified walls, built up in different forms, but mostly as rings, spirals or plates. Absorption of water by sphagnum mosses is a mechanical capillary system which is maintained even by the dead plants in the form of peat (Puustjärvi and Robertson, 1975).

Milling is the most common means of peat harvesting nowadays. Usually, a peatland is drained by ditching at 20 to 40 m intervals and the surface vegetation removed. The soil surface is harrowed repeatedly to a depth of 5 to 10 cm, breaking up the dried peat that is collected by vacuums in North America. This method enhances sustainability as 5 to 10 cm of peat may be removed from the top per year over several decades (Campbell et al., 2002).

Peat deposits are not limited by climatic conditions, and are found where large amounts of biomass are available and decomposition of residues is inhibited (Gondar et al., 2005). Three factors control peat formation and deposition: (1) physical properties of the biomass; (2) humicity or the decomposition degree of the organic substance; and (3) the nature of the elements such as the metals comprising the deposit (Aaby and Berglund, 1986). Thus, peat deposits have been reported in South Africa and some other African countries like the Benin Republic, although the largest peat deposits are found in the Northern hemisphere.

2.5.3 Peat Distribution (Global and Local)

On a country-by-country and peat to land ratio basis, Canada is second to Finland (CSPMA, 2007) although the largest peat deposits of the world are located in Russia

(Spedding, 1988). Canada's peatlands are among the most extensive in the world and the least threatened by development pressures (Irish Peatland Conservation, 2007). Figure 2.3 depicts the global peat and peatland distribution while the distribution of peatland by province or territory in Canada is given by Table 2.4 with Newfoundland and Labrador being the sixth largest peatland province.

Newfoundland peatlands though comparatively small are a significant portion of the great peatland ecosystem that stretches around the world. Studies have shown that bogs (wetlands that accumulate acidic peat) and fens (wetlands that are supplied by surface/or groundwater) dominate Newfoundland's peatlands with the inherent nutrients from the parent-forming plants aiding the formation of this peatland (Pollett and Wells, 1977) and contributing to its characteristics. This might not be the case with peatlands elsewhere.
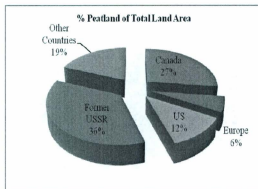
Fig. 2.3: World's extensive peatland distribution (Adapted from CSPMA, 2007)

Table 2.4: Peatland distribution in Canada

Province or Territory	Peatland Area	
	Ha x 10^6	% of Total Land Area
Alberta	18	27.2
British Columbia	4.9	5.1
Manitoba	19.2	29.5
New Brunswick	0.2	4.4
Newfoundland and Labrador	5.4	13.4
Northwest Territories and Nunavut	16.9	4.9
Nova Scotia	0.4	4.9
Ontario	31.3	29.3
Prince Edward Island	< 0.01	< 1
Quebec	11.2	7.2
Saskatchewan	4.9	7.5
Yukon	1.1	2.3
Canada (Total)	**113.4**	**11.4**

Source: Adapted from Daigle and Gautreau-Daigle (2001)

2.6 Peat Characterization and Classification

Peat application, on an industrial, agricultural or domestic/small scale requires a form of characterization and or classification (Bohlin et al., 1989). Due to differences in the environment in which peat is formed and the variation in vegetation involved in formation, classification of peat has remained a difficult task (Spedding, 1988). Classification often refers to the natural composition and location from which the peat is harvested. Characterization of peat on the other hand though reported to be a well investigated area (Bohlin et al., 1989; Nordén et al., 1992), cannot be said to be as simple as stated.

Peat can be highly humified or poorly humified, an indication of the level of decomposition or formation that the parent biomass has undergone. Peat could in simple terms, be classified as: fibric, hemic, or sapric. Fibric peats are the least decomposed, hemic peats are somewhat decomposed, and sapric peats are the most decomposed (Crum and Planisek, 2004; Pérez et al., 2005).

Since 1922, the von Post scale (FAO, 2008) has been a useful means of classifying peat. This method is based on the physical appearance of peat, its water content and the presence of fibers. Peat on the von Post scale is classified into 10 different classes, based on the observed results after pressure is applied by hand and the extruded matter physically examined. On the von Post scale, peat in class 1H is incompletely decomposed and class 10H means completely decomposed peat as shown in Table 2.5.

Table 2:5: The Von Post scale for peat classification

Scale Number	Physical Description	Plant Structure	Expressed Fluid	Peat Lost	Peat Retained Consistency/Colour
H1	Completely unhumified		Colourless, clear		
H2	Virtually unhumified		Yellow-brown clear		
H3	Little humified		Noticeably turbid	None	Not porridge - like
H4	Poorly humified		Very turbid	None	Somewhat porridge - like
H5	Fairly humified, distinct structure	Plain, but somewhat obscured	Strongly turbid	Some	Very porridge - like
H6	Fairly humified	Indistinct but still clear		~ 1/3	Very porridge - like
H7	Quite well humified	Much still visible		~ 1/2	Gruel – like, very dark
H8	Well humified	Vague		~2/3	Only roots and fibrous matter remain
H9	Almost completely humified	Almost none visible		~ all	Homogenous
H10	Completely humified	None visible		All	Porridge

Source: Adapted from Bozkurt et al., (2001)

Peat can be characterized with respect to the bog or vegetation from which it is taken. Characterization can also be on the basis of the metal, organic and inorganic contents. Peat characterization usually presents more detailed information which is desirable, compared to classification. There is however no unique method of peat

characterization as methods chosen are influenced by investigations planned and the number of parameters to be examined before application.

Nowadays, a complete peat characterization in its natural state could be done by a combination of one or more of the following analytical methods: (i) X-ray diffractometry (XRD) – for crystallographic study (Bloom and McBride, 1979; Summa and Tateo, 1999; Romão et al., 2007) (ii) Scanning electron microscopy (SEM) – for surface morphology (Coupal and Lalancette, 1976; Fox and Edil, 1996; Romão et al., 2007), (iii) Fourier transform infra red (FTIR) spectrometry – for functional groups identification (Durig et al., 1988; Romão et al., 2007), (iv) [13]carbon nuclear magnetic resonance (NMR) spectrometry – for functional groups identification (Preston et al., 1989; Almendros et al., 2003) (iv) Particle Size Distribution (PSD), (v) Determination of Metallic Content of peat using Inductively coupled plasma atomic emission spectrometry (ICP-AES) (Ho and McKay, 1998), (vi) Degree of Decomposition (von Post scale), and (vii) Moisture and Ash Contents (Smuts, 1996; Gondar et al., 2005).

2.7 Statistical Design of Experiment

Many of the peat-metal adsorption studies have been conducted with the method of keeping one or two factors constant and varying the factor of interest. An elegant way of conducting experiments with minimal use of materials and reduced bias is to employ a statistical design of the experiment. In statistical design of an experiment, a set of experiments is conducted in a randomized format. In this method, the individual effects of factors known as main effects and the interdependent effects of factors known as

interactions are obtained. The parameters of interest under investigation are known as the responses. Three ways of conducting the design of an experiment are: screening, full and fractional factorial and response surface methods (Montgomery and Runger, 2003).

Screening in design of experiments is used to reduce the experimental runs when little is known about the responses. While the main effects are evaluated, interaction effects cannot be evaluated with screening. However, factors that has significant effects on the responses can be isolated from the less important factors. Factors are run on two – level designs or low and high levels as defined by the range of each factor (Czitrom, 1999).

In full factorial design, all treatment combinations of the factor levels are used in evaluating the response variables. These types of experimental designs are more efficient than one factor at a time designs (Czitrom, 1999). The design allows for the testing of linear and non-linear behaviour in the factors by duplicating experiments at mid point conditions of the factors. However, in this design, it is difficult to differentiate between main effects and interactions as the complexity of the experiment increases. Fractional factorial design provides a reduction in the number of experiments without the loss of information (Montgomery and Runger, 2003).

Response surface design is used to obtain precise information about factor effects and especially magnitude and direction. They are most often three-level designs that allow the estimation of linear, two factor interactions and non-linear effects of all factors under investigation. They are employed when there is an indication of non-linear behaviour or when a factorial design experiment reveals the presence of non-linear

behaviour. They are useful in identifying optimum conditions (Montgomery and Runger, 2003).

The design of experiment by any of the above method involves the use of statistical packages that can be found in MINITAB, Design Expert and others. In this study, Design Expert 8.04 was employed first, in a full factorial design to screen the experimental factors, and followed by the use of the Box-Behnken design of the surface response method.

2.8 Summary of Literature Search

Peat, especially the fibrist type is a promising adsorbent for treating metal contaminated water and wastewater. Various studies have shown that many parameters are involved in the chemistry of the metal uptake on the fibrist peat. Solution pH and initial metal concentration in solution have been reported (Coupal and Lalancette, 1976; Ho et al., 1995; Kalymkova et al., 2008) to be capable of influencing the amount of metal removed from metal contaminated water. Solution temperature (Viraraghavan and Dronamraju, 1993; Kalymkova et al., 2008) has also been reported as an influencing parameter when peat is used as a metal adsorbent.

Peat, though it has been studied as a good adsorbent for metal uptake in metal contaminated water, the understanding of the uptake mechanisms, sequence of reactions and extent of uptake has been inadequately reported and most times reports are contradictory when available. These contradictions need to be clarified, if peat is to be

used on a large scale, as one of the most viable adsorbent materials for metal removal from metal contaminated water and wastewater.

The study reported in this thesis seeks to clarify these issues and as well, list the performance of the saprist Newfoundland peat (referred to as NL peat by the author) used in the study. It also seeks to compare the single ion Ni and Co uptake performance of the saprist NL peat against multiple ions uptake as widely done with the fibrist peat. One of the significance of the use of this peat type is in the management of peat vegetation because it is a non-renewable natural material.

CHAPTER THREE

PEAT CHARACTERIZATION

3.1 Chapter Overview

Characterization methods, results and comparison of poorly decomposed peat (fibrist or horticultural) and highly decomposed (saprist) peats obtained from the same bog in Torbay, St. John's, Newfoundland, Canada, are reported in this chapter. The combination of selected facilities and analytical techniques utilized at Biology, the CREAIT, Chemistry, and Earth Science departments of Memorial University of Newfoundland (MUN), St. John's campus were used to determine the metal content of the virgin peats, the surface morphology, and inherent functional groups. The cation exchange capacity and physical properties of the peats associated with their use as adsorbents, and the peats' particle size distribution by dry granulometry were also determined and presented.

3.2 Physico-chemical Properties of the Newfoundland Peats

3.2.1 Peat Harvesting, Storage and Sample Preparation

Horticultural (fibrist) and highly decomposed (saprist) peats were harvested on 14th August, 2008 from a natural peat bog owned by Traverse Nursery, in Torbay, St. John's NL. Figure 3.1a is a typical sphagnum moss plant and Figure 3.1b is the cleared natural peat bog. According to Pollet et al., (1968) peatlands in this area belong to the

largest single peatland area of the Avalon Peninsula. The horticultural peat was harvested at ~ 4 cm from the surface after clearing some partly decomposed plant materials while the saprist peat was harvested at about 1.6 m from the surface of the bog.

Fig. 3.1a: Sphagnum moss plant

Fig.3.1b: Cleared natural peat bog

The peat samples were transferred on site into large high density polypropylene bags for storage in the Environmental Engineering Laboratory, Faculty of Engineering and Applied Science, MUN, St. John's. The wet bulk density of the samples was determined immediately on arrival at the laboratory. 1500 g of peat samples were weighed and spread on plastic trays for air drying at room temperature. Air drying was the chosen option not only to lower the moisture content of the peats but also to maintain an approximate equilibrium with the air of the laboratory thereby reducing possible changes in the moisture content of the sample during experiments.

Dried peat samples were thoroughly mixed by removing pebbles and undecomposed woody materials by hand-picking, followed by the separation into particle

sizes by dry granulometry. The air dried peat samples are as shown in Figures 3.2a and 3.2b. These air dried peat samples were used in the crystallographic, morphologic and functional groups identification studies.

Fig.3.2a: Air dried saprist NL peat

Fig.3.2b: Air dried fibrist NL peat

3.2.2 Cation Exchange Capacity of Newfoundland Peats

One of the most important parameters for consideration in the choice of a material as an adsorbent is the cation exchange capacity (CEC). The capacity of soils to adsorb and exchange cations expressed in milliequivalent per 100 grams of soil is known as the CEC. It is a significant parameter in the determination of the metal retention capacity of a soil.

The CEC values of the fibrist and saprist NL peats were determined in triplicates by the pH 7.0 calcium acetate ($CH_3CO_2)_2Ca$ – calcium chloride ($CaCl_2$) method (Sheldrick, 1984) and the average values are reported as shown in Table 3.1. This method was selected because of the high organic content of the peat samples and in such cases, the pH dependent changes are known to be high. The CECs of the peats were obtained

45

prior to air drying of the NL peats. The exchangeable Ca in meq/100g in the peats was obtained using equation 3.1 (Shelderick, 1984).

$$\frac{\mu g / mL\ measured}{equivalent\ weight.\ of\ Ca \times 1000} \times \frac{100}{weight\ of\ soil} \times volume\ of\ extract\ (mL) \times dilution$$

(3.1)

3.2.3 Other Physico-Chemical Parameters of Newfoundland Peats

The other physico-chemical properties that can influence peat in the metal adsorption process include the peat pH, moisture content, fiber content, ash content and bulk density. Each of these parameters was determined using applicable ASTM methods for soils by reporting the average of the triplicate samples. Table 3.1 summarizes the values of these properties for the two Newfoundland peat types.

Table 3.1: Physico-chemical properties of the fibrist and saprist NL peats

Parameter	Method of Evaluation	Values	
		Fibrist Peat	Saprist Peat
Degree of Decomposition	Von Post	3H	7 - 8H
pH (in de-ionized water)	ASTM D2976-71	4.2	4.2
Moisture content (%)	ASTM D2974-07A	82	86
Fiber content (%)	ASTM D1997-91	75	69
Ash content (%)	ASTM D2974-07A	16	9
Organic matter (%)	ASTM D2974-07A	84	91
Fresh bulk density (g/cm³)	ASTM D4531-86	0.60	0.65
Dry bulk density (g/cm³)	ASTM D4531-86	0.21	0.28
pH 7.0 CEC (meq/100g)	Calcium acetate/chloride	45	70

46

From Table 3.1, saprist Newfoundland peat has a larger CEC, dry bulk and fresh bulk densities (the dry bulk density was determined after air drying while the fresh bulk density was determined just after harvesting the peats), organic matter content and moisture content compared with the fibrist Newfoundland peat. This trend is connected with the composition of the saprist peat particles which was determined by the high level of decomposition resulting in fine and smaller materials compared with the fibrist peat particles that were coarse and larger in size. The two peat types are however rich in organic content which could be one of the reasons why the Newfoundland peat is mainly used in gardening in the US and Canada.

3.2.4 Particle Size Distribution of the Peats

Particle size distribution or dry granulometry of the air dried peats was determined by sieving triplicate dried peat samples over a series of mechanically stacked sieves of selected sizes. The sizes selected were based on the ease of separation of the peats. The size distribution was obtained using USA standard test sieves (ASTM 11 specification) of 4.75 mm, 2 mm, 850 µm, 425 µm, 300 µm, 150 µm, 75 µm and < 75 µm diameters. The sieves were arranged placing the 4.75 mm diameter and 2 mm diameter sieves on top for the horticultural and saprist peats respectively with a collecting pan placed at the bottom.

Each peat sample was placed onto the upper sieve and shaken on the WS E-Tyler vertical shaker for 15 minutes with vibration amplitude between 2 and 3 mm. Peat fractions above the sieves' diameter were retained on the corresponding sieve while sizes below passed onto the next sieves. The process of separation was repeated three times for

three different air dried peat samples and the average values recorded for the samples as shown in Table 3.2.

Table 3.2: Dry granulometry results of the fibrist and saprist NL peats

Sieve No.	Seive Size (µm)	Average % Retained (Fibrist Peat)	Average % Retained (Saprist Peat)
4	4750	15	13
8	2000	19	-
20	850	-	52
40	425	45	15
50	300	-	5
60	250	9	-
100	150	4	6
200	75	6	3
	<75	2*	6*

*Material less than <75 µm mostly dust lost during the particle size analysis

Table 3.2 showed that the saprist NL peat contained over 50% by weight of 850 µm particle sized peat grains. However, further examination of this fraction during the dry granulometry study, showed that it contained lumped fine particles that resulted in less than 2% of the total saprist peat material (retained in sieve No. 20) when the lumps were broken up by hand. Thus the lumped fine particles of the saprist NL peat affected its particle size distribution as shown in Table 3.2. The fibrist peat on the other hand, had more undecomposed material (between 4.75 and 2.00mm) compared with the saprist peat. Particle size distribution could influence the porosity and make the fibrist NL peat more porous than the saprist NL peat.

3.3 Instrumental Analytical Characterization of the NL Peats

Peat surface analysis is an important step towards identifying the inherent characteristics that could influence peat use as a metal adsorbent. Air dried virgin Newfoundland peats were therefore subjected to analytical characterization using X-ray diffractometry (XRD) for crystallographic study at the Earth Sciences department, Scanning electron microscope (SEM) for morphological and surface profile study at the Biological department and, Fourier transform infra red spectroscopy (FTIR) and ^{13}C Nuclear magnetic resonance (NMR) for the identification of functional groups at the CREAIT, in the Chemistry department. Inductively coupled plasma mass spectrometry (ICP-MS) available at the Earth Sciences department, was employed for the determination of initial metallic content and was the only method that involved the destruction of the peat samples. All the departments are at the St. John's campus of MUN.

3.3.1 Peat Crystallographic Study

Adsorption in peat has been reported to be influenced by the presence of impurities (Couillard, 1994; Twardowska and Kyziol, 2003). If inorganic matters are present in a significant proportion, the understanding of the organic matter metal uptake chemistry could be difficult because of the stronger affinity of the inorganic materials for metals. Peat is generally organic in composition and amorphous in nature while most inorganic matters are crystalline in nature. This difference in composition was used in the crystallographic study of the Newfoundland peats.

The powder X-ray diffractometer (XRD) technique has been used in the identification of multiple phases in microcrystalline mixtures such as rocks, determination of crystalline structure of identified compounds and, identification and analysis of clay materials and recognition of amorphous materials in mixtures (Pecharsky and Zavalij, 2003).

From each of the main twelve particle size fractions shown in Table 3.2 (excluding dust), a statistically infinite amount of randomly oriented powder particles were packed on a vertically placed stud of the Rigaku Rotaflex D/Max 1400 rotating anode powdered x-ray diffractometer with Cu-Kα radiation source operated at 40 kV and 100 mA from Rigaku/MSC (Japan) equipped with an X-ray stream 2000 low temperature system. A coherent beam of monochromatic X-rays of known wavelength (1.54Å) were generated by high energy electrons in a sealed vacuum tube through the Cu (Kα) pure anode. X-rays diffracted by the specimen were measured and a pattern specific to the various crystalline structures were obtained. The interaction of x-rays with the samples created secondary diffracted beams which were related to the interplanar spacings in the material according to the Braggs law given by equation 3.2.

$$n\lambda = 2dSin\theta \qquad (3.2)$$

where, n is an integer, λ is the wavelength of the X-rays in Å, d the interplanar spacing in Å generating the diffraction and θ is the diffraction angle.

The diffraction maxima or peaks were measured along the 2θ diffractometer circle which had a fixed x-ray tube and the specimen moving at half the rate of the detector to

maintain θ-2θ geometry. The diffractograms obtained were matched through the JADE data software.

The diffractograms obtained as shown in Figure 3.3a for the saprist Newfoundland peat of particle size ≤ 425 µm (representative of all other fractions for the two peats), and Figure 3.3b for the fibrist Newfoundland peat of particle size < 75 µm. The diffractograms for all other fractions of particle sizes for both peat types were similar to Figure 3.3a except for fibrist Newfoundland peat of particle size < 75 µm. As shown in Figure 3.3b, identifiable peaks that showed the presence of calcium and silicon oxide minerals were obtained for this case.

The hump-shaped peak occurring between 18° and 32° is a unique characteristic of peat (Romão et al., 2007). The spectrum showed that the Newfoundland saprist peat was completely amorphous as no mineral peak was identified while the Newfoundland fibrist peat at < 75µm contained identifiable inorganic fractions. Some studies have reported the presence of known minerals in peat such as quartz and feldspar in a New York woody peat (Bloom and McBride, 1979) and calcite, kaolinite and quartz in an Alder-peat from Poland (Twardowska and Kyziol, 1996); but no known minerals especially clays were detected in the Newfoundland peat particles except for the fibrist NL peat particles of size < 75 µm.

ID: Second trail I glass
File: 425.MDI   Scan: 5-99.95/.03/. 36/#3166, Anode: CU
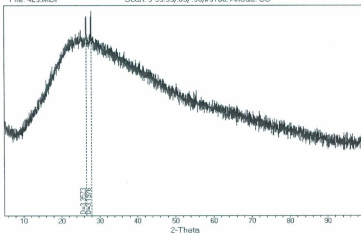
Figure 3.3a: Diffractogram of saprist NL peat fraction ≤ 425 μm

ID: Second trail I
File: LESS75.MDI   Scan: 5-99.95/.03/. 36/#3166, Anode: CU

1) 12-0708: Si 02 - Silicon Oxide

2) 23-0430: Ca - Calcium

2-Theta
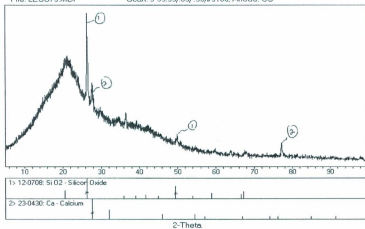
Figure 3.3b: Diffractogram of fibrist NL peat for fraction ≤ 75 μm (1 is associated with

the peaks for silicon oxide and 2 associated with the peaks for calcium)

52

3.3.2 Peat Surface Morphology

Surface characteristics of peat influence properties such as porosity, permeability and water holding capacity. The surface profile and morphology of solid matters can be studied using Scanning Electron Microscopy (SEM) (Bozolla, 2007). In SEM, the lenses act as condensers in a demagnification series to focus on extremely small spots (Egerton, 2005). This is highly essential in understanding the peats' pores orientations.

Samples from each fraction obtained in the dry granulometry stages were spread over a carbon taped stud, coated with 550X Sputter Coater for gold to obtain ~15nm thick coating on the peat. This process, in the opinion of the author, greatly enhanced the resolution of the micrographs since biological specimens such as peat are known to yield poor signals on conventional SEM (Egerton, 2005). The Hitachi-S570 SEM was operated at 20 mA in a 0.2 mbar vacuum that allowed generated electrons to reach the specimen after ~2.5 minutes resulting in signals that included secondary and backscattered electrons, X-rays, light and heat.

Secondary electrons gave information on the specimen topography while, light and heat provided insight on the composition of the material being probed (Egerton, 2005 and Bozzola, 2007). As the probes struck the specimen, each point impacted provided information displayed on a monitor. Image quality, presented as micrographs, depended on the signal strength and overall yield of secondary electrons from the specimen. Areas that appeared darker in the micrographs were due to fewer secondary electrons.

Micrographs of the twelve different size fractions for the two Newfoundland peat types specimen were obtained at different magnifications. Different magnifications on the

Hitachi-S570 SEM were employed so as to obtain the best possible resolution for the twelve specimens from which the twelve fractions for the dry granulometry (Table 3.2) were obtained. Figures 3.4a and 3.4b are the micrographs of fibrist and saprist Newfoundland peats at a magnification of 1000 times and at different scales.

Figure 3.4a: Micrograph of fibrist NL peat (Magnification X 1000)
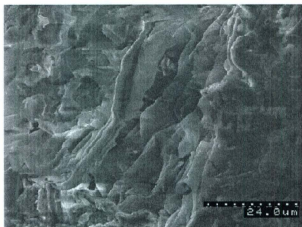
Figure 3.4b: Micrograph of saprist NL peat (Magnification X 1000)

54

The micrographs showed that pores in the fibrist peat were more distinct compared with those of the saprist peat. The microstructures of the peats showed highly inter-connected fibres with large and thick cell wall pores in the fibrist NL peat while, the saprist NL peat contained collapsed and overlapping pores. Each pore in the peat type consisted of a unique internal cellular arrangement. The pore structure in the saprist peat could be due to the compressive forces from the decomposed particles with light and fragile cell walls, while that of the fibrist peat could originate directly from the plant forming materials. Coupal and Lalancette, (1976) reported this pore structure in a fibrist peat to be cellular. Bozkhurt et al., (2001) reported that a higher decomposition (in saprist peat) reduced the pore fraction, leading to smaller particles being packed together, increasing the bulk density of the material. This is evident as the fibrist peat had the lower bulk density and moisture content, compared to the saprist peat (Table 3.2).

At higher peat decomposition level, pore sizes tended to be smaller and inseparable (powder-like) resulting in a compact peat matrix with reduced permeability, leading to higher water holding potential. The fibrist peat should therefore have a higher porosity which could be one reason why it is favoured in gardening and horticulture; but in the adsorption process, its residence time could be shorter reducing its ability to quickly trap metals from the percolating wastewater.

3.3.4 Identification of Functional Groups

The ability of a soil to hold metals is influenced by the presence of organic matter which is made of various functional groups. The identification of these functional groups

is one major step in understanding the chemistry of metal uptake by soil organic matter. Chemical compositions of peats can be identified by Fourier Transform Infra-Red (FTIR) and Nuclear Magnetic Resonance (NMR) spectrometry. The FTIR spectrometry is capable of identifying the presence of organic functional groups which can then be used in the classification of the parent material. Organic compounds such as carbohydrates, lignins, celluloses, fats and/or lipids, and proteinaceous compounds have been identified based on the vibrational characteristics of their structural bonds (Artz, et al., 2008). These techniques have been applied in the study of extracted humic fractions from various peats with variations in the functional groups reported (Niemeyer et al., 1992; Baran, 2002; Li et al., 2004; Gondar et al., 2005; Fong and Mohamed, 2007).

The FTIR microscope accessory allows spectra from a few nanograms of material to be obtained quickly, with little sample preparation and low operation cost. In some cases, thin films of residue are identified with a sensitivity that rivals or even exceeds electron or ion-beam-based surface analysis techniques. FTIR is based on the principle that some molecules absorb light in the infra-red region of the electromagnetic spectrum (Smith, 1996) with the wavelength of the absorption being a function of the bond types in the molecule (Griffiths and de Haseth, 1986). The essential components of the FTIR are shown in Figure 3.5.

Figure 3.5: Essential components of FTIR spectrophotometer

The interferometer is the unique feature of the FTIR. This component helps to superimpose the released waves from the infra red source making them easy for interpretation (Smith, 1996).

The Bruker TENSOR 27 FTIR equipped with a MIRacle ATR accessory coated with crystallized ZnSe with absorbance range from 4000 and 650 cm^{-1} was used. A few particles of each of the air dried homogenized fibrist peat of sizes 425, 250, 150 and 75 µm, and saprist peat of 850, 425, 300, 150 and 75 µm (4.75 and 2.00 mm of the fibrist peat and 4.75mm of the saprist peat were left out because they were mostly undecomposed materials) were analyzed.

Each sample from the selected particle size fractions was placed on the pressure tip, compressed onto the sampling area at the center of the ZnSe crystal plate, and was scanned for one minute in transmission mode double sided forward/backward at a spectral resolution of four wavenumbers. The equipment incorporates a KBr beam splitter which transmits ~ half of the radiation from the source, and reflects the other half through the aperture set at 6 mm through to the detector. Final spectra were obtained from the interferogram through a Fourier transform presenting a quantitative analysis.

Spectra for the various fractions of the peats were similar in profile and shape. Thus the fibrist and saprist NL peats from the same peat bog could consist of the same functional groups. The spectra in Figure 3.6 (similar for all fractions of both peat types) and the probable functional groups present in the peats are summarized in Tables 3.3 following matches with Lange's Chemistry Handbook (2005) or as otherwise indicated.
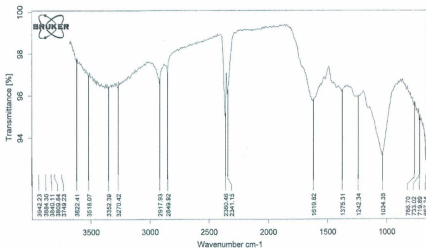
Figure 3.6: FTIR spectra of saprist or fibrist NL peats

The functional groups in the fibrist and saprist NL peats are dominated by the presence of oxygenated organic species such as carboxylic acid - RCOOH, alcoholic and phenolic hydroxyls – ROH and ethers - ROR in addition to amines – RNH_2, or R_2NH and or amides – R-CO and where R could be an aliphatic, straight chain, branched chain or heterocyclic. All these groups contain active electron sites in their primary structures and their fluctuating polarization can allow their electrons to be positioned at different locations in their structures to be shared by incoming metals deficient in electrons. Reactions involving electron movement or influenced by opposite charges may therefore govern the peat metal binding chemistry.

Table 3.3: Probable functional groups present in the saprist NL peat samples

Wavenumber (cm⁻¹)	Probable Functional Group Assigned and Band, cm⁻¹	Comparable Studies
3518	Primary amines (aliphatic) 3550-3300[a] Secondary amines 3550-3400	
3352	Normal polymeric OH stretch[1]	Niemeyer et al., 1992
3270	Ammonium ion 3300-3030 [b]	
2918	Carboxylic acids –CO₂H, OH stretching 3000-2500	Orem et al., 1996
2850	Carboxylic acids –CO₂H, OH stretching 3000-2500 Methylene (CH₂) C-H asymmetric/symmetric stretch[1]	Orem et al., 1996 Niemeyer et al., 1992
2360	Tertiary amines R₁R₂R₃NH⁺ 2700-2250	
2341	Aliphatic CN	
1620	Primary amines (aliphatic) 1650-1560[a] C=C conjugated with aromatic ring 1640-1610 α, β unsaturated carbonyl compounds 1640-1590	Orem et al., 1996
1412	Ammonium ion 1430-1390[b] Vinyl C-H in-plane bend[1]	
1375	=C(CH₃)₂ Alkane residues attached to C ≈ 1380 Nitro C-NO₂ aromatic 1380-1320 (s)[c]	Orem et al., 1996
1242	Aromatic ethers, aryl –O stretch (Φ-O-H)[1]	Artz et al., 2008
1150	Tertiary alcohol C-O stretch[1]	Niemeyer et al., 1992
1034	Hydroxyl O-H primary aliphatic alcohols 1085-1030[d] -O-CH₃ ethers - 1030 Peroxides –O-O- 1150-1030[1 e] Alkyl	Orem et al., 1996 and Artz et al., 2008
915	Silicate ion[1]	
845	Nitro C-NO₂ aromatic 865-835[c]	
825	Peroxides -O-O- 900-830[e]	
767	-CH₂- Rocking vibration	
720	Saturated CH₂ c 720	Artz et al., 2008
667	Hydroxyl O-H primary aliphatic alcohols 700-600[d]	

[1] John Coates in Encyclopaedia of Analytical Chemistry (2000)
[a] primary amine bands at 3550-3300 and 1650-1560
[b] ammonium ion bands at 3300-3030 and 1430-1390
[c] nitro C-NO₂ aromatic bands at 1380-1320 and 865-835
[d] primary aliphatic alcohols bands at 1085-1030 and 700-600
[e] peroxide bands at 1150-1030 and 900-830

Solid state ^{13}C NMR was also employed in this research to support and provide additional information on the functional groups present in the air dried NL peats. In NMR, the samples are usually placed in a magnetic field and excited through pulsations from the radio frequency input. The magnetic fields after re-alignment induce an output radio signal that generates a spectrum. Fourier analysis of the complex output produces the monitored spectrum. Several pulsations were carried out allowing for the identification of signals from background noise (Teng, 2005).

Solid state ^{13}C NMR of the peats from a size fraction of ≤ 425 µm was undertaken to identify dominant functional groups. This was done partly because fractions ≤ 425 µm were selected for use in the Ni and Co uptakes experiments. The spectra were obtained at 298 K using a Bruker Avance II 600 spectrometer, equipped with an SB Bruker 3.2 mm MAS triple-tuned probe operating at 600.33 MHz for 1 h and 150.97 MHz for ^{13}C. Chemical shifts are referenced to tetramethylsilane (TMS) using adamantane as an intermediate standard for ^{13}C. The samples were spun at 20 kHz for the ^{13}C NMR spectra. Cross-polarization spectra were collected with a Hartmann-Hahn match at 62.5 kHz and 100 kHz with 1h decoupling. The recycle delay was 2 s and the contact time was 2000 ms.

The spectra obtained were similar for both the saprist and fibrist NL peats. Figure 3.7 was one of the spectra and a summary of the identified functional groups are given in Table 3.4; these are similar to the functional groups identified with the FTIR. In NMR, functional groups are identified based on their chemical shift δ (ppm) range defined by equation 3.3 (Duer, 2004).

$$Chemical\ shift\ (\delta) = \frac{frequency\ of\ signal - frequency\ of\ reference}{Spectrometer\ frequency} \tag{3.3}$$
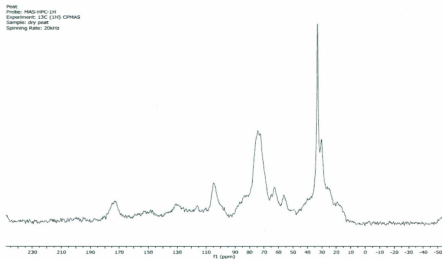
Figure 3.7: ^{13}C NMR Spectra of a fibrist or saprist NL peat

Table 3.4: Probable functional groups in fibrist and Saprist NL peats from ^{13}C NMR

Chemical shift range δ (ppm)	Probable functional groups	Similar Studies
18.05 – 40.06	CH$_3$ (in long polymeric chains)	Preston et al., (1989), Baldrock et al., (1992), Mao et al., (2000).
56.28 – 84.15	Amine Carbon, Alcohol, ethers, methoxyl	Preston et al., (1989), Baldrock et al., (1992), Mao et al., (2000), Almendros et al., (2003).
100.37 – 129.43	Phenol, N-substituted aromatic	Preston et al., (1989), Mao et al., (2000).
150.78 – 173.38	Carboxyl, amide, esters	Preston et al., (1989), Mao et al., (2000), Almendros et al., (2003).

From Figure 3.7 and Table 3.4, the ^{13}C NMR spectrometry provided further insights to the functional groups present in the saprist NL peat. These functional groups included the carboxyl, amide, esters, phenol, alcohols and ethers. The presence of long chain polymeric methylene (- CH_2 -) was also detected.

While the FTIR spectrometry can be employed independent of the ^{13}C NMR spectrometry, and vice versa, the combination of the two analytical tools have given a clearer functional groups analysis of the saprist and fibrist NL peat as the results summarized in Tables 3.3 and 3.4 corroborated each other. The two techniques also have the added advantage of being non-destructive and peat samples can therefore be reused. The two techniques showed that peats from the same bog are likely to consist of the same functional groups but in different proportions depending on the degree of decomposition.

Functional groups such as carboxyls, phenols, amines and amides are known to react with metals and have been identified to be present in the saprist NL peat. Therefore, Ni and Co uptakes by this peat would be influenced by the availability and ease of accessibility of the functional groups by the metal ions when the peat is used as an adsorbent.

The presence of amine and amide groups in the NL peats could be a reason why these peats (especially the fibrist peat) are mostly employed in gardening in Canada and the US rather than heating as obtained in Europe especially in Ireland and Finland.

3.3.5 Peat Metallic Content

Inductively coupled plasma mass spectrometry (ICP-MS) is a simultaneous multi-element and the fastest growing trace element detection and evaluation technique. The major components of most designs are the nebulizer, spray chamber, plasma torch, (used to generate positively charged ions rather than photons) and detector. Ions produced are directed towards the mass spectrometer via an interface which is a vacuum maintained at a pressure of 267 Nm^{-2} (~ 2 Torr) considered also as the most important part of the ICP-MS (Thomas, 2004).

With the ICP-MS technique, the virgin peats were destroyed to release the metals present in them. In this research, the air-dried homogenized saprist and fibrist peats were each crushed in a mortar, acidified with 14.55 N HF and 8N HNO_3 and left on a hot plate for several days until completely digested. 6N HCl and 8N HNO_3 were then added to dissolve the samples further. Finally 8N HNO_3 was added and diluted with nano-pure water according to the rock dissolution procedure used in the Earth Science department at MUN the samples were finally analyzed with a model ELAN DRC-2 ICP-MS.

Two random samples of the fibrist and saprist peats from the peat bog were analyzed and the instrument took duplicate readings for each samples with average of the duplicate for each sample reported. The metal concentrations in each peat sample are presented in Table 3.5. Some metals were detected at concentrations below 1 mg/kg and included As, Ni, and Pb. The presence of these metals could be due to both natural and anthropogenic sources; the results however show that these peat soils have a natural affinity for the detected metals with calcium and iron being the predominant metals.

Table 3.5: ICP-MS results of NL peats

Metal	Concentration (mg/g)	
	Fibrist Peat	**Saprist Peat**
Ca	2743	2392
^{54}Fe	971	1012
Ti	98	34
Zn	88	15
Sn	8	8
Mn	27	7
^{52}Cr	ND[a]	4
Ni	0.7	4
Cu	0.3	2
^{77}Se	ND[a]	1

[a] not detected

From Table 3.5, the fibrist NL peat had more Ca, Ti, Zn and Mn and less of Ni and Cu compared to the saprist NL peat. The saprist NL peat had more Fe compared with the fibrist NL peat. An equal amount of Sn was detected in both peat types with no ^{52}Cr and ^{77}Se in the fibrist peat. It is however interesting to note that more Ni was detected in the saprist peat compared to the fibrist peat while no Co was detected in either peat types. The detection and proportions of the metals could be related to the location of the peat bed within the peat bog, the characteristics of the parent forming plants, microbial activities and the bog surrounding soils characteristics.

3.4 Chapter Summary

Fibrist and Saprist Peats from a Newfoundland peat bog were characterized and compared where possible, using analytical techniques that are mainly non-destructive (except in the determination of the ash content and the metallic content by ICP-MS) to determine the physico-chemical properties, and surface morphology and identify functional groups in the peat material. The characterization study showed that the saprist peat was denser, and finer, and had a larger organic and moisture content, and CEC compared with the fibrist peat. The surface morphological study showed that the fibrist peat had more identifiable pores while the saprist peat had collapsed and overlapped pores that were not easily identified. FTIR and ^{13}C NMR studies showed that the two peats contained similar functional groups. Metallic content analysis of the virgin peats showed that the fibrist peat had larger Ca, Ti, Zn and Mn contents while the saprist peat had larger Fe, Ni, and Cu contents.

CHAPTER FOUR

EXPERIMENTAL METHODS USING SAPRIST PEAT AS ADSORBENT

4.1 Chapter Overview

Adsorption is influenced by many factors such as solution pH, concentration of contaminants, method of contact of the adsorbent with the contaminant, residence or holding time of the adsorbent, quantity of adsorbent, adsorbent surface area and others (Ruthven, 1984; Al-Duri, 1995; Cooney, 1999; Yong, 2001). The evaluation of the impact of these factors has usually been done on a one-factor basis. This involves the determination of values of a parameter on the adsorbed quantity with all other factors constant. However, the complexity of industrial wastewaters and the interplay of factors are such that this simple approach might be inadequate.

This chapter reports on the materials and the batch and column experiments conducted using the saprist NL peat as an adsorbent. This peat type was selected because it was the adsorbent of interest from the physico-chemical analysis reported in Chapter Three of this study; it was nearly a homogeneous material which can provide added understanding to the metal uptake chemistry. The conditions of the experiments were based on the response surface method using the Box-Behnken design after screening of the factors. The kinetic experiments and the adsorption isotherm studies were then based on the significant factors determined from the Box-Behnken design of the experiment.

4.2 Materials

The test adsorbent used was the untreated air dried highly humified or saprist NL peat with particle size fractions ≤ 425 µm which had been kept in sealed dry plastic containers after the dry granulometry and characterization studies. Saprist peat particle size fractions > 425 µm were not used because these fractions contained large proportions of undecomposed materials.

The stock adsorbates used in the study were prepared from analytical grade nitrate hexahydrates $M(NO_3)_2.6H_2O$ (M is either Ni or Co) supplied by Anachemia Chemicals, Canada. The solutions' pHs were adjusted by the addition of 0.25 M sulphuric acid from Anachemia Chemicals, to lower the pH or a pH 10 solution containing potassium carbonate-potassium borate-potassium hydroxide buffer 0.05M from Fischer Scientific, Canada to increase the solution pH. The pH was measured with an ATI Orion model 3000 VWR brand pH/mV/temperature meter from VWR Scientific, Canada.

4.3 Methods

The research consisted of:

1. <u>Design of experiment</u>: To simultaneously evaluate the reaction conditions that could influence metal adsorption efficiency;

2. <u>Kinetic study</u>: To establish metal adsorption reactions order and equilibrium rates;

3. <u>Batch study</u>: To determine sorption parameters through the use of established adsorption isotherms;

4. <u>Desorption study</u>: To investigate and evaluate the degree of metal desorption on the adsorbent; and

5. <u>Fixed bed column study</u>: To determine the breakthrough, the active mass transfer zone and the bed Ni and Co sorption capacities.

4.3.1 Response Surface Design – Box Behnken Design

Six reaction factors, namely, initial metal concentration, stock solution pH, time of contact, agitation level, peat dose, and peat particle size were investigated in a screening step using batch tests with a two-level full factorial design with two replicates and two mid-points. The factors were designated as low (-), mid-point (0) and high (+). Stock metal solutions of 50, 125 and 200 mg/L were prepared and solution pHs adjusted to 3, 6.5 and 10. Air dried saprist peat of masses 0.08, 0.84 and 1.6 g of particle sizes $\leq$ 425 µm, > 850 µm and the thoroughly mixed fractions ($\leq$ 425 to > 850 µm) were weighed on an analytical balance into plastic serum bottles to which 40 mL of prepared metal solutions of 50, 125 and 200 mg/L were added, before being capped and thoroughly shaken.

The bottles were agitated on a 5900 Eberbach reciprocal shaker bed at low (45 rpm) and high (80 rpm) levels for 12, 18 and 24 hours. At the end of the selected times, samples were removed from the shaker bed, allowed to settle and filtered with 45 µm quantitative filter paper from Anachemia Chemicals, Canada. The filtrates were acidified with a drop of 0.25 M sulphuric acid and stored in sample bottles kept in a dark cupboard for analysis of the metal content. The storage environment was to first, inhibit the actions

of any photo–sensitive bacteria and also to prevent possible precipitation of metals in the solution prior to analysis.

Since the screening experiment determined that agitation level and peat particle size were insignificant, the experimental procedure was repeated for the Box-Behnken response surface design with only four significant factors (because they had larger percentage contribution, > 10%), viz, initial metal concentration, stock solutions pH, peat dose and contact time.

4.3.2 Kinetic Experiments

Kinetic tests of Ni and Co adsorption conducted in triplicate were carried out in 50 mL plastic serum bottles containing 0.08, 0.16, 0.84 and 1.6 g air dried saprist peat of particle sizes ≤ 425 µm and 40 mL of 25, 50, 125 and 200 mg/L of Ni or Co stock solutions adjusted to pHs of 3, 5.5, 8 or 10 (pHs 5.5, 8 and 10 were buffered). The serum bottles were quickly capped and thoroughly shaken.

The capped bottles were agitated on the 5900 Eberbach reciprocal shaker bed at a low speed of 45 rpm. At 0.5, 1.0, 1.5, 2.0, 3.0, 4.0, 5.0, 6.0, 8.0, 10, and 12 h periods, serum bottles were removed from the shaker bed. Samples were filtered with 45 µm quantitative filter paper from Anachemia Chemicals, Canada. The filtrates were acidified with a drop of 0.5 M sulphuric acid, labelled and stored in sample bottles kept in a dark cupboard for analysis of the Ni or Co content. Two blank experiments were carried out to estimate the effects, if any, of the serum bottle and the filter paper on Ni and Co sorption

and also to determine if there was any significant Ni (no Co in the virgin peat) elution from the saprist NL peat.

4.3.3 Batch Equilibrium Experiments

These tests were conducted in 50 mL plastic serum bottles which contained 0.08, 0.16, 0.84 and 1.6 g of air dried saprist peat of particle size fraction ≤ 425 µm. Stock metal solutions of Ni or Co concentrations of 12.5, 25, 50, 125 and 200 mg/L, adjusted to the desired pHs of 3, 5.5, 8 and 10, were added to the bottles, and the bottles were capped and thoroughly shaken.

The capped bottles were agitated on the 5900 Eberbach reciprocal shaker bed at 45 rpm for 24 h. The agitation time of 24 h was considered adequate for equilibrium based on the kinetics data and also, it is generally the duration in most equilibrium studies (Ho et al., 1995; Ho and McKay, 1999; Ringqvist et al., 2002; Kalymkova et al., 2008). Serum bottles' contents were filtered with 45 µm quantitative filter paper from Anachemia Chemicals, Canada. The filtrates were acidified with a drop of 0.25 M sulphuric acid, labelled and stored in sample bottles kept in a dark cupboard for analysis of the Ni or Co contents.

Competitive sorption on the NL saprist peat was investigated by preparing 200, 100, 50, 25 and 12.5 mg/L equal mass solutions of Cd, Co, Ni, Pb and Zn using the chloride of each metal supplied by Anachemia Chemicals, Canada. The solutions were pH adjusted to 5.5 by adding a few drops of 0.25 M sulphuric acid. 0.08, 0.16, 0.84 and 1.6 g of air dried saprist peat were weighed into serum bottles and 40 mL of the solutions

added. Bottles were capped and thoroughly shaken on the 5900 Eberbach reciprocal shaker bed at 45 rpm for 24 h. Filtration and determination of filtrates concentrations were carried out as with the single ion system.

4.3.4 Desorption Study

After each batch adsorption test was concluded, the peat-metal material on the filter paper was gently washed off into a 100 mL conical flask with ~ 25 mL of water. The flask was well shaken and the contents divided into 5 other 100 mL conical flasks. Each flask containing ~ 5 mL of peat-metal solution was treated by adding 40 mL of 0.1, 0.2, 0.5, 1, and 2 M HCl. Each mixture was thoroughly shaken and allowed to settle for 2 h. Each mixture was decanted and the Ni and Co concentrations present were analyzed.

4.3.5 Fixed Bed Column Experiments

Vertical, downward flowing fixed bed column experiments were carried out in fabricated Plexiglass columns 14 cm long, 6 cm internal diameter and at room temperature. A constant 1 L- head aspirator bottle was used as the solution tank and was repeatedly filled with the metal stock solutions. A variable speed peristaltic pump with flow rate between 250 mL/h and 2500 mL/h was used to suck out water at the column exit (see the schematic and experimental set up in Figures 4.1a and 4.1b).

The columns were charged with 110 g of air dried NL saprist peat of fraction $\leq$ 425 μm. Ceramic plates of pore size 60 microns and thickness of 0.5 cm were placed at

the top and the bottom of the column to prevent migration of the peat particles. This gave an effective peat depth of 12.5 cm which was later subdivided into 7 sections of approx. 2 cm depth. Two blank fixed bed column experiments were carried out: 1) without peat to investigate the effect of the Plexiglass material and ceramic plates on Ni and Co sorption; and 2) with peat but with no metal in the influent to investigate if there was any significant elution of the initial Ni in the peat into the effluent. The fixed bed column experiments were conducted in duplicate for Ni and Co single metal systems and for the blank tests.

Metal stock solutions at a concentration 100 mg/L, adjusted to a 5.5 pH, were fed to the top of the column and the pump speed adjusted such that 1 L or 2 L of the metal solution passed through the bed in 1 h which gave an equivalent flow rate of 1.0 L/h and 2.0 L/h with an approximate residence or holding time of 3 and 1.5 minutes within the peat fixed bed. Effluent from the column was collected at the end of each 1 L volume of treated solution, acidified with a drop of 0.25 M sulphuric acid, labelled and stored in a sample bottle kept in the dark for analysis of the metal concentration.

At breakthrough, the column set up was dismantled and ~ 0.5 cm of the top layer of each of the seven marked zones was collected for metal analysis. The columns were marked from the top to the bottom with tiny flexi plastics placed inside the packed peat beds for identification. From the single ion-fixed bed column results, the top layer (~0.5 cm) of each zone of the spent saprist peat was collected into a 100 mL beaker sealed for ICP-MS analysis to determine the Ni and Co accumulation on the selected layers and the distribution of the metals along the column depth.
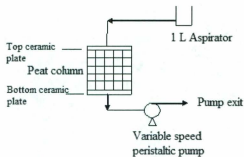
Fig 4.1a: Schematic diagram of the saprist NL peat column set up
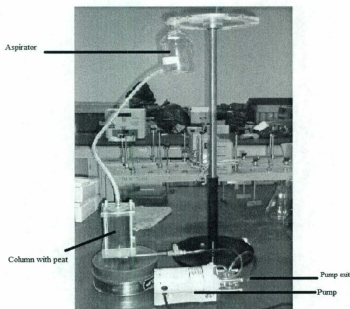
Fig. 4.1b: Fixed bed column set up as conducted

4.4 Analysis of Metal Concentrations

Residual metal concentrations in the acidified and stored samples from the batch and column tests were analyzed using a Varian SpectrAA-55 flame atomic absorption spectrometer and an air-acetylene flame. The spectrometer was operated at a slit width of 2 nm, a lamp current of 4 A for Ni or 7 A for Co, an air flow of pressure of approx. 60 psi and an acetylene flow pressure of ~ 76 KNm^{-2} (11 psi). For measurement of the Ni concentration, the wavelength of the lamp was set at 232 nm while for Co, it was 240.7 nm. Reported values of the metals were based on calibration of standard solutions (usually between 100 – 1.75 mg/L) which were usually made before any analysis was undertaken.

A blank solution was aspirated. This was to set to zero to stabilize the equipment. The equipment was then calibrated at the appropriate range of the metal solutions. The metal samples were then aspirated and the READ button pressed to read off the mean absorbance value of the samples given at a maximum of 3 % relative standard deviation (RSD) with any value > 3% RSD rejected and the run repeated.

Tests conducted, results obtained and the subsequent analyses are presented in subsequent chapters (five, six and seven).

CHAPTER FIVE

BOX – BEHNKEN DESIGN, KINETIC RESULTS AND DISCUSSION

5.1 Chapter Overview

This chapter presents all the results obtained from the Box-Behnken design and kinetic experiments carried out during the research. Metal concentrations in treated effluents were analysed by Flame Atomic Absorption Spectrometer (FAAS) using a varian model SpectrAA 55 atomic spectrometer available at the MUN Chemistry department, and reported as percent metal removed or adsorbed quantity of metal in the saprist NL peat. Results from the blank samples were also analyzed to check the stability of the experiment and the consistency of the FAAS equipment. The trends observed for each experiment and discussions of the probable Ni and Co uptake mechanisms through analysis of the data are reported.

5.2 Response Surface Method (Box – Behnken Design)

The Box - Behnken surface response design with four factors was selected for the design after the two-level factorial screening experiments showed that the particle size and agitation levels were statistically insignificant in determining metal adsorbed by the saprist NL peat at a 5% confidence level. The percent metal removed was also noted to be non-linear thus the model obtained from the factorial design would not be adequate. This necessitated the use of a second order response surface method employing the Box-

Behnken design that excluded the particle size and the level of agitation. The four factors investigated and their levels during the experiment are summarized in Table 5.1

Table 5.1: Independent factors, units and levels for the Box-Behnken design

Factor (treatment)	Units	Levels		
		Low (-1)	Mid (0)	High (+1)
Metal concentration	mg/L	50	125	200
Peat dose	g/L	2	21	40
Time of contact	h	12	18	24
pH	-	3	6.5	10

The percent of metal adsorbed on the NL saprist peat was fitted to a second-order polynomial function given by equation 5.1,

$$Y_{z,s} = \beta_o + \sum_i \beta_i Z_i + \sum_i B_{ii} Z_{ii}^2 + \sum_{i<j} B_{ij} Z_i Z_j + \varepsilon_{z,s} \quad (5.1)$$

where Y was the percent metal adsorbed, Z was the factor, β_i, was the linear effect, β_{ii} was the quadratic effect, β_{ij} was the interaction effect or cross product effect between ith and jth factors, and ε was the random error or noise.

The Box-Behnken response surface design input and response (metal removed, %) was as shown in Table 5.2 where metal sorbed in % was defined by equation 5.2. The analysis of variance (ANOVA) was then used to obtain the polynomial second order predictive model for the removal of Ni or Co by the saprist NL peat.

$$Metal\ sorbed,\ \% = \left(1 - \frac{C_{effluent}}{C_{initial}}\right)100 \qquad (5.2)$$

Table 5.2: Box-Behnken design with 3 levels and 4 variables

Run No.	Coded Factors				Metal Removed, %	
	Metal Conc. (mg/L).	Peat dose (g/L)	Time (hr)	pH	Co	Ni
1	50	2	18	6.5	45	98.04
2	200	2	18	6.5	30	58.7
3	50	40	18	6.5	93.8	98.8
4	200	40	18	6.5	84.6	99.6
5	125	21	12	3	77.2	93
6	125	21	24	3	78.7	94.4
7	125	21	12	10	94.6	23.7
8	125	21	24	10	94.8	26.2
9	50	21	18	3	86.4	94
10	200	21	18	3	73.6	79.7
11	50	21	18	10	96.2	32.8
12	200	21	18	10	93.5	23.4
13	125	2	12	6.5	36.3	69.9
14	125	40	12	6.5	87.9	99.6
15	125	2	24	6.5	33.4	70.8
16	125	40	24	6.5	88.9	83.6
17	50	21	12	6.5	89.6	95.5
18	200	21	12	6.5	78.8	80.5
19	50	21	24	6.5	90.4	96.1
20	200	21	24	6.5	74	87.3
21	125	2	18	3	33.1	31.7
22	125	40	18	3	87.3	97.3
23	125	2	18	10	54.9	17.5
24	125	40	18	10	95.7	30.4
25	125	21	18	6.5	81.3	78.8
26	125	21	18	6.5	78.6	88.9
27	125	21	18	6.5	80.7	91.4
28	125	21	18	6.5	80.2	90.2
29	125	21	18	6.5	79.4	99.7

The number of experimental runs was obtained from equation 5.3 as,

$$Number\ of\ runs = \binom{k}{2} \times 2^2 + n_c \qquad (5.3)$$

where k was the number of factors (4 in this experiment) and n_c was the center point (5 was chosen in this experiment). The term 2^2 is from the two-level factorial on which Box-Behnken design is based (Myers and Montgomery, 2002). With 4 factors, the design is exactly rotatable (Box-Behnken designs are generally not rotatable except with 4 and 7 factors) (Myers and Montgomery, 2002; Box et al., 2005). The choice of 5 center points was to approach a stable design which is generally rotatable. In rotatable design, the variance of the predicted response is constant at all points that are equidistant from the center of the design (imagine the design to be a cube) (Box et al., 2005).

The predictive model equations were developed after satisfying the necessary statistical conditions. These were: 1) normal probability plot of the studentized residuals to check for normality of residuals; 2) studentized residuals versus predicted values to check for constant error; 3) externally studentized residuals to look for outliers or influential values; and 4) suggestions for any transformations.

From the ANOVA, the models obtained were significant for the selected factors that had Prob > F values (test for comparing lack of fit variance with pure error variance) less than 0.05. The Adjusted R-squared being 0.9911 and Predicted R-Squared as 0.9811 for the % Co sorbed and for the % Ni sorbed, Adjusted R-squared was 0.9242 and the Predicted R-squared was 0.8217. The Adjusted and Predicted R-squared values were within 0.2 of each other which is the acceptable margin. The detailed ANOVA results for Ni and Co uptake by saprist NL peat are presented in Appendices B1 and B2.

Equations 5.4 and 5.5 given below are the predictive model equations for Co and Ni respectively and provided the solutions and values to the coefficients in equation 5.1 with A as the metal concentration, B as the peat dose, C as the time of contact and D as the pH of the metal solution. AB was the interaction between the metal concentration and the peat dose, AD was the interaction between the metal concentration and the pH, and BD was the interaction between the peat dose and the pH.

$$Co\ sorbed, \% = +80.44 - 5.58A + 25.46B + 7.78D + 2.53AD - 3.35BD \\ + 1.91A^2 - 18.72B^2 + 5.67D^2$$ (5.4)

$$Ni\ sorbed, \% = +91.50 - 7.17A + 13.55B - 28.01D + 10.03AB - 13.18BD \\ - 8.51B^2 - 34.99D^2$$ (5.5)

The interaction plots between peat dose/Ni concentration, and pH/peat dose for Ni sorption are depicted in Figures 5.1a and 5.1b, while, the optimum conditions for these interactions are shown in Figures 5.2a and 5.2b.

(a)

(b)
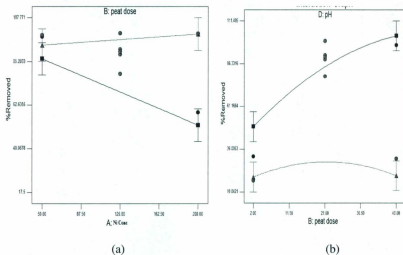
Figure 5.1: Interaction of factors on % Ni sorbed (a) peat dose (g/L) and Ni ion concentration (mg/L) and (b) peat dose (g/L) and pH (red and black are the low and high values while green is the mid-point for the factors).
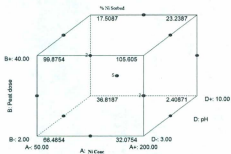
Figure 5.1c: Cubic plot of the Box-Behnken design for the sorption of Ni^{2+} (red is the mid-point of the factors)

Figure 5.1a shows that a large % of Ni was removed at low Ni concentration (50 mg/L) and a large peat dose (40 g/L), while Figure 5.1b shows that a large of % Ni was

removed at low solution pH (3) and at large peat dose (40 g/L). Figure 5.1c is the cubic representation of the Box-Behnken design for the sorption of Ni^{2+} on the saprist NL peat.

Ni concentration/peat dose interaction was one of the interactions observed for Ni uptake. At 2 g/L peat dose, an increase in Ni concentration decreased percent Ni removed from the solution from 66 to 32% (see Figure 5.1c). This was because more Ni ions were available as the concentration was increased without a corresponding increase of available active sites. It has been reported that the water held by the peat matrix is not thermodynamically bound to the peat but by capillary forces that exist between the water molecules and the peat matrix (Forsberg and Aldén, 1989); thus metal ions diffusion due to concentration could determine the uptake of metals. At higher Ni concentrations, there existed a diffusion gradient which could have led to the binding of the kinetically energized Ni ions in the solution. Since the corresponding sites for complexation have not been increased, less of the highly energized Ni ions were adsorbed at high concentration of 200 mg/L.

On the other hand, at a low concentration, the increased peat dose increased the percent Ni uptake from 66 to 99% (see Figure 5.1c) because more than enough active sites were available and the metal ions could bind with the nearest sites with less energy requirements. At a large peat dose, an increased Ni concentration increased the percent Ni sorbed from 99 to almost 100 (see Figure 5.1c) which could be partly due to the mobility of the ions, and the corresponding increase in the active sites on the saprist NL peat that provided binding sites.

From the cubic plot of Figure 5.1c, the percent Ni uptake decreased from 66 to 37 at a 2g/L peat dose when pH was increased from 3 to 10. At peat dose of 40 g/L, the percent Ni uptake decreased from 100 to 18% as pH was increased from 3 to 10. When pH was increased from 3 to 10, the percent Ni uptake decreased from 37 to 2% at a peat dose of 2 g/L.

As the peat dose was increased, the available active sites were increased thus binding was increased. But as pH was simultaneously increased especially above pH of 7, more hydroxyl ions become available in the system which may have resulted in the formation of metal hydroxides. The continuous dissociation of the Ni hydroxide could have created a local repulsive environment between the negatively charged active sites and the hydroxyl ions. Generally, a double layer is formed on a surface because electrons are beyond the limits of the lattice formed by the positive ions. When this metal layer comes in contact with a negatively charged adsorbent layer, the layer is thickened lowering the migration of the positively charged ions to the surface of the adsorbent (Sparks, 2003). The thickening of the diffuse double layer at larger peat dose and pH could have contributed to the reduced percent Ni uptake at basic pH (above pH 7). The strength of the interference of the repulsion from the diffuse double layer within the peat matrix could also depend on the stability of the Ni hydroxide that was formed. At a higher peat dose of 40 g/L (larger coverage of the diffuse double layer), and pH of 10 (more hydroxyls), the repulsive forces could have accounted for the reduced uptake of Ni as observed at an increased pH and peat dose.

In solution, chelation effect is observed when there is a preferential formation of a chelate complex (MX) where the metal ion M coexists with the polydentate ligand X (ligand with multiple donor sites) and the monodentate ligand L (ligand with single donor site) whose concentration should be equivalent to that of X in relation to the donor atom (Frausto da Silva, 1983). At a lower pH of 3, a high percent Ni uptake was reported because the chelation effect could have been pronounced. According to Crist et al., (1996) the chelation effect could release protons (H^+) from a carboxylic acid group when a divalent metal ion binds to an adjacent phenolic OH or an adjacent carboxylic acid as shown in equation 5.6. Large chelation effects, where they exist, are known to occur at lower values of pH (Frausto da Silva, 1983).

$$(5.6)$$
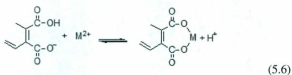
One of the goals of this study was to achieve a high percent Ni or Co uptake at a reduced quantity of the saprist NL peat consumed. It was therefore necessary to optimize the uptake conditions as represented by the significant factors that influenced the percent Ni or Co uptake. If minimum peat dose is the desired goal for an optimum % Ni removal, using the multiple response optimization approach, the optimization tool in the software, Design-Expert® 8.04 (Stat-Ease, Inc,), could be used to predict the experimental conditions needed. Table 5.3 summarizes the results of the optimum % Ni removed for two scenarios using Design-Expert® 8.04.

Table 5.3: Summary of % Ni removed for two optimization cases

Case	Constraints	Goal	Lower Limit	Upper Limit	Solutions
1	Conc. (mg/L)	in range	50	200	~100 % Ni removed at Ni
	Peat dose (g/L)	minimize	2	40	conc. of 50 mg/L, peat
	pH	in range	4.5	6.5	dose of 14 g/L and pH 5.3
2	Conc. (mg/L)	maximize	50	200	~ 100 % Ni removed at Ni
	Peat dose (g/L)	minimize	2	40	conc. of 200 mg/L, peat
	pH	in range	4.5	6.5	dose of 28 g/L and pH 4.9

In Table 5.3, the pH range for the two cases was set between 4.5 and 6.5 because mining wastewaters are generally known to be acidic (Dickerson and Brooks, 1950; Drury, 1999) with pH values within the given range. The optimization results suggested that a minimum peat dose of 28 g/L was required for the maximum sorption (~100%) of Ni at the initial Ni concentration of 200 mg/L and pH 4.9. On the other hand, a minimum peat dose of 14 g/L was required if the initial Ni concentration is minimized (50 mg/L) at a pH of 5.3.

For Co uptake, the interactions between pH/Co concentration and pH/peat dose are depicted by Figures 5.2a and 5.2b.

(a)   (b)
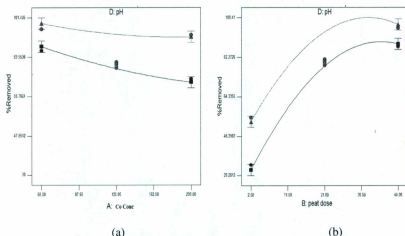
Figures 5.2: Interaction of factors on % Co sorbed (a) pH and Co ion concentration (mg/L), and (b) peat dose (g/L) and pH (red and black are the low and high values while green is the mid-point for the factors).
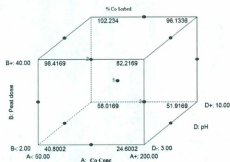
Figure 5.2c: Cubic plot of the Box-Behnken design for the sorption of Co^{2+} (red is the mid-point of the factors)

Figure 5.2a showed that high % Co removal was achieved at low Co concentration (50 mg/L) and low solution pH (3). Figure 5.2b showed that high % Co was removed at

high peat dose (32 g/L) and high solution pH (10). Figure 5.2c shows the cubic plot of the Box-Behnken design for Co^{2+} sorption on the saprist NL peat.

As indicated in Figure 5.2(a), Co concentration/pH interaction was one of the interactions observed for Co uptake on the saprist NL peat. At a low Co concentration (50 mg/L), the percent Co sorbed increased from 41 to 58 as pH was increased from 3 to 10 (see Figure 5.2c). This could be due to chemistry of the uptake. In solution, a double layer exists between the surface of the solid and the bulk solution due to the action of charges of the ions in solution and on the solid surface. The thickness of this layer is dependent on the concentration of ions in the solutions and increase in the solution pH could have nullified the increase in the thickness of the diffuse double layer around the peat surface due to increase in the concentration of Co. Increase in Co concentration to 200 mg/L led to increase in Co sorption from 25 to 52% as the pH was increase from 3 to 10.

As indicated in Figure 5.2(b), the second interaction observed was peat dose / pH, and at low peat dose, the percent Co retained increased from 25 to 52% as pH was increased from 3 to 10 (see Figure 5.2c). At the low peat dose, Co tends to actively occupy the available active sites even as pH was increased because Co uptake could be through complexation at pH of 3 and this changed to ion exchange at pH of 10. At pH of 3, the percent Co retained increased from 41 to 98% as peat dose increased from 2 to 40 g/L (see Figure 5.2c). This is because more active sites were made available and complexation of the Co with the functional groups on the saprist NL peat could have been rapid.

Co uptake according to equation 5.4 was optimized for two cases of experimental conditions using Design-Expert® 8.04 and the results are summarized in Table 5.4. The optimization results could provide additional operational information when using the saprist NL peat as a Co adsorbent.

Table 5.4: Summary of % Co removed for two optimization cases

Case	Constraints	Goal	Lower Limit	Upper Limit	Solutions
1	Conc. (mg/L)	in range	50	200	~94 % Co removed at Co
	Peat dose (g/L)	minimize	2	40	conc. of 50 mg/L, peat
	pH	in range	4.5	6.5	dose of 27 g/L and pH 6.5
2	Conc. (mg/L)	maximize	50	200	~ 90 % Co removed at Co
	Peat dose (g/L)	minimize	2	40	conc. of 104 mg/L, peat
	pH	in range	4.5	6.5	dose of 30 g/L and pH 6.5

Table 5.4 shows that an optimum % (~94) of Co could be sorbed at a minimum peat dose of ~27 g/L and at a Co concentration of 50 g/L and a pH of 6.5. If a maximum Co concentration within the range used in the experiment was desired, a minimum peat dose of ~ 30 g/L would be required at a maximum Co concentration of 104 mg/L at pH 6.5.

Co and Ni are members of the d- block of the transition elements. The chemistry of the d- block elements are influenced by the valence electron and some other electronic parameters. Some selected Co and Ni basic chemical data are as summarized in Table 5.5.

Table 5.5: Some selected basic chemical data for Co and Ni

Chemical data	Co	Ni
Valence electron	$[Ar]\,d^7 s^2$	$[Ar]\,d^8 s^2$
First Ionization energy, kJ/mol	758	737
Atomic radius, pm	116	115
*Ionic radius (M^{2+}), nm	75	69
Electron gain energy E^a, kJ/mol	-64	-112
*Hydration energy, kJ/mol	-2051	-2134
Electronegativity, χ_b	1.9	1.9

Sources: Jones (2001) and *Barrett (2003)

where [Ar] is the electronic configuration of argon ($1s^2\,2s^2\,2p^6\,3s^2\,3p^6$)

For the Ni and Co sorption by the saprist NL peat, hydrolysis of the metal ions played a significant role leading to the interactions discussed. Hydrolysis of metal ions can be considered in two steps as shown in equations 5.7. and 5.8.

$$M^{2+} + H_2O \Leftrightarrow MOH^+ + H^+ \qquad (5.7)$$

$$MOH^+ + H_2O \Leftrightarrow M(OH)_2 + H^+ \qquad (5.8)$$
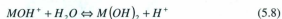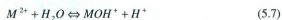
The overall reaction can be represented by equation 5.9.

$$M^{2+} + 2H_2O \Leftrightarrow M(OH)_2 + 2H^+ \qquad (5.9)$$
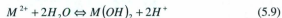
Metal ions that are easily hydrated will be least adsorbed. The ease of hydration of a metal ion could be obtained from the hydration energy. Co has a slightly lower hydration energy compared to Ni and is therefore expected to be the more adsorbed metal

because lower heat of hydration favours easy bond formation. Co also has a larger atomic and ionic radii compared to Ni which could favour electron sharing with electron donors leading to more adsorption. This however was not the case suggesting that uptake mechanisms of the two metals were affected by the interactions between some of the experimental factors.

For the purpose of this research, the author has defined adsorption as either a physical or chemical phenomenon. The physical adsorption or physisorption occurs with less interaction between the cation and the peat matrix and is mainly due to the weak forces of attraction between the negatively charged peat surface and the positively charged cation. In chemical adsorption or chemisorption, exchange of electrons is involved and this can be through ion exchange or a complexation reaction between the cation deficient in electron and the ligands with the exchangeable proton (H^+) or functional groups capable of donating electrons for sharing. Similarly, removal, retention, uptake, and sorption are all words used by the author in this study to refer to adsorption of Ni or Co by the saprist NL peat.

5.4 Results and Discussion of the Kinetic Study

The kinetic study of the Ni and Co uptake on the saprist NL peat was discussed in terms of the time taken to attain equilibrium and fitting of the adsorption data to the pseudo-second order kinetic model with the determination of the kinetic constants.

5.4.1 Equilibrium Time for Kinetic Study

The time taken to attain equilibrium at the various experimental combinations is summarized in Table 5.6 while the kinetic data obtained for the Co or Ni uptake are presented in Appendixes C and D.

Table 5.6: Time (h) to attain equilibrium during kinetic study of Ni^{2+} and Co^{2+} uptake

pH	Metal Conc. (mg/L)	Peat dose (g/L)							
		2		10		21		40	
		Ni	Co	Ni	Co	Ni	Co	Ni	Co
3	25	8	6	10	2	5	2	3	1.5
	50	8	1.5	6	1	6	1	4	1.5
	125	10	-	8	1	6	1	5	1
	200	6	-	5	-	8	1	8	1
5.5	25	6	1.5	2	1.5	2	1	1	1
	50	5	1.5	5	1.5	4	1	3	1
	125	8	8	12	2	6	1	3	1
	200	10	-	6	-	8	1	4	1
8	25	6	1.5	3	1.5	1.5	1	3	3
	50	4	1.5	12	1.5	1.5	5	5	4
	125	8	1	5	12	4	12	2	4
	200	8	1	8	1	5	1	3	5
10	25	3	4	1	3	4	2	3	1.5
	50	5	2	4	4	3	3	1.5	1
	125	10	2	6	5	4	4	3	10
	200	10	1.5	8	6	5	5	6	1

[-] indicates no experimental result

From Table 5.6, the shortest Ni removal equilibrium time was 1.0 h at a pH of 10, Ni concentration of 25 mg/L and a peat dose 10 g/L, and at pH of 5.5, Ni concentration of 25 mg/L and at a peat dose of 40 g/L. For Co, the lowest recorded equilibration time was 1 h at all peat doses though this short equilibration time occurred more frequently at higher peat doses and lower pHs. An equilibrium time of 10 h was observed at a pH of

10, Co concentration of 125 mg/L and a peat dose of 40 g/L. Table 5.6 also showed that the uptake of Co was more rapid compared to the sorption of Ni on the saprist NL peat at the experimental conditions selected which might not be unconnected with the overall uptake mechanism of the metals.

The equilibrium times could be related to the mechanisms of metal uptake for Ni uptake, which seems to be mainly through ion exchange while Co sorption was through complexation. Bunzl (1974) reported that the kinetics of ion exchange is slower in nature, and with Ni uptake being slower as shown by this study, the uptake is suggested to be through ion exchange. The attainment of equilibrium as shown in Table 5.6 was dependent on pH, peat dose and metal concentration.

The equilibrium time obtained for Ni and Co on the NL saprist peat is longer than the time reported in most studies in which horticultural/fibrist peat was the adsorbent. Viraraghavan and Dronamraju (1993) reported 2 hours as the equilibrium time for Cu, Ni and Zn on dried ($103^{o}C$) Saskatchewan horticultural peat. Ho et al., (1995) reported about 1.5 hours as the equilibration time for an Irish peat used in the adsorption of Ni. Al-Faqih et al., (2008) reported an initial rapid uptake of 100 minutes within which most of the Cd, Cu, Ni and Zn adsorption took place in a single system study. In this study, on saprist NL peat, the uptake time was found to be longer for different values of pH, peat dose and metal concentration.

The relative longer equilibrium time observed could also be attributed to the small particle size of the peat that enhanced the external surface area and increased the binding sites. Although with this peat type, larger surface area per unit mass was available, the

smaller pore size between the particles, and the resultant compression between the overlapped and collapsed cell walls of the peat material could have reduced the porosity which reduced the uptake at shorter contact times (see the micrographs of the saprist peat on page 51). Similarly, because the saprist peat particles were small and air dried, swelling of the pores was reduced and this could have affected the hold up and uptake of the metal ions at shorter contact times, a view corroborated by Gosset et al., (1986) that the level of drying could lower the degree of swelling and the metal binding kinetics.

Variations in the equilibrium times for both Co and Ni uptake could also be due to the modes of uptake mechanism of the ions from the solution to the surface of the saprist peat and these modes could have been affected by solution pH, metal concentration and the peat dose. The uptake mechanism could have been physical adsorption when attainment of equilibrium was fast ~ 1 h or chemical adsorption when attainment of equilibrium was slow > 1.5 h.

5.4.2 Pseudo-second Order Kinetics of Ni and Co Uptake

The adsorption data for Ni and Co uptake by the saprist NL peat were fitted to the pseudo-second order kinetic equation developed by Ho et al., (1996) (equation 2.5, page 20). Kinetics data obtained at peat doses of 2 and 10 g/L for Co concentrations of 125 and 200 mg/L at pH of 3 and 5.5 were inconsistent as the values of the uptake by saprist NL peat gave large fluctuations; hence they were omitted in the subsequent analysis. The pseudo-second order kinetic plots are shown in Figures 5.3a to 5.6d for Ni sorption and, from Figures 5.7a to 5.10d for Co sorption.

The kinetics parameters from the pseudo-second order plots are summarized in Table 5.7 for Ni sorption at Ni concentrations of 25, 50, 125 and 200 mg/L for pH of 3, 5.5, 8 and 10 with peat doses of 2, 10, 21 and 40 g/L.

These experimental conditions were selected based on some of the earlier studies of metal adsorption on fibrist peat (Gosset et al., 1986; Ho et al., 1995; Ho et al., 1999) and on the results of the response surface method using the Box-Behnken design carried out in this study.

Fig. 5.3a: Pseudo-second order sorption kinetics of Ni^{2+} on saprist NL peat at pH 3.0, temp., 22°C, conc., 25 mg/L and different peat doses.

Fig. 5.3b: Pseudo-second order sorption kinetics of Ni^{2+} on saprist NL peat at pH 3.0, temp., 22°C, conc., 50 mg/L and different peat doses.

Fig. 5.3c: Pseudo-second order sorption kinetics of Ni^{2+} on saprist NL peat at pH 3.0, temp., 22°C, conc., 125 mg/L and different peat doses.

Fig. 5.3d: Pseudo-second order sorption kinetics of Ni^{2+} on saprist NL peat at pH 3.0, temp., 22°C, conc., 200 mg/L and different peat doses.
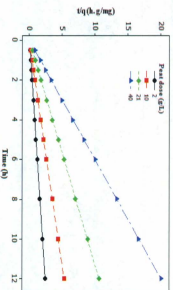
Fig. 5.4a: Pseudo-second order sorption kinetics of Ni^{2+} on saprist NL peat at pH 5.5, temp., 22°C, conc., 25 mg/L and different peat doses.
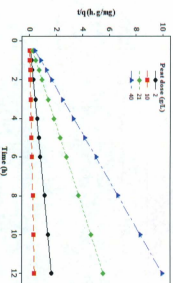
Fig. 5.4b: Pseudo-second order sorption kinetics of Ni^{2+} on saprist NL peat at pH 5.5, temp., 22°C, conc., 50 mg/L and different peat doses.
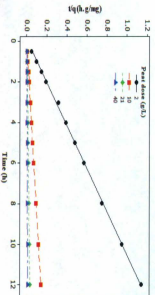
Fig. 5.4c: Pseudo-second order sorption kinetics of Ni^{2+} on saprist NL peat at pH 5.5, temp., 22°C, conc., 125 mg/L and different peat doses.
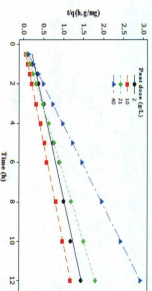
Fig. 5.4d: Pseudo-second order sorption kinetics of Ni^{2+} on saprist NL peat at pH 5.5, temp., 22°C, conc., 200 mg/L and different peat doses.
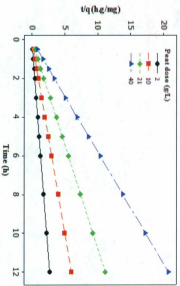
Fig. 5.5a: Pseudo-second order sorption kinetics of Ni^{2+} on saprist NL peat at pH 8, temp., 22°C, conc., 25 mg/L and different peat doses.

Fig. 5.5b: Pseudo-second order sorption kinetics of Ni^{2+} on saprist NL peat at pH 8, temp., 22°C, conc., 50 mg/L and different peat doses.
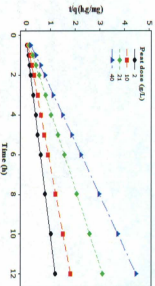
Fig. 5.5c: Pseudo-second order sorption kinetics of Ni^{2+} on saprist NL peat at pH 8, temp., 22°C, conc., 125 mg/L and different peat doses.
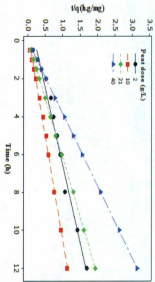
Fig. 5.5d: Pseudo-second order sorption kinetics of Ni^{2+} on saprist NL peat at pH 8, temp., 22°C, conc., 200 mg/L and different peat doses.
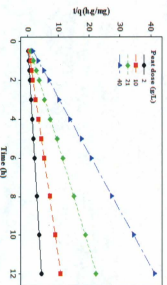
Fig. 5.6a: Pseudo-second order sorption kinetics of Ni^{2+} on saprist NL peat at pH 10, temp., 22°C, conc., 25 mg/L and different peat doses.
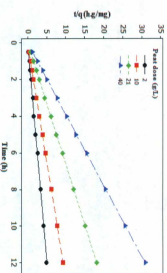
Fig. 5.6b: Pseudo-second order sorption kinetics of Ni^{2+} on saprist NL peat at pH 10, temp., 22°C, conc., 50 mg/L and different peat doses.
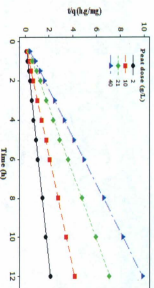
Fig. 5.6c: Pseudo-second order sorption kinetics of Ni^{2+} on saprist NL peat at pH 10, temp., 22°C, conc., 125 mg/L and different peat doses.
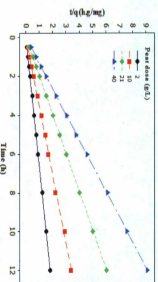
Fig. 5.6d: Pseudo-second order sorption kinetics of Ni^{2+} on saprist NL peat at pH 10, temp., 22°C, conc., 200 mg/L and different peat doses.

The kinetics of a reaction controls the reaction rates which in turn determines the holding or residence time, and governs the efficiency of the overall reaction. The kinetics of the Ni uptake was fitted to the pseudo-second order kinetic equation and since this equation was based on chemisorption as the adsorption mechanism, Ni uptake could be mainly due to chemical bonding via complexation and/or ion exchange with the active sites on the saprist peat. This observation is consistent with the equilibrium times obtained, viz; (i) in cases where attainment of equilibrium by Ni solutions were generally > 1.5 h – this could have been due to ion exchange in which exchangeable cations and protons on the peat were involved at pHs > 5.5; and (ii) in cases where complexation with ligands were involved at pH of 3

The kinetics data obtained for Ni sorption at the selected conditions satisfied the pseudo-second order kinetics equation in most of the cases, but did not satisfy the equation at the smaller peat dose of 2 g/L; this could have been aided by intra-particle diffusion of the Ni ions. At larger peat dose, the data obtained suggested chemical bonding either by ion exchange or complexation as the likely Ni uptake mechanism. The equilibrium adsorption, q_e in mg/g, equilibrium rate constant, $K_{1,ad}$ in $gmg^{-1}h^{-1}$, and the regression coefficient, r^2, at the kinetics conditions are summarized in Table 5.7 and were used in providing the basis for uptake mechanisms.

Table 5.7: Estimated pseudo-second order kinetics parameters for Ni^{2+} adsorption at the selected experimental conditions

pH	Peat dose (g/L)	Conc. 25 mg/L			Conc. 50 mg/L			Conc. 125 mg/L			Conc. 200 mg/L		
		q_e	$K_{1,ad}$	R^2	q_e	$K_{1,ad}$	R^2	q_e	$K_{1,ad}$	R^2	q_e	$K_{1,ad}$	R^2
3	2							5.16	0.14	0.913	1.47	0.48	0.972
	10	1.86	1.43	0.999	3.29	1.43	0.997	6.21	0.58	0.997	9.76	0.49	0.999
	21	1.07	26.47	1	2.01	12.71	1	3.99	5.62	1	6.05	0.7	0.999
	40	0.59	-502.3	1	1.16	67.88	1	2.62	15.64	1	3.89	12.25	1
5.5	2	4.98	3.05	1	7.26	1.79	0.999	10.59	1.17	0.999	9.24	0.08	0.983
	10	2.24	-34.31	1	30.86	0.18	0.999	82.64	0.11	0.999	10.27	0.54	0.998
	21	1.13	980.8	1	2.16	-143	1	384.6	0.01	0.999			1.0
	40	0.6	-632.9	1	1.2	59.02	1	1.11	0.004	0.999	4.11	45.65	1
8	2	4.31	6.41	1	6.49	0.65	1	10.02	1	1	8.14	0.07	0.98
	10	1.97	9.99	1	3.27	2.88	1	6.67	0.68	1	10.82	0.17	0.997
	21	1.07	46.86	1	2.05	16.23	1	3.9	2.3	1	6.2	0.003	1
	40	0.58	321.93	1	1.13	39.16	1	2.7	4.47	1	3.81	28.73	1
10	2	2.67	-19.29	1	2.42	1.8	0.998	5.8	0.59	0.999	8.14	0.07	1
	10	1.11	59.3	1	1.28	9.28	1	2.88	5.51	1	10.82	0.17	0.999
	21	0.53	241.29	1	0.66	23.97	1	1.7	7.49	1	1.99	11.27	1
	40	0.29	194.98	1	0.39	96.39	1	1.22	27.1	1	1.32	26.47	1

As indicated in Table 5.7, the amount of Ni sorbed at equilibrium given by q_e (mg/g) was highest with a value of 384.6 at pH of 5.5 at peat dose 21 g/L for Ni concentration of 125 mg/L with the corresponding equilibrium rate constant ($gmg^{-1}h^{-1}$) of the pseudo-second order, being the lowest at 0.01. The regression coefficient was nearly unity for almost all the combinations investigated.

At pH of 3 and at constant peat dose, the adsorbed Ni at equilibrium q_e, in mg/g, increased as concentration was increased while, the equilibrium rate constant, $K_{1,ad}$ in $gmg^{-1}h^{-1}$, decreased except at the peat dose of 40 g/L where a negative value was computed. Increased concentration favoured more Ni sorption at all peat doses employed and complexation of Ni ions with the active sites could be the uptake mechanism. Chen et al., (1990) reported that where applicable, the higher the initial concentration, the stronger the occurrence of complexation reactions.

At pH of 5.5, at constant peat dose, adsorbed Ni at equilibrium increased as concentration was increased up to a Ni concentration of 125 mg/L and significantly decreased at 200 mg/L Ni concentration. Based on earlier discussions, a switch in Ni uptake mechanism could have been encountered with complexation reaction being the dominant route up to 125 mg/L Ni concentration and a change to ion exchange at 200 mg/L except around the peat dose of 40 g/L where ion exchange could have dominated from a Ni concentration of 125 mg/L. This observation was justified by the equilibrium rate constant, $K_{1,ad}$ values, which did not show a consistent pattern as Ni concentration was increased compared with the $K_{1,ad}$ at pH of 3. The attainment of equilibrium was

reaction driven and if more than two reactions were involved in the reactions, the values of the rate constants could have been significantly affected by the dominant reaction.

At pH of 8, Ni adsorbed at equilibrium q_e, increased as concentration was increased at constant peat dose but no consistent pattern was manifested in the values of the equilibrium rate constant. At pH of 10, Ni adsorbed at equilibrium increased as concentration was increased at constant peat dose with decreased equilibrium rate constants. The values were however generally larger than the corresponding equilibrium rate constants at pH of 3. Therefore the Ni uptake mechanism at pH of 8 and 10 were suggested to be mainly chemisorption via ion exchange.

The release of protons, most likely in the carboxylic group in peat, was reported to be accompanied by a decrease in pH (Ho et al., 1995). Also, complexation reactions have been reported to be less dependent on solution pH (Chen et al., 1990). An attempt was therefore made using the solution pHs to identify the mechanism of Ni uptake at various conditions. This was accomplished by monitoring the pH of the filtrates for each concentration at the corresponding peat dose and pH prior to the determination of the Ni contents. The average pHs over 12 h where significant changes were noticed are shown in Table 5.8 (no significant changes were noticed at pH 3 and so not reported).

Table 5.8: Average Ni^{2+} filtrate pHs at various peat doses

Conc. (mg/L)	Av. of pH^1 at peat dose (g/L)				Av. of pH^2 at peat dose (g/L)				Av. of pH^3 at peat dose (g/L)			
	2	10	21	40	2	10	21	40	2	10	21	40
25	5.3	5.3	5.3	5.2	7.7	7.6	7.6	7.5	9.6	9.6	9.6	9.5
50	5.3	5.2	5.1	5.0	7.7	7.6	7.6	7.3	9.6	9.5	9.5	9.4
125	5.2	5.2	5.1	4.9	7.6	7.5	7.5	7.3	9.4	9.4	9.3	9.3
200	5.2	5.1	5.0	4.9	7.6	7.5	7.4	7.1	9.4	9.3	9.3	9.3

where pH^1, pH^2 and pH^3 are the average pHs at initial pHs of 5.5, 8 and 10, respectively

From Table 5.8, it was evident that slightly lower pHs were obtained as the Ni concentration increased and also as the peat dose was increased. This trend could be attributed to the level of ion exchange that took place at these experimental conditions and because no significant changes were noticed at pH of 3, Ni uptake on the saprist NL peat could have been via complexation at pH of 3 and through a combination of ion exchange and complexation at pH 5.5, 8 and 10.

The pseudo-second order plots of Co sorption at various peat doses, pHs and concentrations are shown in Figures 5.7a to 5.10d and the computed pseudo-second order kinetics parameters are summarized in Table 5.9.
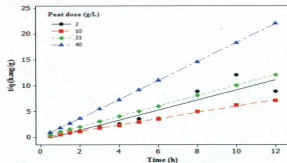
Fig. 5.7a: Pseudo-second order sorption kinetics of Co^{2+} on saprist NL peat at pH 3.0, temp., 22°C, conc., 25 mg/L and different peat doses.
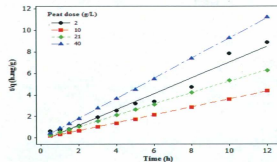
Fig. 5.7b: Pseudo-second order sorption kinetics of Co^{2+} on saprist NL peat at pH 3.0, temp., 22°C, conc., 50 mg/L and different peat doses.
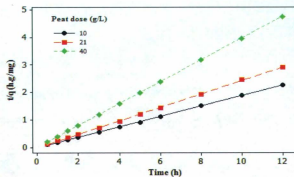
Fig. 5.7c: Pseudo-second order sorption kinetics of Co^{2+} on saprist NL peat at pH 3.0, temp., 22°C, conc., 125 mg/L and different peat doses.
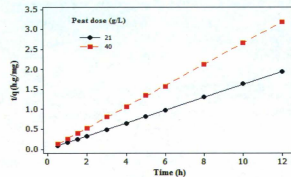
Fig. 5.7d: Pseudo-second order sorption kinetics of Co^{2+} on saprist NL peat at pH 3.0, temp., 22°C, conc. 200 mg/L and different peat doses.
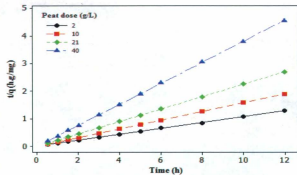
Fig. 5.8a: Pseudo-second order sorption kinetics of Co^{2+} on saprist NL peat at pH 5.5, temp., 22°C, conc., 25 mg/L and different peat doses.
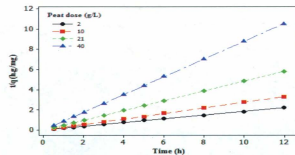
Fig. 5.8b: Pseudo-second order sorption kinetics of Co^{2+} on saprist NL peat at pH 5.5, temp., 22°C, conc., 50 mg/L and different peat doses.
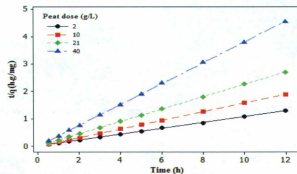
Fig. 5.8c: Pseudo-second order sorption kinetics of Co^{2+} on saprist NL peat at pH 5.5, temp., 22°C, conc., 125 mg/L and different peat doses.
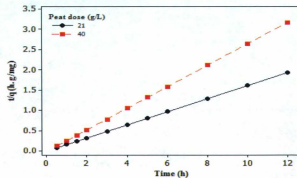
Fig. 5.8d: Pseudo-second order sorption kinetics of Co^{2+} on saprist NL peat at pH 5.5, temp., 22°C, conc. 200 mg/L and different peat doses.
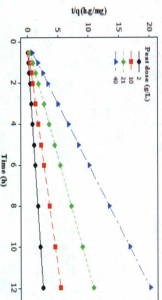
Fig. 5.9a: Pseudo-second order sorption kinetics of Co^{2+} on saprist NL peat at pH 8.0, temp., 22°C, conc., 25 mg/L and different peat doses.
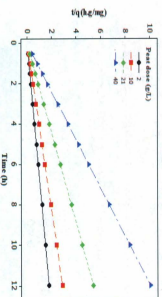
Fig. 5.9b: Pseudo-second order sorption kinetics of Co^{2+} on saprist NL peat at pH 8.0, temp., 22°C, conc., 50 mg/L, and different peat doses.
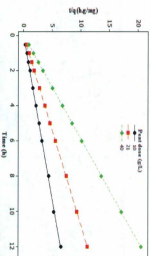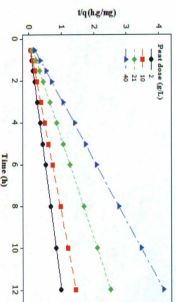

Fig. 5.9c: Pseudo-second order sorption kinetics of Co^{2+} on saprist NL peat at pH 8.0, temp., 22°C, conc., 125 mg/L, and different peat doses.
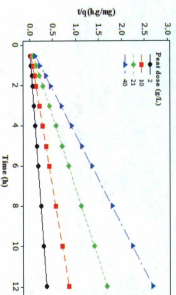
Fig. 5.9d: Pseudo-second order sorption kinetics of Co^{2+} on saprist NL peat at pH 8.0, temp., 22°C, conc. 200 mg/L, and different peat doses.
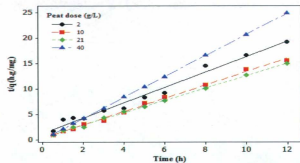
Fig. 5.10a: Pseudo-second order sorption kinetics of Co^{2+} on saprist NL peat at pH 10.0, temp., 22°C, conc., 25 mg/L and different peat doses.
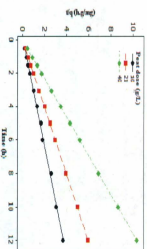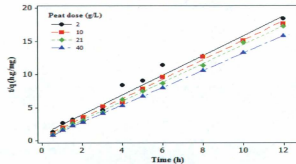

Fig. 5.10b: Pseudo-second order sorption kinetics of Co^{2+} on saprist NL peat at pH 10.0, temp., 22°C, conc., 50 mg/L and different peat doses.
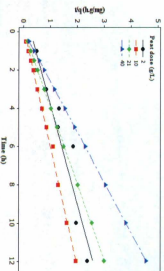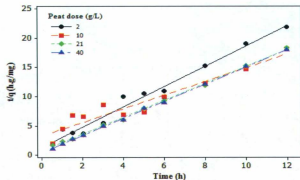

Fig. 5.10c: Pseudo-second order sorption kinetics of Co^{2+} on saprist NL peat at pH 10.0, temp., 22°C, conc., 125 mg/L and different peat doses.
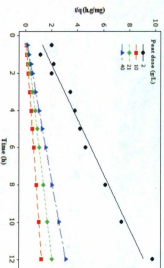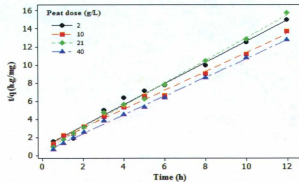

Fig. 5.10d: Pseudo-second order sorption kinetics of Co^{2+} on saprist NL peat at pH 10.0, temp., 22°C, conc. 200 mg/L and different peat doses.

Figures 5.7a to 5.7d showed that the Co uptake kinetics satisfied the pseudo-second order kinetic equation at all the experimental conditions with regression coefficient values, r^2, nearly unity except at pH of 3, for Co concentration of 25 mg/L and at peat dose of 2 g/L. No consistent Co uptake data was obtained at peat dose of 2 and 10 g/L at a Co concentration of 200 mg/L, and at peat dose of 2 g/L for Co concentration of 125 mg/L. Peat dose of 2 g/L and Co concentration of 125 mg/L gave higher Co sorption kinetics data than peat dose of 10 and 21 g/L. Since the pseudo-second order kinetic equation was based on the assumption that uptake is through chemisorption (Ho et al., 1995) which can either be ion exchange and/or complexation, then, Co sorption at the above experimental conditions from the data obtained, seems to suggest chemisorption as the main uptake mechanism.

At pH of 5.5 graphically illustrated by Figures 5.8a to 5.8d, Co uptake kinetics data showed a consistent pattern for all peat doses and Co concentrations except at Co concentration of 200 mg/L where no consistent kinetics data were obtained for peat doses of 2 and 10 g/L. At pH 8 shown by Figures 5.9a to 5.9d, no abnormal Co sorption pattern was obtained. Figures 5.10a to 5.10d showed that Co sorption kinetics was nearly the same for all concentrations and peat doses. Also at pH of 10, Co uptake showed nearly the same behaviour for all peat doses and concentrations used.

The kinetic constants from these plots are shown in Table 5.9.

Table 5.8: Estimated pseudo-second order kinetics parameters for Co^{2+} adsorption at the selected experimental conditions

pH	Peat dose (g/L)	Conc. 25 mg/L			Conc. 50 mg/L			Conc. 125 mg/L			Conc. 200 mg/L		
		q_e	$K_{1,ad}$	R^2	q_e	$K_{1,ad}$	R^2	q_e	$K_{1,ad}$	R^2	q_e	$K_{1,ad}$	R^2
3	2	1.02	-1.55	0.872	1.37	-1.93	0.969						
	10	1.64	-14.24	0.998	2.73	-3.71	0.999	5.28	-2.15	1			
	21	0.99	203.7	1	1.9	-86.69	1	4.09	-4.42	1	6.15	-14.69	1
	40	0.55	-223.8	1	1.07	-16.56	1	2.52	-54.18	1	3.76	33.72	1
5.5	2	4.24	7.33	0.999	5.48	4.33	0.999	9.34	1.43	1			
	10	2.1	225.82	1	3.63	252.82	1	6.3	4.5	0.998	6.22	14.36	1
	21	1.09	132.11	1	2.07	63.05	1	4.45	13.31	1	3.77	-41.34	1
	40	0.58	-98.83	1	1.14	80.14	1	2.63	26.3	1			
8	2	4.71	-0.09	1	6.87	2.08	1	12.2	1.29	1	33.44	1.12	1
	10	2.18	10.22	1	4.18	8.8	1	8.31	2.3	1	14.04	1.37	1
	21	1.11	29.63	1	2.23	34.65	1	4.8	4.57	1	7.17	4.42	1
	40	0.59	313.83	1	1.2	162.85	1	2.9	10.61	1	4.5	3.75	1
10	2	0.67	121.77	0.981	0.68	2.08	0.975	0.58	2.14	0.981	0.86	1.36	0.991
	10	0.76	5.09	0.996	0.69	3.61	0.997	0.86	0.41	0.925	0.96	1.06	0.995
	21	0.83	3.03	0.999	0.7	7.25	0.999	0.69	3.13	0.998	0.8	2.96	0.997
	40	0.48	49.22	1	0.77	8.48	1	0.68	5.36	0.999	0.97	2.96	0.998

From Table 5.9, at pH of 3, and at constant peat dose, the Co adsorbed at equilibrium, q_e (mg/g), increased as the Co concentration was increased. At this pH, negative values of the equilibrium rate constants, K ($gmg^{-1}h^{-1}$) were also computed. The negative values of equilibrium rate constants could be related to the sorption mechanism as suggested by the time taken to attain equilibrium. With Co, ≤ 1.5 h was the time needed to attain equilibrium at most reaction conditions (refer Table 5.6, page 86), and where negative values of equilibrium rate constant were reported, the times to attain equilibrium were generally low compared to other times with positive equilibrium rate constants. The negative value of K also implies that the concentration of the peat and Co formed during the reaction was decreasing or being consumed as the reaction proceeded. The product formed when Co reacted with the saprist peat could be migrating out of the peat matrix leading to its concentration being reduced at the corresponding pH.

Increase in the initial concentration has been reported to increase the strength of the complexation reaction (Chen et al., 1990). At pH 3 the maximum Co sorbed at equilibrium increased as the initial concentration was increased. Co uptake at pH of 3 is therefore suggested to be through complexation of Co on the active sites of the saprist NL peat.

At pH 5.5, the Co adsorbed at equilibrium, q_e (mg/g) also increased with increased Co concentration at constant peat dose. The q_e at pH of 5.5 for Co concentration of 25 and 50 mg/L were lower than that of Ni at the same pH and concentration; and at other concentrations no consistent pattern was obtained which was the trend for other pHs and

conditions. At pH of 5.5, the equilibrium rate constant values were positive except at concentrations of 25 and 200 mg/L for peat dose of 40 g/L.

At pH 8, q_e values increased as concentration was increased at constant peat dose. The equilibrium rate constant values at this pH for all peat doses were positive. For constant peat dose and concentration, the q_e increased as pH was increased to 8. Complexation is therefore suggested as the dominant Co uptake mechanism at the pH of 8. The q_e values for Ni uptake did not show this consistent pattern as pH was increased to 8 at constant metal concentration and peat dose. The maximum Co sorbed at equilibrium q_e, was 33.44 mg/g at pH of 8 with the corresponding pseudo-second order rate constant being 1.12 $gmg^{-1}h^{-1}$.

At pH 10, q_e values did not show a consistent pattern when concentration was increased and in addition, the values obtained where generally smaller than those reported for pHs of 3, 5.5 and 8 at constant metal concentration and peat dose. The irregular pattern of the values of q_e was similar to the pattern obtained with Ni uptake at pH 10. Therefore Co uptake at pH of 10 could be mainly due to ion exchange.

As previously stated for Ni, ion exchange via the release of proton was the dominant metal uptake mechanism by the saprist NL peat especially at pHs > 3. For the sorption of Co, when the pHs of the Co filtrates for each concentration at the corresponding peat dose were monitored during the experiment, no significant change in pHs was obtained except at pH of 10. Table 5.10 is a summary of the pH values obtained during the experiment. A decrease in pH values would have been obtained if ion

exchange was the dominant uptake mechanism at all the solution pHs, but this was not so; thus it seems Co sorption was predominantly by complexation.

Table 5.10: Average Co^{2+} filtrate pHs at various peat doses at initial pH of 10

	Average pH at the peat doses (g/L)			
Conc. (mg/L)	2	10	21	40
25	9.7	9.6	9.5	9.5
50	9.7	9.5	9.4	9.4
125	9.6	9.5	9.4	9.4
200	9.6	9.4	9.4	9.3

From Table 5.10, a general decrease in pH was observed as the Co concentration and peat dose were increased. This was similar to the trend obtained for Ni concentrations and suggested similar reaction mechanisms at the pH of 10 which would be mainly ion exchange. In this case, two protons (H^+) were exchanged for every one Co^{2+} sorbed and the released protons migrated into the solution decreasing the pH.

5.5 Summary on Kinetics of Ni or Co Adsorption on Saprist NL Peat

The kinetics of Ni or Co sorption in saprist NL peat was discussed in this chapter. The data showed that different uptake mechanisms were involved in the sorption of these metals. From the chemical properties of Ni and Co, Co should be adsorbed more compared to Ni because, large ionic radius of Co favoured more adsorption as covalent

bonds are easily formed. Similarly lower heat of hydration of Co would favour easy bond formation. Co had a larger atomic radius and lower heat of hydration compared to Ni. This could have been the reason for the rapid adsorption of Co as shown by the equilibrium times in Table 5.6. For most of the experimental conditions investigated in this study, the adsorption of Ni was generally larger than that of Co; this is most likely due to the combination of ion exchange and complexation reactions in the Ni adsorption compared to complexation only in Co adsorption.

The uptake of these two metals therefore could mainly be a function of their chemistry. Co and Ni are members of the borderline metals (others are Fe^{2+} and Cu^{2+}) that are known to react with ligands such as ROH, RCO_2H, NR_3 (Jones, 2001), where R is an alkyl group such as methyl - CH_3, ethyl -C_2H_5, etc. The reactivities of these metals with ligands are not easily quantifiable in any sequence because they are influenced by the ligand environment such as its size and position.

The adsorption of the two metals in saprist NL peat satisfied the pseudo-second order kinetics equation which was based on chemisorption as the dominant mechanism. Data obtained showed that a combination of ion exchange and complexation could have accounted for the uptake of Ni at pH of 3 and 5.5. As the pH was increased, the reaction became predominantly ion exchange. On the other hand, Co sorption was through complexation reaction at pHs of 3, 5.5 and 8, and the uptake mechanism became more of ion exchange at pH of 10.

112

Ni or Co sorption was a function of concentration, peat dose and solution pH. According to Poots et al., (1978), when the adsorbed metal quantity is plotted against the square root of the time, the graph should be linear through the origin if mass transfer only controls the adsorption kinetics. The data obtained for Ni and Co uptake failed this check (see appendix E, plots E1 to E32), and this showed that mass transfer process alone did not control the overall sorption of Ni or Co on the saprist NL peat but also chemical reactions that involved the exchange of ions and/or the sharing of electrons.

CHAPTER SIX

BATCH ADSORPTION AND DESORPTION

6.1 Chapter Overview

Batch adsorption isotherms are very useful in the evaluation of adsorbent capacity as they provide information on the interaction between the adsorbent and adsorbate, helping in process optimization and or design. This chapter reports only the adsorption isotherm models that were fitted by the experimental data. Competitive sorption using Cd, Pb and Zn was also carried out and finally, desorption results in % of the metal sorbed during the batch adsorption experimental are also reported.

6.2 Batch Tests – Adsorption Isotherms

The average concentrations of the triplicate batch adsorption tests conducted over 24 hours at five Ni^{2+} or Co^{2+} concentrations (200, 125, 50, 25 and 12.5 mg/L) at various peat doses and solution pHs were used to calculate the Ni or Co sorbed. This approach was similar to that of Ho et al., (1995). The average raw data of the effluents and corresponding metal adsorbed are presented in Appendix F. A maximum metal concentration of 200 mg/L was selected because it was the highest of the concentrations during the kinetics study and is mostly used in related studies (Ho et al., 1995; Ho and McKay, 1999). The unit of mg/L (equivalent to part per million, ppm when solution is

114

dilute with a density of 1.0 g/cm^3) is the normally reported unit in the industry and has been maintained in this study. The minimum peat dose of 4 g/L was chosen because the kinetics study showed that the peat dose of 2 g/L was unstable at the Ni concentrations of 25 and 50 mg/L at pH of 3 and at Co concentrations of 125 and 200 mg/L at pHs of 3 and 5.5 and gave large fluctuations of values. The fitting of the batch tests results to some commonly used isotherms such as the Elovich model, Fractional Power model, and the Dubinin-Radushkevich isotherm, was attempted but the data only fit the Langmuir and Freundlich isotherms.

6.2.1 Langmuir Isotherm

The Langmuir isotherm relates the adsorptive capacity of the adsorbent to the coverage of the active sites given by the Langmuir monolayer saturation capacity and also, the level of desorption at specified conditions. The Langmuir isotherm plots for the five Ni concentrations (200, 125, 50, 25 and 12.5 mg/L) at pHs of 3, 5.5, 8 and 10 and at a temperature of 22°C with varied peat doses are shown in Figures 6.1a to 6.1d. The summary of the Langmuir parameters from the Langmuir isotherm model (equation 2.9, page 23) is presented in Table 6.1 for Ni adsorption by the saprist NL peat.
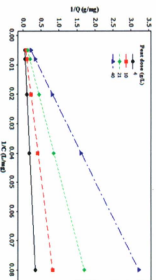
Fig. 6.1a: Langmuir adsorption isotherms for Ni²⁺ at pH 3 and specified peat doses.
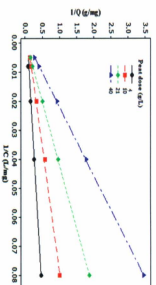
Fig. 6.1c: Langmuir adsorption isotherms for Ni²⁺ at pH 8 and specified peat doses.
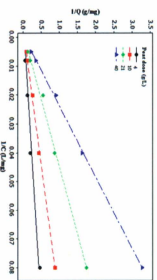
Fig. 6.1b: Langmuir adsorption isotherms for Ni²⁺ at pH 5.5 and specified peat doses.
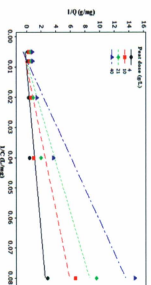
Fig. 6.1d: Langmuir adsorption isotherms for Ni²⁺ at pH 10 and specified peat doses.

The Langmuir model gave good fits for the batch experiments carried out at different peat doses and pHs as shown by the regression coefficient, r^2, which were near unity. The Langmuir constants given by b, in L/mg and the Langmuir monolayer saturation capacity q_m, in mg/g at the various conditions for Ni uptake on the saprist NL peat are summarized in Table 6.1.

Table 6.1: Langmuir parameters for Ni^{2+} adsorption over the range of Ni^{2+} concentrations at specified peat doses and pHs

Peat dose (g/L)	pH 3			pH 5.5			pH 8			pH 10		
	$b*10^{-3}$	q_m	r^2	$b*10^{-3}$	q_m	r^2	$b*10^{-3}$	q_m	r^2	$b*10^{-3}$	q_m	r^2
4	6.45	39.68	0.994	8.41	24.04	0.928	14.58	14.20	0.960	8.98	-3.16	0.856
10	2.09	47.85	0.999	3.76	25.38	0.998	7.43	11.61	0.998	9.56	-1.26	0.869
21	8.75	54.35	1.000	2.29	20.58	0.995	1.62	26.88	1.000	8.08	-1.04	0.903
40	4.07	61.35	1.000	1.04	23.87	0.999	1.57	15.06	1.000	7.66	0.70	0.929

From Table 6.1, the Langmuir monolayer saturation capacity, q_m generally decreased with increasing pH at constant peat dose. At the pH of 3, q_m increased as the peat dose was increased. For other pHs, no consistent pattern was observed. This might be connected with the uptake mechanism which had been suggested (Chapter 5) to be predominantly a complexation reaction at pH of 3 and a combination of ion exchange and complexation as pH was increased from 5.5 to 10. At pH 3, larger values of q_m was

obtained compared to other pHs. The maximum q_m was obtained at peat dose of 40 g/L at pH 3.

At pH of 10, negative values of the Langmuir monolayer saturation capacity, q_m, were obtained for all peat doses except at 40 g/L. Although, a negative value of q_m was not accounted for in the development of the equation, it could possibly imply that Ni uptake at pH 10, was by electronic exchange since the solution could have been saturated with electrons released from hydrolysable functional groups in the celluloses and lignins at this pH. Coupal and Lalancette (1976), have reported that at higher pHs (>8.5), peat is not stable in terms of its physical strength. This physical instability could have contributed to the negative values of the q_m at lower peat doses until 40 g/L

The ratios of desorption to adsorption given by the Langmuir constant, b in L/mg, were generally low for all the experimental conditions which showed that desorption of Ni from the saprist NL peat during the experiments was not pronounced. This could be due to the ability of the peat to hold firmly the Ni in solution when bonded to the matrix of the peat.

The Langmuir isotherms for the Co^{2+} concentrations range (200, 125, 50, 25 and 12.5 mg/L) at 22°C for different peat doses and pHs are shown in Figures 6.2a to 6.2d and the Langmuir constants are summarized in Table 6.2.
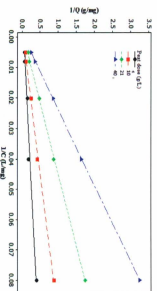
Fig. 6.2a: Langmuir adsorption isotherms for Co²⁺ at pH 3 and specified peat doses.
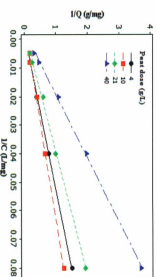
Fig. 6.2c: Langmuir adsorption isotherms for Co²⁺ at pH 8 and specified peat doses.
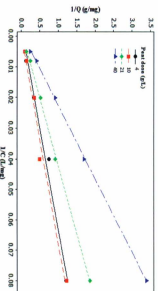
Fig. 6.2e: Langmuir adsorption isotherms for Co²⁺ at pH 5.5 and specified peat doses.
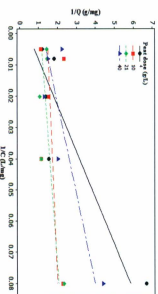
Fig. 6.2d: Langmuir adsorption isotherms for Co²⁺ at pH 10 and specified peat doses.

The adsorption data for the Co^{2+} concentrations range gave good fits for the Langmuir isotherm at pHs of 3, 5.5, and 8 but poor fits were observed at pH of 10 with the regression coefficients as low as 0.1227 at a peat dose 10 g/L as seen in Figures 6.2a to 6.2d.The Langmuir constants, b in L/mg and Langmuir monolayer saturated capacities, q_m in mg/g at the indicated peat doses are summarized in Table 6.2

Table 6.2: Langmuir parameters for Co^{2+} adsorption over the range of Co^{2+}

concentrations at specified peat doses and pHs

Peat dose	pH 3			pH 5.5			pH 8			pH 10		
(g/L)	$b*10^{-3}$	q_m	r^2	$b*10^{-3}$	q_m	r^2	$b*10^{-3}$	q_m	r^2	$b*10^{-3}$	q_m	r^2
4	10.80	21.55	0.975	3.68	18.15	0.984	5.81	11.86	0.998	6.70	2.19	0.801
10	3.34	28.49	0.998	1.13	60.98	0.982	2.31	23.81	0.998	218.3	0.68	0.123
21	2.50	18.98	0.999	2.31	19.31	0.999	3.29	13.00	0.998	95.20	0.89	0.520
40	1.36	18.38	1.000	1.64	14.75	1.000	2.87	7.75	0.999	35.80	0.81	0.742

From Table 6.2, the Langmuir monolayer saturation capacity, q_m in mg/g, increased to maximum values as the peat dose was increased from 4 to 10 g/L for pHs of 3, 5.5 and 8. A general decrease was observed in q_m for peat doses from 10 to 40 g/L for all the pHs studied. The peat dose of 10 g/L at pHs of 3, 5.5 and 8 gave the highest q_m. This could imply that the coverage of the active sites on the peat by the Co ions through the dominant reaction mechanism was optimum at this peat dose.

The lowest q_m was observed at a peat dose of 10 g/L at pH 10. Low values of the q_m at pH 10 also corresponded to larger Co desorption to adsorption ratios given by b in

L/mg compared to the values observed at other pHs. In fact, the largest q_m, 60.98 mg/g observed at pH of 5.5 at peat dose of 10 g/L had the lowest desorption to adsorption ratio. This could imply that the stronger the mechanism of Co adsorption, the less likely for desorption to occur. Co could therefore be forming more stable complexes with the ligands in the peat matrix and these complexes might be less reactive at the pH of the environment.

As the pH was increased, q_m decreased except at pH 5.5 where increases in q_m were observed from pH 3 at peat doses of 10 and 21 g/L. The relative consistent pattern of the q_m values for Co sorption on the saprist NL peat compared to that of Ni could be related to one, rather than multiple uptake mechanisms. Uptake mechanisms were thus, suggested to be a function of the metal chemistry as well as the metal concentration, peat dose and solution pH.

The q_m for Ni was larger than that of Co at pH of 3 for all peat doses. At pHs of 5.5 and 8, Co had a larger q_m at peat dose of 10 g/L; at pH of 10, Co had a larger q_m compared to Ni. Large values of q_m is an indication of the level of coverage of the active sites by the cation which was governed by the reaction path (adsorption mechanisms).

The chemical properties of Co (Table 5.3) favoured the larger values of q_m observed at pH of 10 compared to Ni. With ion exchange suggested as the predominant adsorption mechanism at this pH, the slightly larger ionic radius and lower hydration energy of Co compare to Ni would enhance easy exchange of electrons with its d-orbital with the available ligands leading to slightly more uptake. On the other hand where larger Ni uptakes compared to Co were observed, a combination of ion exchange and

complexation could have influenced and accounted for the values of the q_m. The equilibrium adsorption from the Langmuir isotherm for Ni and Co was influenced by the peat dose and the solution pH.

6.2.2 Freundlich Isotherm

The Freundlich isotherm relates the adsorptive capacity of the adsorbent to the concentration of the contaminant through the constant known as the Freundlich isotherm constant. Ni and Co adsorption data on the NL saprist peat were fitted to the Freundlich isotherm for all the peat doses and pHs used at the five metals' concentrations of 200, 125, 50, 25 and 12.5 mg/L. The plots obtained are presented in Figures 6.3a to 6.3d for Ni uptake and Figures 6.4a to 6.4d for Co sorption on the saprist NL peat.
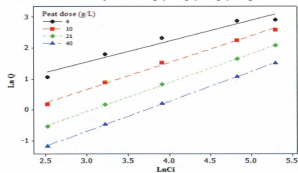
Fig.6.3a: Freundlich adsorption isotherms for Ni^{2+} at pH 3 and specified peat doses.
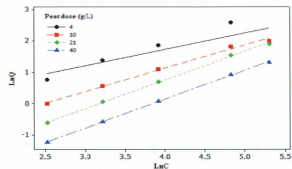
Fig.6.3c: Freundlich adsorption isotherms for Ni^{2+} at pH 8 and specified peat doses.
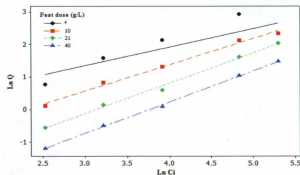
Fig.6.3b: Freundlich adsorption isotherms for Ni^{2+} at pH 5.5 and specified peat doses.
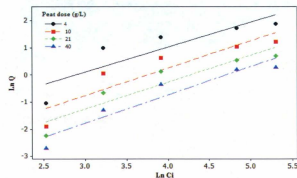
Fig.6.3d: Freundlich adsorption isotherms for Ni^{2+} at pH 10 and specified peat doses.

The Ni batch adsorption data gave good fits (regression coefficient, r^2, being closer to unity) with the Freundlich adsorption model with data obtained at pH of 3 giving better fits than other pHs investigated as shown in Figures 6.3a to 6.3d. The Freundlich parameters for Ni adsorption at the experimental conditions are summarized in Table 6.3 with the Freundlich isotherm constant K expressed in $mg^{(1-1/n)} kg^{-1} L^{1/n}$ and the Freundlich exponent, $1/n$ being dimensionless.

Table 6.3: Freundlich parameters for Ni^{2+} adsorption over the range of Ni^{2+}
concentrations at specified peat doses and pHs

Peat dose (g/L)	pH 3			pH 5.5			pH 8			pH 10		
	K x10^{-3}	$1/n$	r^2	K x10^{-3}	$1/n$	r^2	K x10^{-3}	$1/n$	r^2	K x10^{-3}	$1/n$	r^2
4	345.3	0.669	0.958	465.7	0.563	0.655	704.1	0.521	0.753	2.22	0.921	0.771
10	12.1	0.861	0.996	14.2	0.809	0.993	161.3	0.738	0.994	0.17	1.011	0.822
21	1.36	0.936	0.999	1183.6	0.934	0.995	54.3	0.916	0.999	0.06	0.993	0.870
40	2.52	0.968	1.000	0.2	0.961	0.999	28.5	0.925	1.000	0.01	1.045	0.907

From Table 6.3, the Freundlich isotherm constant K, a measure of the adsorbent capacity, increased as the pH increased from 3 to 8 for the Ni concentration except at pH of 5.5 for peat dose 40 g/L where it decreased and at peat dose 21 g/L where the maximum K value was observed.

At constant pH, increased peat dose led to decrease in K as observed at pH 3 except for peat dose of 40 g/L, and pHs of 8 and 10; but at pH of 5.5, a maximum K of

1.183 mg$^{(1-1/n)}$ kg^{-1} L$^{1/n}$ at peat dose 21 g/L was observed followed by a large decrease at peat dose of 40 g/L. This trend could have been influenced by the natural pH of the saprist NL peat which was 4.2 (Table 3.1, page 43) and also, by the uptake mechanism. Uptake is generally known to be higher at and around the natural pH of the adsorbent (Schwarzenbach et al., 2003) while complexation is less pH dependent compared with ion exchange. Thus, as complexation became less dominant at pH > 3, less Ni was sorbed.

The Freundlich exponent (1/n) increased as peat dose was increased. This implied that the bonds sites at larger peat doses were more than sites at lower peat doses. Also the strength of the bond could be stronger and Ni held more tightly than at lower peat doses. This fact was corroborated by the Langmuir constant, b, which measures desorption to adsorption ratios, which have been observed to be generally lower at larger peat doses (Table 6.1). The regression coefficients were lower in values compared to those of the Langmuir isotherms especially at a peat dose of 4 g/L. Peat being a biomass could react with metals well beyond the 24 h used as bench-mark during this study. This could be one reason why the Langmuir and Freundlich isotherms gave good fits for the same data with the Langmuir isotherm providing better fits based on the value of the computed regression coefficients over the pH, concentration and peat dose ranges.

The Freundlich isotherms, for Co adsorption over the concentrations range, with varied peat doses and pHs, are shown from Figures 6.4a to 6.4d.
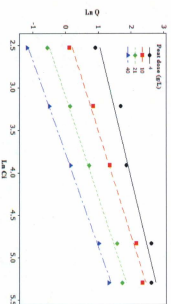
Fig.6.4a: Freundlich adsorption isotherms for Co^{2+} at pH 3 and specified peat doses.
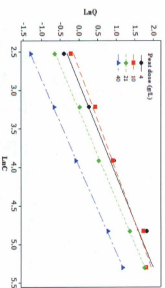
Fig.6.4c: Freundlich adsorption isotherms for Co^{2+} at pH 8 and specified peat doses.
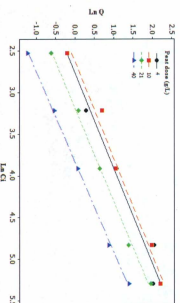
Fig.6.4b: Freundlich adsorption isotherms for Co^{2+} at pH 5.5 and specified peat doses.
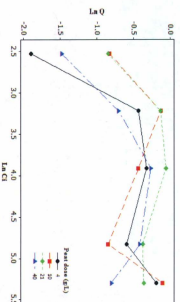
Fig.6.4d: Freundlich adsorption isotherms for Co^{2+} at pH 10 and specified peat doses.

The Co adsorption data gave good fits for the Freundlich isotherm at pH of 3, 5.5 and 8 but not at the pH of 10 where regression coefficients were low especially at peat doses of 10 and 21 g/L as seen in Figures 6.4a to 6.4d. The Freundlich parameters for the Co adsorption at the experimental conditions are summarized in Table 6.4 with the Freundlich isotherm constant K expressed in $mg^{(1-1/n)}$ kg^{-1} $L^{1/n}$ and the Freundlich exponent, $1/n$ being dimensionless.

Table 6.4: Freundlich parameters for Co^{2+} adsorption over the range of Co^{2+} concentrations at specified peat doses and pHs

Peat dose (g/L)	pH 3			pH 5.5			pH 8			pH 10		
	$K \times 10^3$	$1/n$	r^2	$K \times 10^3$	$1/n$	r^2	$K \times 10^3$	$1/n$	r^2	$K \times 10^3$	$1/n$	r^2
4	322.3	0.614	0.949	3.86	0.875	0.971	88.03	0.836	0.970	3.73	0.44	0.521
10	14.4	0.811	0.991	5.73	0.859	0.982	128.92	0.753	0.984	165.4	0.080	0.064
21	2.27	0.851	0.991	1.36	0.899	0.996	59.04	0.866	0.999	183.4	0.096	0.026
40	0.35	0.916	0.998	0.29	0.926	0.999	28.13	0.896	1.000	21.6	0.236	0.323

From Table 6.4, the Freundlich isotherm constant K decreased as the peat dose was increased from 4 to 40 g/L at pH of 3. The values of K increased at peat doses of 10 and 21 g/L between pHs of 5.5 and 10. The Freundlich isotherm constant at pH of 3 showed a consistent pattern compared to other pHs as the peat dose was increased. At constant peat dose, the Freundlich isotherm constant had lower values at pH of 5.5 compared to other pHs of 8 and 10 where it was much higher. The maximum K value of

$0.3223 \text{ mg}^{(1-1/n)} \text{ kg}^{-1} \text{ L}^{1/n}$ for Co over the concentrations range was however, obtained at peat dose 4 g/L and at pH 3.

At constant peat doses, the influence of pH on the K values did not follow a consistent pattern like the adsorption of Ni (refer Table 6.3). At a lower peat dose of 4 g/L, the largest K was reported at pH 3. However at peat doses of 10 and 21 g/L, larger K values were observed at pH 10, while at peat dose of 40 g/L, the largest K was observed at pH 8. The inconsistent pattern could have been as a result of the selective reaction between the Co and the different functional groups present in the peat which could have led to the formation of different Co–peat complexes at different peat doses and pHs. Kalymkova et al., (2008), suggested that at higher peat decomposition, more fulvic acid (the fraction of humic matter soluble at all pH) compared to humic acid (humic matter that can be precipitated at pH 1) is present and, the hydroxyl functional group is more reactive compared to the carboxylic functional group at certain pH levels. The reactivity of the hydroxyl group and the presence of amine and or amide as determined from the functional groups identification in this study could have influenced the Co-peat complexes formation. The influence of these functional groups might not be pronounced in the adsorption of Ni, hence more consistent adsorption patterns were observed.

The Freundlich exponent for the Co adsorption generally increased as peat dose was increased except at pH 10 where the pattern was inconsistent. This trend corroborated that of the Langmuir isotherm model for the Co adsorption where an inconsistent Langmuir constant, being a measure of desorption to adsorption was observed at pH 10.

The increase in the Freundlich exponent suggested that the bond strength between the available active sites and Co ions increased as peat dose was increased.

From the 24 h, Ni and Co adsorption test results, the percents of initial Ni and Co adsorbed at the various peat doses and pHs were obtained and summarized as shown in Table 6.5.

Table 6.5: Percent of initial concentration of Ni^{2+} and Co^{2+} adsorbed at various conditions

pH	Conc. (mg/L)	Percent of initial metal concentration adsorbed							
		Ni^1	Co^1	Ni^2	Co^2	Ni^3	Co^3	Ni^4	Co^4
3	200	36.5	27.5	66.5	52.7	83.6	59.8	90.8	75.5
	125	56.3	43.9	76.3	69.0	87.0	81.5	94.1	88.8
	50	80.4	51.0	91.4	77.8	96.0	86.6	98.0	93.0
	25	95.6	86.0	98.0	93.2	99.2	95.6	99.6	97.2
	12.5	92.8	80.0	96.8	90.4	98.4	96.0	99.2	98.4
5.5	200	15.3	15.0	52.6	46.0	80.4	74.5	88.0	80.8
	125	60.0	24.8	67.8	58.4	85.2	67.2	91.0	76.6
	50	68.0	23.6	75.0	57.6	76.0	79.2	88.0	86.4
	25	78.8	21.2	92.0	81.2	97.2	91.6	98.4	94.0
	12.5	69.6	26.4	90.4	65.6	96	90.4	97.6	94.4
8	200	14.1	11.8	36.8	30.4	70.1	60.5	74.6	64.3
	125	42.5	19.6	49.4	44.8	78.4	66.0	80.8	69.1
	50	51.6	20.4	60	49.5	83.5	70.9	86.3	73.5
	25	63.4	20.9	70.2	62.1	88.2	84.8	90.2	81.4
	12.5	68.9	21.3	80.3	63.8	90.0	86.2	93.1	86.8
10	200	13.2	1.7	17.1	4.5	21.1	7.3	26.6	9.0
	125	18.0	1.8	23.0	3.44	28.8	11.52	39.0	21.12
	50	32.0	5.8	38.0	13	48.0	39.6	56.0	61.6
	25	43.2	10.4	42.8	35.2	43.2	73.6	43.6	79.2
	12.5	11.2	4.8	12.0	35.2	17.6	72.0	21.6	72.8

Superscripts 1, 2, 3 and 4 are the peat doses at 4, 10, 21 and 40 g/L respectively.

From Table 6.5, the percent of Ni or Co sorbed generally decreased as metal concentration was increased at a constant pH and peat dose although this trend was not usually observed between the two lowest metal concentrations. This may have been because of the interaction between the experimental factors (metal concentration, solution pH and peat dose) which could have been pronounced at these two concentrations compared to others.

At constant metal concentration and pH, the percent metal sorbed increased as the peat dose increased. This trend was due to increase in active sites as the peat dose was increased. For both metals, at a constant peat dose, percent metal sorbed generally decreased as pH was increased with only two exceptions (at 25 mg/L Co at pH 8 and 25 mg/L Ni at pH 10). The largest percent of metals sorbed was obtained at pH of 3 and at peat dose of 40 g/L. This could have also been possible since adsorbents are known to be more effective around their natural pHs (Schwarzenbach et al., 2003).

The percent of Ni sorbed was generally higher than that of Co with only few exceptions. These exceptions were: i) at pH 5.5 for peat dose of 21 g/L and for metals concentration of 50 mg/L; ii) at pH 10 for peat dose of 21 g/L and at metals concentrations of 25 and 12.5 mg/L; and iii) at pH 10 for peat dose of 40 g/L and for metals concentrations of 50, 25 and 12.5 mg/L.

6.3 Separation Factor R* for Ni or Co Sorption

From the Langmuir isotherm, separation factors R*s, for Ni and Co were calculated. The R* was used to check if the Ni and Co adsorptions under the experimental

conditions were favourable or not. This factor was calculated from equation 2.10 (see page 24).

$$R^* = \frac{1}{1 + bC_o} \qquad (6.1)$$

where, b is the Langmuir constant (L/mg), and C_o is the initial metal concentration (mg/L). Ni or Co adsorption is favourable if $0 < R^* < 1$, unfavourable if $R^* > 1$, irreversible if $R^* = 0$ and is of linear isotherm if $R^* = 1$. Table 6.6 summarizes the separation factors obtained at the experimental conditions for Ni and Co uptake on the saprist NL peat using the b values from Tables 6.1 and 6.2 for Ni and Co respectively.

Table 6.6: Calculated separation factors for Ni and Co adsorption

Peat dose	Ni separation factor,				Co separation factor,			
(g/L)	R* at pH				R* at pH			
	3	5.5	8	10	3	5.5	8	10
4	0.437	0.373	0.255	0.358	0.316	0.576	0.463	0.427
10	0.705	0.571	0.402	0.343	0.600	0.816	0.684	0.022
21	0.364	0.686	0.755	0.382	0.667	0.684	0.603	0.050
40	0.551	0.828	0.761	0.395	0.786	0.753	0.635	0.123

From Table 6.6, it can be concluded that Ni or Co uptake by the saprist NL peat was favourable since the experimental conditions gave $0 < R^* < 1$. This peat is therefore a good adsorbent for the treatment of wastewater containing Ni or Co over a wide pH range and at 10 fold peat changes.

6.4 Desorption of Adsorbed Metals

The extent to which the sorbed Ni or Co concentrations were held by the saprist NL peat was investigated with various concentrations of HCl. Desorption with water and HCl have been used in proposing the adsorption mechanisms of some peats from China (Zhipei et al., 1984) and when significant desorption was obtained with HCl, the adsorption mechanism was suggested to be ion exchange. The Ni or Co desorption results were reported as a percentage of the amount of metal desorbed compared with that initially adsorbed.

No significant Ni desorption was observed at pH 3 and no Co desorption at pHs of 3, 5.5 and 8. Ni however, showed significant desorption at all other pHs > 3, while Co was desorbed at pH 10 only (see Table 6.7). Maximum desorption of ~ 97% of the initially sorbed Ni was reported at pH 10 for a peat dose of 40 g/L (see Table 6.7). For Co, ~ 84% desorption was obtained at pH 10 for a 40 g/L peat dose (see Table 6.7). The detailed desorption results are presented in Appendix G.

Table 6.7: Percent Ni^{2+} and Co^{2+} desorbed by the addition of HCl on the peat-metal material

pH	Ci (mg/L)	HCl (M)	% of Co $C_{desorbed}$ at 40 g/L peat dose					% of Ni $C_{desorbed}$ at 40 g/L peat dose				
			C_1	C_2	C_3	C_4	C_5	C_1	C_2	C_3	C_4	C_5
	12.5	0.1	38.5	43.8	49.6	54.2	58.5	60.1	63.8	68.6	74	77.3
	25	0.2	42.8	50.1	55.4	59.2	63	69.6	75.5	79.9	83.7	86.5
10	50	0.5	50.6	62.5	66.7	65.4	69.1	78.5	81	87.2	90.5	93.5
	125	1	61.7	67.2	71	72.5	75.7	82.4	88.6	94.2	95.4	96.9
	200	2	67.1	70.9	77.3	80.1	83.5	87	92	96.1	96.8	97.5

where Ci was the initial metal concentration, and C_1, C_2, C_3, C_4 and C_5 were the concentrations of 12.5, 25, 50, 125 and 200 mg/L.

With Ni, desorption was observed at all solution pHs except at pH 3. At low pH, the reactive potential of functional groups in an adsorbent is unchanged but as the pH is increased, neutralization is introduced changing the reactivity and affinity of the functional groups with metals (Gupta et al., 2009). At pH 3 for Ni and Co, and at pHs of 5.5 and 8 for Co, the likely uptake reaction was complexation. At other pH (5.5, 8 and 10 for Ni and 10 for Co) ion exchange was the dominant uptake mechanism. With ion exchange, two carboxylic H^+ ions were exchanged by one Ni^{2+} or Co^{2+} ion where applicable. This exchange step was then reversed in the presence of the H^+ (as HCl), and the extent of reversal was indicated by the percent of the Ni^{2+} or Co^{2+} obtained.

6.5 Competitive Sorption Test

Wastewaters are generally complex in nature containing many cations, anions and organic compounds. The ability of the saprist NL peat to treat solutions with more than two cations was tested with a simulated wastewater containing Cd, Co, Ni, Pb and Zn. Five equal mass concentrations (200, 125, 50, 25 and 12.5 mg/L) of Cd^{2+}, Co^{2+}, Ni^{2+}, Pb^{2+} and Zn^{2+} was investigated in a competitive batch sorption test at an adjusted pH of 5.5 and at 4, 10, 21 and 40 g/L peat doses. The percent of the initial metal concentration sorbed is presented in Table 6.8, and the raw results and the calculated metals sorbed are presented in Tables G1 and G2 of appendix G.

Table 6.8: Percent of initial concentration of metal cations adsorbed in competitive batch adsorption test at pH 5.5

Peat dose (g/L)	Initial conc. (mg/L)	% of initial metal conc. adsorbed				
		Cd	Co	Ni	Pb	Zn
4	200	2	1	5.5	96.6	1.5
	125	9	3	24	97.5	2
	50	46	28	48	99	40
	25	68	56	68	99.6	60
	12.5	87.2	76.8	84	100	84
10	200	9.5	6	17	98.2	7.5
	125	47	34	54	99.3	39
	50	72	62	72	99.6	66
	25	88	80	88	100	83.2
	12.5	95.2	89.6	92.8	100	91.2
21	200	41.5	33	55.5	99.4	37.5
	125	74	62	78	99.5	68
	50	88	82	88	99.6	85.6
	25	95.2	92	94	100	93.2
	12.5	97.6	94.4	96.8	100	96
40	200	65.5	58	75.5	99.6	62.5
	125	85	81	88	99.5	83.6
	50	84	78	84	99.8	80.8
	25	97.2	94.8	96.8	100	95.6
	12.5	98.4	96.8	97.6	100	97.6

From Table 6.8, Pb was the most adsorbed with 100% reported at all the peat doses at metal concentrations of 12.5 and 25 mg/L. The sequence of adsorption was

generally $Pb^{2+} > Ni^{2+} > Cd^{2+} > Zn^{2+} > Co^{2+}$ at most peat doses with few exceptions depending on the metal concentration. For Ni or Co, the percent uptake slightly increased during competitive sorption when compared with a single ion system at peat doses greater than 4 g/L (Table 6.5, page 128).

With the competitive sorption at pH 5.5, it was evident that not all the active sites in the saprist NL peat were covered by the single ion system and this showed that this peat type is an efficient universal metal adsorbent. Competitive sorption data obtained at the experimental conditions did not fit the Langmuir or Freundlich adsorption isotherms. Competition could have enhanced the coverage of a large proportion of the active sites present in the saprist NL peat. An active site is made up of low and high metal affinity sites. The low affinity sites are occupied at high concentrations of metal while the high affinity sites are occupied at low metal concentrations (Kalymkova et al., 2008). Competition between metals could have led to the occupation of both sites at constant metal concentration as shown by the high metal uptake percentages.

6.6 Chapter Summary

The equilibrium sorption of Ni and Co by a saprist NL peat at different experimental conditions was investigated in this chapter. The Freundlich and Langmuir isotherms were used to assess the capacity of this peat and the trends observed were related to the metal uptake mechanisms at the various experimental conditions.

Ni was generally adsorbed more than Co due to a likely combination of ion exchange and complexation reactions especially at acidic pH (3, and 5.5). At pH of 8 and 10, ion exchange dominated the uptake mechanism resulting in lesser uptake of Ni when compared with Ni sorbed at pHs of 3 and 5.5. Co on the other hand could have been adsorbed via complexation only with the Co sorbed being less than that of Ni at most experimental conditions.

For both metals, sorption was dependent on metal concentration, solution pH and peat dose. Adsorbed metals at equilibrium increased with increased metal concentration. Two active sites containing different ligands could have existed in the peat. Kalymkova et al., (2008) reported that high metal affinity sites on the peat were occupied at low metal concentration while low metal affinity sites were occupied at high metal concentration. Increased metal concentrations, however, led to the decrease in percent metal uptake, a trend also reported Viraraghavan and Dronmraju (1993).

Increased peat dose provided more active sites which would be occupied by the cations. This was reflected in the percent of metals sorbed which increased with increasing peat doses, consistent with the conclusion of Sharma and Foster (1993), viz; as peat dose was increased, active sites become unsaturated leading to a higher removal efficiency. Competitive sorption test also showed that more sites were occupied in the presence of multiple cations.

Higher metal uptakes were reported at lower pHs which could have been due to the natural pH of the saprist peat. With complexation being less dependent on pH

compared to ion exchange, results suggested that at pH 3, complexation was dominant while ion exchange was dominant at pH 10.

CHAPTER SEVEN

FIXED BED LEACHING COLUMN RESULTS AND DISCUSSION

7.1 Chapter Overview

This chapter presents the results and discussion of the fixed bed leaching column for the uptake of 100 mg/L of Ni and Co at pH 5.5. Bed depth service time (BDST) equation was used to determine the adsorbent capacity and the adsorbent exhaustion rate. The cumulative Ni or Co accumulation on the layers within the fixed bed column to determine the active metal transfer zones, and the possible Ni or Co uptake mechanisms are also presented.

7.2 Fixed Bed Ni and Co Column Results

The column experiments provided an estimate of the adsorption capacity during continuous operations and the determination of the breakthrough points for Co and Ni adsorption on the saprist NL peat. In soil sorption processes, the breakthrough point is defined as occurring when the effluent concentration equals 50% of the initial influent concentration (Yong, 2001)

The Ni and Co influent pH 5.5 and concentration of 100 mg/L were chosen because the pH of 100 mg/L of Ni or Co solution at the room temperature of ~ 22°C was nearly 5.5 (100 mg/L of Ni had a pH of 5.6 and 100 mg/L of Co had a pH of 5.3) and both required minimal pH adjustment before use. The breakthrough curves are presented

in Figures 7.1a and 7.1b while the raw average effluent concentrations for 100 mg/L initial concentration of Ni at pH 5.5 at two flow rates on the saprist NL peat fixed bed column experiments are presented in Tables H1 and H2 of Appendix H.
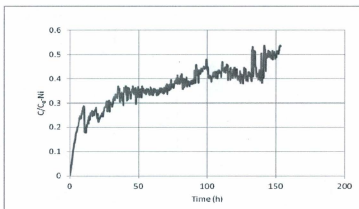
Fig. 7.1a: Breakthrough curve for Ni^{2+} adsorption at pH 5.5, conc., 100 mg/L, 22°C and at a flow rate of 1.0 L/h (data points at every 1 L).
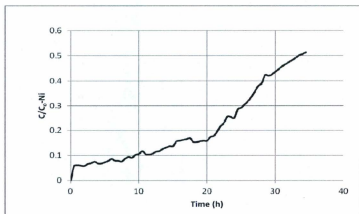
Fig. 7.1b: Breakthrough curve for Ni^{2+} adsorption at pH 5.5, conc., 100 mg/L, 22°C and at a flow rate of 2.0 L/h (data points at every 1 L).

The breakthrough for the 100 mg/L Ni concentration at pH 5.5 with the continuous downward flow of 1.0 L/h was obtained at 153 hours after 160 L of the solutions had been used while at a downward flow of 2.0 L/h, the breakthrough point was attained at 34 hours and after 63 L of the Ni solution had been treated. Maintaining the flow in a column experiment with the application of the BDST equation is known to be a limitation of the column experiment (Hutchins, 1973). The use of the variable speed peristaltic pump connected to the column exit helped maintain the linear flow. The pump speed was varied to maintain flow as the experiment progressed, but this contributed to the change in the breakthroughs which did not correspond exactly to the flow rates. Since breakthrough at a lower flow rate occurred after a larger volume had been treated, a lower flow rate that would allow more retention of Ni is therefore recommended for the design of adsorption column.

During the continuous downward flow fixed bed column experiment, Ni sorption gradually increased as the volume of influent increased. However, at some points, there were sharp decreases in the Ni effluent concentration corresponding to 11, 21, 29, 39, 49, 83, 90, 102, 124 and 140 L of the influent Ni solution. The sharp decrease in Ni effluent concentrations was pronounced at the lower downward flow rate of 1.0 L/h. Peat bed saturation will certainly require the consumption of a large volume of the 100 mg/L Ni concentration at pH 5.5, if attainable.

The pH of the Ni effluent concentration of the column corresponding to the points of decrease as monitored are presented in Table 7.1. Initial pH was 5.5 and the general pH of the effluent Ni concentration at the column exit was ~ 5.2.

Table 7.1: pH of Ni^{2+} concentrations at the column exit

Volume (L)	11	21	29	39	49	83	90	102	124	140
pH	4.9	4.8	4.9	4.7	4.7	4.7	4.9	4.9	4.8	4.7

From Table 7.1, the pHs at the points of decrease on the breakthrough curve in Figure 7.1a suggest that ion exchange was pronounced and significant at these points, compared to a general decrease of pH 0.3 otherwise. The overall retention trend suggests that a combination of ion exchange and complexation of Ni with the active sites could have accounted for the larger Ni uptake. The above trend corroborated the earlier suggestions from the kinetics and equilibrium batch and desorption studies where decrease in pH was attributed to ion exchange and relatively constant pH was attributed to complexation.

The breakthrough curves for the 100 mg/L initial Co concentration at pH 5.5 on the saprist NL peat in a continuous downward fixed bed column at flow rates of 1.0 and 2.0 L/h are presented in Figures 7.2a and 7.2b while the raw average Co effluent concentrations are shown in Table H3 and H4 of Appendix H.
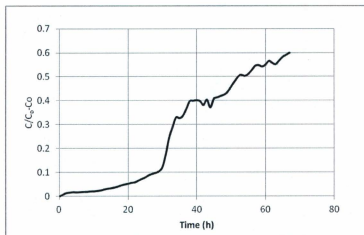
Fig. 7.2a: Breakthrough curve for Co^{2+} adsorption at pH 5.5, conc., 100 mg/L, 22°C and at a flow rate of 1.0 L/h (data points at every 1 L).
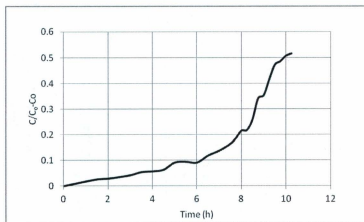
Fig. 7.2b: Breakthrough curve for Co^{2+} adsorption at pH 5.5, conc., 100 mg/L, 22°C and at a flow rate of 2.0 L/s (data points at every 1 L).

The breakthrough for the 100 mg/L Co concentration at pH 5.5 was obtained at 56 hours after 51 L of the Co solution had been used at a downward flow of 1.0 L/h. At the downward flow of 2.0 L/h, the breakthrough point was attained after 10 hours and 25 L of the 100 mg/L Co concentration solution had been used.

It was evident that less Co was retained compared to Ni at both flow rates although the two metals were retained more at the lower flow rates. At lower flow rate, the holding time of the solution in the column was higher and this allowed some measure of equilibrium to be attained leading to larger retention of the metals. At the higher flow rate, contact with the peat matrix was shorter and equilibrium attainment was far less; thus less retention was observed.

Ni and Co retentions could have been influenced by the uptake mechanisms and the products formed during the reaction. Although, Co was expected to be adsorbed more due to its larger ionic radii and lower heat of hydration (Table 5.3, page 83) compared to Ni, the products formed by the peat-Co interaction at the pH of 5.5, could have reduced the availability of more active sites for the Co uptake while Ni may not have behaved in the same way. Also at this pH (5.5), the kinetics investigation in this study suggested a likely combination of ion exchange and complexation for Ni uptake and these two reactions could have led to more Ni retention. Table 7.1 suggested that, ion exchange could have occurred at some zones along the column height during the sorption of Ni because of the drop in the effluent pH. These points also corresponded to the observed sharp declines in the profile of the Ni uptake at lower flow rate. With Co, lower flow rate did not give any significant effluent pH change.

At lower downward flow rates < 0.5 L/h, the experiment was discontinued after 300 L of 100 mg/L Ni at pH of 5.5 had been treated; the breakthrough point was not achieved at this time. Ni concentration in the effluent of the column decreased to about 0.08 mg/L with the first 20 L of the solution after which gradual increase was noted. This experiment was discontinued partly because of the large clogging effect noticed within the column that significantly reduced the flow and also because of the low exit concentration which was < 24 mg/L even after 300 L of solution had been treated. Although a lower flow rate of 0.5 L/h is desirable as more volume of the metal contaminated solution can be treated, the porosity of the saprist peat needs to be enhanced to maintain the flow rate. If porosity cannot be enhanced, a flow rate of 1.0 L/h is recommended for the adsorption column because better contact would be enhanced than at higher flow rates and more metal solution can be treated.

The saprist NL peat capacity in the column was determined using the simplified form of the equation 2.12 (page 25) given as equation 7.1 used in similar studies (Sharma and Forster, 1995; Volesky et al., 2003; Goel et al., 2005; Aksu and Gönen, 2006; Malkoc et al., 2006).

$$\ln\left(\frac{C_t}{C_o}\right) = kC_o t - N_o k \frac{H}{v} \qquad (7.1)$$

where, C_o and C_t were the influent and effluent concentrations (mg/L), with the C_t being the 50% of the C_o, k was the rate constant (L/mg.h), N_o was the adsorption capacity of the peat bed (mg/L), H was the effective height of the column (m), t was the time taken to attain the breakthrough (h) and v was the linear flow rate (m/h) obtained by dividing the

actual flow rate (cm^3/min) by the column cross sectional area (cm^2). A plot of $\ln\left(C_t/C_o\right)$ against t was used to determine k and N$_o$ at the breakthrough for the two flow rates for Ni and Co retentions. The results are summarized in Table 7.2. The plots in terms of volume treated are shown in Appendix I.

Table 7.2: Summary of Breakthrough constants from a simplified Bohart-Adams model

Flow rate (L/h)	Ni^{2+}						Co^{2+}					
	BV (L)	t$_{50}$ (h)	k x 10^{-6} (L/mg.h)	N$_o$*10^4 (mg/L)	AER (g/L)	r^2	BV (L)	t$_{50}$ (h)	k x 10^{-6} (L/mg.h)	N$_o$*10^4 (mg/L)	AER (g/L)	r^2
1.0	160	153	18	3.56	0.69	0.79	51	56	106	0.25	2.16	0.93
2.0	63	34	132	0.089	1.75	0.88	25	10	472	0.11	4.4	0.79

In Table 7.2, BV is the breakthrough volume (L), t$_{50}$ is the breakthrough time (h) and AER is the adsorbent exhaustion rate which is defined as the mass of adsorbent in column (g) per the treated volume (L) of liquid at breakthrough.

From Table 7.2, the kinetic rate constant, k, increased as the flow rate was increased. This implied that during the column test, the rate of transfer of Ni ions into the peat matrix was larger as the flow rate was increased. Similarly, the rate of Co ions transfer from solution to the peat matrix increased as flow rate was increased. With wide variations in values, the trend suggested that the adsorption mechanism of each metal was

not the same on the saprist NL peat. With small particle sized materials, cross linking of the material matrix is enhanced and intra particle diffusion is reduced during the ion exchange process. Ni was therefore suggested to be sorbed via ion exchange in the column. For Co, complexation with the ligands present at the active sites of the peat could have dominated the sorption reaction and as the flow rate was increased, the Co ions were quickly snatched from the solution thus giving a larger kinetic rate constant at higher flow rate.

The adsorption capacity of the peat bed, N_o, for Ni and Co decreased as the flow rate was increased. The observed trend could be related on one hand, to the attainment of equilibrium. At lower flow rate, longer contact between the peat matrix and metal ion was enhanced and equilibrium could be attained which led to lower adsorbent exhaustion rate in Ni and Co uptake in the peat column. On the other hand, variation in the uptake mechanism and products formation could have contributed to the observed values. While more Ni was sorbed, less Co was sorbed despite the promising nature of the initial Co uptake. The products that were formed by the peat-Co interaction could have gradually inhibited the sorption rate as the reaction progressed.

The AER as computed in Table 7.2 decreased as flow rate was increased. For Ni, 0.69 g/L at a flow rate of 1.0 L/h was computed, while for Co, 2.16 g/L at a flow rate of 1.0 L/h was computed. AER is one of the parameters that determine the capital and operating costs of a treatment system (the other is the empty bed residence time EBRT-time taken for liquid to fill empty column) (McKay and Ng, 2002). Low flow rate is therefore recommended for design purposes to achieve lower capital and operating costs.

146

The retentions of Ni and Co on a fixed saprist NL peat bed could be explained by the simplified Bohart–Adams model, since the regression coefficients were reasonable ranging between 0.79 and 0.99, with the sorption of Co giving higher regression coefficient values.

7.3 Effective Mass Transfer Zone

In fixed bed column adsorption, the zone that is first acted upon by the contaminant solution is referred to as the upstream and is always the point where a high initial concentration of the contaminant interacts with the column bed. This zone in a downward fixed bed column is expected to move downward as the bed gets saturated (Hutchins, 1973; Cooney, 1999) with the sorption of the metal in the solution by the active sites on the saprist NL peat. The behaviour of the movement of the saturated zone along the fixed bed is largely influenced by the establishment of equilibrium between the contaminant in solution and the fixed bed. The area covered by this equilibrium movement is the mass transfer zone which is often difficult to measure. Naja and Volesky (2006) suggested that the mass transfer zone (MTZ) is the region where the highest concentration of the contaminant in the solution phase is reduced to the lowest concentration i.e. the zone where sorption is most effective in the adsorbent.

In this study, the ratio of the accumulated metal concentration ($C_{acc.}$) at the selected depth to the initial metal concentration (C_o) was plotted against the column depth (H) from the inlet to determine the effective mass transfer zone along the column. Figure

7.3 depicts the results obtained for a flow rate of 1.0 L/h. The raw data from the analyzed spent saprist peat are presented in Appendix J.
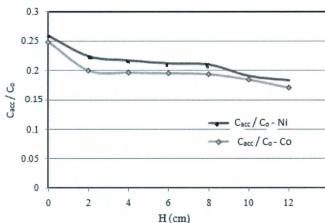
Fig. 7.3: Comparison of the mass transfer zone for Ni^{2+} and Co^{2+} column experiments at pH 5.5 for 100 mg/L metal concentration at flow rate of 1.0 L/h

Figure 7.3 shows that there was a decrease in the accumulation of metal retained along the column depth (with values given, representing the top layer of each marked depth). Exchange equilibrium is therefore not maintained along the column for the saprist NL peat for the adsorption of Ni and Co. Crist et al., (1996) expressed a contrary view using Ca-impregnated peat of similar organic content and pH. They stated that equilibrium was maintained, and increase in metal concentration was reported along the column depth. In this study, the metal concentration was observed to slightly decrease along the column depth except at the thin layer at the top of the column. It is evident from this study also, that within an adsorption zone in the column, only the top layer was

148

actively involved in metal retention because more of the metals' concentration was detected at this layer. This fact is corroborated by similar studies where it was reported that the retention of pollutants in peat was on the surface where a filtering layer was formed by accumulation which increased the retention capacity of particles (Perez et al., 2005), and Egger et al., (1980) reported that the trace metal concentration in a natural peat bog decreases as depth in the peat bog increases. The overall transfer zone pattern was similar for both Ni and Co as seen in Figure 7.3 with a steeper decrease observed at 2 cm followed by a slight decrease along the depth to the column exit.

Figure 7.3 suggests that the column top layer accounted for more uptake of Ni and Co than any other section. With this profile, a single long fixed bed column might not be an economical use for the saprist NL peat. Multiple columns with shorter heights operating in parallel (receiving the metal solution at the same time) or series (cascade arrangement) is recommended. This will allow for the efficient use of the peat.

7.4 Effect of Column Height on Ni and Co Retentions

The breakthrough for Ni and Co uptakes was tested at a flow rate of 1.0 L/h with three different column heights (5.5, 12.5 and 26.5 cm). Figure 7.4 shows the profile of the breakthrough time (t_{50}) versus the height of the column used. The data obtained during the study is presented in Appendix K. Foster and Sharma (1995) reported that if a plot of breakthrough time and column height passed through the origin, then, one uptake mechanism of the metal was involved in the adsorption. In Fig. 7.4, the data points did

not pass through the origin suggesting that more than one uptake reactions was involved in Ni and Co retentions on the saprist NL peat.
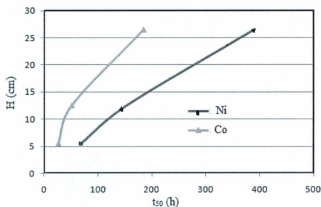
Fig. 7.4: Profiles of breakthrough time (t_{50}, h) against column height (H, cm) at pH of 5.5

From Figure 7.4, high Ni and Co uptakes were obtained at the highest peat bed height. This is due to the increased surface area and equivalent increase in the available active sites. Thus a longer breakthrough time was observed with the highest peat bed and larger percent of Ni and Co retentions obtained at this height, although more of Ni was retained compared with Co.

Figure 7.4 gave a nearly linear profile with the three column heights used for Ni compared with that of Co but did not pass through the origin in both cases which suggested that more than one uptake mechanism was involved in the Ni and Co sorption on the saprist NL peat at the pH of 5.5 in the fixed bed column. This observation corroborated earlier suggestions in this study in which the metals uptake mechanisms on

the saprist NL peat have been suggested to be dominated either by ion exchange or complexation, and a combination of both reactions depending on the solution pH.

7.5 Summary on Column Experiments

The column experiments were conducted with Ni or Co solution at pH 5.5 because the pH of the 100 mg/L concentration of the metals was nearly 5.5. Also, from the optimization results (see Table 5.4 page 83), a concentration of ~100 mg/L of Co was desirable for minimum peat dose and for comparison 100 mg/L Ni concentration was selected. In chapter 5, the batch kinetics study suggested that at pH 3, Ni and Co were predominantly sorbed by complexation. As the pH was increased, a combination of complexation and ion exchange was responsible for Ni uptake while Co was sorbed by ion exchange at pH 10. Results from the batch equilibrium adsorption experiments in chapter 6 corroborated the suggestions made in chapter 5. The results of the Ni and Co desorption tests with different concentrations of HCl in chapter 6 were significant in terms of the sorption mechanisms inferred especially with the change in metal solutions pH.

The results obtained in the column tests showed that more than one uptake reaction mechanisms were responsible for the retention of Ni at the selected pH 5.5 while, the retention of Co was mainly by a single mechanism. This was inferred based on the pHs of the effluent from the saprist NL peat column and the breakthrough pattern obtained for the two metals especially at a flow rate of 1.0 L/h (Figures 7.1a and 7.2a).

The conclusions drawn from the column experiments were therefore in tandem with those made in chapters 5 and 6.

7.6 Ni and Co Uptake Mechanisms

The uptake mechanisms for Ni and Co on the NL saprist peat were proposed based on the trends of results and observations made during the investigations, thus providing suitable explanations for the most likely chemistry of the sorption mechanisms leading to the removal of the metals. Chemisorption through ion exchange or complexation of the metal ions was the main uptake mechanism. While it is difficult to completely isolate metal uptake mechanisms, effort is made to justify the proposed uptakes within the scope of the experiments conducted for the chosen conditions.

The uptakes of Ni or Co could be described by the percent sorbed or the adsorbed quantity per mass of peat. For convenience, the percent sorbed was selected for the analysis of the uptake mechanism by the functional groups present on the surface of the saprist NL peat. Ni and Co retentions started at pH 3, and steadily increased to an optimum pH of 5.5 and 10 for Ni and Co respectively. This observation was consistent throughout the study using batch tests (in kinetic, equilibrium adsorption and desorption studies, and the Box-Behnke design).

At a solution pH of 3, there was no significant decrease in effluent solution pH during the batch tests with Ni or Co. This trend was the same for Co at all other solution pHs except at pH 10 where significant decrease in pH was observed. Ni uptake however, showed a decrease in solution pH at pH 5.5, 8 and 10. Decrease in solution pH is an

indication of the release of a proton with a corresponding increase in solution acidity (Ho, et al., 1995). Bond formation via the oxygenated functional groups accompanied by the release of a proton is therefore suggested as the main route for metal uptake on the NL saprist peat at these pHs with complexation either being slow or dormant.

The desorption test with various concentrations of HCl showed that a significant amount of Ni was desorbed when absorbed at pH 5.5, 8 and 10, and for Co, at pH 10 (Tables F1 and F2 of Appendix F). The percent metal removed increased with the concentration of HCl and the peat dose. Desorption was very poor at pH of 3 which suggested that the uptake of Ni at this pH was not completely ion exchange. Desorption test is a strong indication of ion exchange as suggested by Zhipei et al., (1984). Thus ion exchange is the dominant mechanism by which Ni was removed by NL saprist peat at the solution pHs of 5.5, 8 and 10 and at pH 10 for Co.

Ni uptake at pH 3 and Co uptake at pHs of 3, 5.5 and 8 is suggested to be primarily through complexation. During metal-peat complexation, the carboxyl, phenolic and possibly amine/amide functional groups are attacked by the positively charged metal ions leading to an initial peat-metal complex, a dinuclear intermediate (an intermediate with two metal ions attached to ligands that are linked, forming a singular compound) by which the removal of the ions took place. At these solution pHs, no significant change in pH was noticed.

Possibly accompanying the complexation reaction at pH 3 also, was the protonation of the sorption sites on the peat leading to the decrease in the ability of the material to retain initial metals resident in the peat. The sites vacated by the unretained

metals could have been occupied by the incoming cations of Ni or Co and this led to their removal in the solution. Thus at pH 3, initial metals present in the peat and deprotonation of carboxylic group caused by electronic re-arrangement could have combined to provides sites that were occupied by the attacking Ni and Co ions. If this is the case, all sites capable of complexing are first occupied before sites capable of exchanging protons get involved in metal uptake.

Kadlec and Keoleian (1986), suggested that carboxylic acid and phenolic hydroxyl groups in peat are the functional groups capable of complexing with metals such as Cu^{2+}, Pb^{2+}, and Zn^{2+}. In addition to these groups, the saprist NL peat contained nitrogen functional groups (amine and amide) and these could have acted as ligands which chelated or coordinated with Ni and Co, and enhanced their uptakes even at low solution pH. According to Henry et al., (1992), the potential of an anion to complex a cation is a function of the charge transfer of the metal-anion intermediate bond, which is determined by electronegativities of the intermediate complex, the anion and its protonated form. Ni is known to be slightly more electronegative compared to Co (Ni is 1.80 and Co is 1.75) (Henry et al., 1992) which could have accounted for higher Ni uptake at pH 3 compared to Co. At low pH, the solution is positively charged and when it came in contact with the peat surface which was initially negatively charged, complexation took place via the surface functional groups that led to the removal of Ni or Co.

As pH steadily increased, the peat surface which was originally negatively charged became surrounded by more hydroxyls with some functional groups at the active

sites being deprotonated. The ease of deprotonation could have been affected by the metal concentration and this could have affected the quantity of metal adsorbed. At pH 10, more of Ni and Co was adsorbed on the saprist NL peat with significant change in the equilibrium pH of the monitored filtrates.

The consistency of the adsorption data of Co over the pH range and peat dose, was an indication that uptake reactions have primarily followed a single reaction path which was possibly a change from complexation at pH 3 to ion exchange as the pH was increased. In the case of Ni, ion exchange and complexation reactions occurred simultaneously with the complexation reaction being the dominant at solution pH of 3. As the pH was increased, ion exchange became the main reaction. This was supported by the lack of 100 % Ni or Co desorption at the related pHs.

In ion exchange, the peat surfaces retained Ni or Co ions by the deprotonation of the active sites. The reaction is summarized in two steps by equations 7.2 and 7.3.

$$2SP-COH + M^{2+} \leftrightarrow (SP-CO)_2 M + 2H^+ \qquad (7.2)$$

$$SP-COH_2^{2+} + M^{2+} \leftrightarrow SP-COM^{2+} + 2H^+ \qquad (7.3)$$
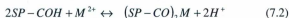
where C is carbon, O is oxygen, H is proton or hydrogen, SP is the peat surface, and M^{2+} is the Ni or Co ion.

On the peat surface (SP), a carbon-oxygen complex binds the metal ions by displacing protons. Equation 7.2 is the suggested route at low pH (acidic) while equation 7.3 is the suggested route as the pH was increased (basic pH).

CHAPTER EIGHT

CONCLUSIONS AND RECOMMENDATIONS

8.1 Chapter Overview

Conclusions and recommendations from this study are based on the use of untreated saprist Newfoundland peat as the adsorbent for Ni^{2+} and Co^{2+} from wastewater. Peat characteristics are known to be uniquely related to the location of harvest; consequently variations in the conclusions drawn from this study might be encountered. The study employed saprist Newfoundland peat as the adsorbent for Ni and Co retention from a simulated water. Kinetics experiments in batch mode were pseudo-second order, and equilibrium adsorption tests fitted the Langmuir and Freundlich isotherms from which the adsorptive capacity of the saprist peat was computed.

Desorption tests showed that Co was predominantly sorbed by complexation of its ion with the active sites through the presence of ligands in the peat matrix while Ni was sorbed by a combination of ion exchange and complexation depending on the solution pH. Competitive sorption tests showed that not all the active sites were occupied in a single ion system and competition enhanced the adsorption of Ni and Co especially at lower metal concentrations. Continuous downward flow column experiments suggested that more Ni was sorbed compared with Co, at a flow rate of 1.0 L/h. The use of a monovalent metal would present a completely different observation compared to the trends reported in this study.

8.2 Conclusions

The following were the conclusions drawn from the research:

1. Saprist NL peat that was characterized using analytical techniques (XRD, SEM, FTIR, and ^{13}C-NMR) and the techniques did not involve the destruction of the material. This study showed the presence of highly oxygenated functional groups and amine/amide groups that could be involved in ion exchange or complexation of metals. ICP-MS results showed that the peat contained several metals, especially Ca, Fe, and Mn in proportions > 100 mg/L.

2. The application of the response surface method through the Box-Behnken design, statistically showed that interactions of concentration/peat dose (50 mg/L and 14 g/L or 200 mg/L and 28 g/L), and peat dose/pH (28 g/L and pH 4.9) were important in the optimum Ni adsorption by the saprist NL peat. On the other hand, the interactions of concentration/pH (~ 100 mg/L and pH 6.5), and peat dose/pH (~30 g/L and pH 6.5) were vital in the optimum Co adsorption by the saprist NL peat.

3. From the interactions of the factors in the Box- Behnken design and by monitoring the effluent pHs during kinetic and desorption tests of Ni and Co sorptions, the data obtained suggested that more than one reaction was involved in the metal sorption chemistry on the saprist NL peat depending on the solution pH, concentration and peat dose.

4. From the response surface method using the Box-Behnken design, optimum batch operational conditions for Ni retention was at a peat dose between 25 and 40 g/L

for solution pH of 3 and Ni concentration ≤ 50 mg/L. For optimum Co uptake, a peat dose of 32 g/L for a solution pH of ~ 6 and Co concentration of 25 mg/L are the desirable operational conditions.

5. Kinetic tests showed that Co was more rapidly sorbed compared with Ni and generally attained equilibrium after 1 h, although more Ni was sorbed over the 12 h experiment time compared with Co. The maximum Ni adsorbed at equilibrium in a 12 h study, 385 mg/g, was obtained at a solution pH of 5.5, peat dose of 21 g/L and a Ni concentration of 125 mg/L and for Co, the maximum adsorbed quantity was 33 mg/g at pH 8, a peat dose of 2 g/L and Co concentration of 200 mg/L.

6. The equilibrium adsorption over a 24 h period showed that the data fitted Freundlich and Langmuir isotherms with regression coefficients near unity. Adsorption efficiencies increased with peat dose at low metal concentrations and pH 3 but the adsorbed quantity per unit mass of peat used decreased with increasing peat dose. The maximum Langmuir monolayer saturation capacity of the peat for Ni was 61.35 mg/g at solution pH of 3 and for a peat dose of 40 g/L; while, the corresponding value for Co, it was 60.98 mg/g at pH of 5.5 and for a peat dose of 10 g/L. For the Freundlich isotherm constant, a maximum value of 1.18 $mg^{(1-n)}kg^{-1}L^{1/n}$ at solution pH of 5.5 and for a peat dose of 21 g/L was computed while for Co, it was 0.32 $mg^{(1-n)}kg^{-1}L^{1/n}$ at solution pH of 3 for a peat dose of 4 g/L.

7. The competitive sorption test at a constant solution pH 5.5, showed that the peat maintained its metal removal capacity with a multi-metal system and Ni and Co adsorptive capacities were enhanced at metal concentrations ≤ 50 mg/L at peat doses ≥ 21 g/L.

8. The fixed-bed column experiments with a 6 cm diameter, 12.5 cm effective peat depth, flow rates of 1.0 and 2.0 L/h which gradually decreased as the peat matrix became saturated, and a solution pH 5.5 for 100 mg/L Ni and Co were reasonable operational parameters that gave a breakthrough for Ni at a volume of 160 L and for Co, at 51 L at the lower flow rate. The breakthrough showed that lower flow rates would enhance better contact and retention of the metals.

9. The modified Bohart-Adams model gave maximum adsorption capacity of 35.6 g/L at flow rate of 1.0 L/h for Ni adsorption at a constant solution pH 5.5. The maximum adsorption capacity of 2.5 g/L at a flow rate of 1.0 L/h was computed for Co also at a constant solution pH 5.5. The AER for Co was generally more than twice that of Ni, which suggested that capital and operating cost of treating Co using the saprist NL peat would be higher for Co compared to Ni.

10. The column experiment showed that more metal adsorption took place at the top layer than at the bottom and not all the layers within the peat depth were actively involved. With a slower flow rate, a higher contact time with the peat surface was achieved and a larger volume of metal solution was treated (160 L for Ni and 56 L for Co).

11. Monitored effluents pH at the end of each litre of solution showed a decrease at some points (> 0.5 units), which corresponded to a possible change in the dominant reaction. This trend was obvious with Ni sorption compared to Co sorption. The decrease in pH was attributed to ion exchange as the dominant sorption reaction.

12. The trend of results at various solution pHs and the desorption tests (no desorption at pH of 3 for both metals) suggested that Ni uptake on the saprist NL peat was a combination of ion exchange and complexation while, Co was sorbed mainly by complexation at solution pH below 10 and above this pH, ion exchange dominated the uptake chemistry. Ion exchange gave higher percentage of metal removal results compared to complexation.

13. The research showed that metal adsorption on the saprist NL peat was metal ion specific and concentration specific, solution pH specific and peat dose dependent while; the uptake chemistry was metal ion and solution pH dependent.

8.3 Original Contributions

Fibrist peat has been widely investigated as a metal adsorbent. This study is the first attempt at using air dried NL saprist peat characterized in its natural state, as an adsorbent for Ni and Co in batch and column experiments. This study established that optimum reaction conditions exist for the maximum uptake of Ni and Co at minimum peat dose. For Ni, the peat dose/concentration and, solution pH/peat dose should be optimized while for Co, solution pH/concentration and, peat dose/solution pH should be

optimized. The saprist NL peat – metal reaction was strongly influenced by the solution pH and large adsorbed metal quantities were obtained under acidic conditions.

The saprist peat contained a large number of active sites as shown by the competitive sorption at pH 5.5 and the percentages of Ni and Co retained were near those at single ion uptake on the peat. The study established that the adsorbent exhaustion rate of the saprist NL peat for Ni was lower than that of Co at a solution pH of 5.5. Desorption with 0.1 M to 2 M HCl and other data during the batch and column experiments suggested that the metals were retained by chemisorption with complexation being the possible route at acidic conditions and ion exchange at basic conditions.

8.4 Recommendations

The use of the saprist NL peat as a Ni and Co adsorbent was investigated in this study. While the availability, application and capacity of the peat to remove metals from wastewater cannot be argued, further studies are needed in order to maximize the potential of this adsorbent to reduce or eliminate under utilization and wastage during applications. The following are recommended:

1. Untreated saprist Newfoundland peat was used in the study. Impregnation with acid, Ca^{2+}, Fe^{3+} and or a monovalent metal or acid washing is suggested. This will further increase the homogeneity in the saprist NL peat.

2. Adsorption trends in terms of the Freundlich and Langmuir parameters were not established under certain conditions investigated. This might not be unconnected

with some materials that could be present in the peat interfering with the peat-metal chemistry. Further investigations to ascertain the level of this interference are suggested.

3. Functional groups identified by FTIR and ^{13}C-NMR could be masked by appropriate masking agents to gain further insight into the sequence of metal uptake reactions.

4. Column experiments showed that adsorption was not effectively distributed along the depth of the column. To reduce peat wastage or under utilization, the peat should be treated by aeration to allow oxidation of the matrix. Counter flow aeration is recommended as this will allow the dispersion of the solution increasing contact with overlapped active sites and improve overall column efficiency. The impact of this form of additional treatment step should be investigated.

5. Saprist Newfoundland peat contained extremely small particle sizes. There was a continuous collapse and overlapping of these particles when packed. This reduced porosity and increased clogging. The mechanism of peat clogging and overall peat-solution hydrodynamics should be studied to improve the column efficiency

6. Shorter columns either in parallel or series are recommended for use since the cumulative metal adsorbed decreased down the peat bed.

REFERENCES

Aaby, B. and Berglund, B. E. (1986): Characterization of Peat and Lake Deposits, In Berglund B. E. (Ed): Handbook of Holocene Palaeoecology and Palaeohydrology, John Wiley & Sons Ltd, pp 231 – 246.

Ajmal, M., Khan, A. H., Ahmad, S. and Ahmad, A. (1998): Role of Sawdust in the Removal of Copper (II) from Industrial Wastes, Water Research, Volume 32, Number. 10, pp 3085 – 3091.

Aksu, Z. And Gönen, F. (2006): Binary Biosorption of Phenol and Chromium(VI) onto Immobilized Sludge in a Packed Bed: Prediction of Kinetic Parameters and Breakthrough Curves, Separation and Purification Technology, Volume 49, Issue 3, pp 205 – 216.

Al-Duri, B., (1995): Adsorption Modeling and Mass Transfer, In McKay G. (Ed): Use of Adsorbents for the Removal of Pollutants from Wastewaters, CRC Press, New York, pp 134 – 173.

Al-Faqih, L., Johnson, P. D. and Allen, S. J. (2008): Evaluation of a New Peat-Based Sorbent for Metals Capture, Bioresource Technology, Volume 99, Issue 5, pp 1394–1402.

Allen S. J. (1987): Equilibrium Adsorption Isotherms for Peat, Fuel, Volume 66, Issue 9, pp 1171 – 1175.

Alloway, B. J. (1995): Heavy Metals in Soils, 2nd Edition, Blackie Academic and Professional London, p 3.

Almendros G., Knicker H., Gonzalez-Vila, J. (2003): Rearrangement of Carbon and Nitrogen forms in Peat after Progressive Thermal Oxidation as Determined by Solid State ^{13}C and ^{15}N-NMR Spectroscopy, Organic Geochemistry, Volume 34, Issue 11, pp 1559 - 1568.

Andreasson, A., Jönsson, B. and Lindman, B. (1988): Surface and Colloid Chemistry of Peat Dewatering (Electrostatic Effects), Colloid and Polymer Science 266, pp 164 - 172.

Annadurai, G., Juang, R-S. and Lee, D-J. (2002a): Factorial Design Analysis for Adsorption of Dye on Activated Carbon Beads incorporated with Calcium Alginate, Advances in Environmental Research, Volume 6, Issue 2, pp 191 – 198.

Annadurai, G., Juang, R-S. and Lee, D-J. (2002b): Adsorption of Heavy Metals from Water using Banana and Orange Peels, Water Science Technology, Volume 47, Number. 1, pp 185 - 190.

Artz, R.R.E., Chapman, S.J., Robertson, A.H.J., Potts, J.M., Laggoun-Défarge, F., Gogo, S., Comot, L., Disnar, J.R., and Francez, A.J. (2008): FTIR spectroscopy can be used as a screening tool for organic matter quality regenerating cutover peatlands, Soil Biology and Biochemistry, Volume 40, Number 2, pp 515 - 527.

ASTM D1997 - 91 (2008): Standard Test Method for Laboratory Determination of the Fiber Content of Peat Samples by Dry Mass, ASTM International, West Conshohocken, PA. DOI: 10.1520/D1997-91R08E01.

ASTM D2974-07A (2007): Standard Test Methods for Moisture, Ash, and Organic Matter of Peat and Other Organic Soils, ASTM International, West Conshohocken, PA. DOI: 10.1520/2974-07A.

ASTM D2976-71 (2004): Standard Test Method for pH of Peat Materials, ASTM International, West Conshohocken, PA. DOI: 10.1520/D2976-71R04.

ASTM D4531-86 (2008): Standard Test Methods for Bulk Density of Peat and Peat Products, ASTM International, West Conshohocken, PA. DOI: 10.1520/D4531-86R08.

Babarinde, N. A. A. (2002): Adsorption of Zinc (II) and Cadmium (II) by Coconut Husk and Goat Hair, Journal of Pure and Applied Sciences, Volume 5, Issue, pp 81 – 85.

Babel, S. and Kurniawan, T. A. (2003): Low-Cost Adsorbents for Heavy Metals Uptake from Contaminated Water – a Review, Journal of Hazardous Materials, Volume 97, Issues 1 – 3, pp 219 – 243.

Bailey, S. E., Olin, T. J., Bricka, R. M., and Adrian, D. D. (1999): A Review of Potentially Low-Cost Sorbents for Heavy Metals, Water Research, Volume 33, No. 11, pp 2469 – 2479.

Baldock, J. A., Oades, J. M., Waters, A. G., Peng, X., Vassallo, A. M. and Wilson, M. A. (1992): Aspects of the chemical structure of soil organic materials as revealed by solid-state[13]C NMR spectroscopy, Biogeochemistry, Volume 16, Number 1, pp 1 - 42.

Baltpurvins, K. A., Burns, R. C. and Lawrance, G. A. (1996): Heavy Metals in Wastewater: Modelling the Hydroxide Precipitation of Cu(II) from Wastewater using Lime as the Precipitant, Waste Management, Vol. 16, No. 8, pp 717 – 725.

Baran, A., (2002): Characterization of Carex Peat using Extinction Values of Humic Acids, Bioresource Technology, Volume 85, Issue 1, pp 99 – 101.

Barrett, J. (2003): Inorganic Chemistry in Aqueous Solution, RSC-Publishers, 128 – 129.

Bel' kevich, P. I., Chistova, L. R., Rogach, L. M. and Sobol, M. I. (1980): Selective Sorption of Cations by Peat, Solid Fuel Chemistry (Khimiya Tverdogo Topliva), Volume 14, Number 4, pp 146 – 151.

Benjamin, M. M., Sletten, R. S., Bailey, R. P. and Bennett, T. (1996): Sorption and Filtration of Metals Using Iron-Oxide Coated Sand, Water Research, Volume 30, Number 11, pp 2609 – 2620.

Bhattacharyya, D., Jumawan (Jr.) A. B. and Grieves, R. B. (1979): Separation of Toxic Heavy Metals by Sulfide Precipitation, Separation Science and Technology, Volume 14, Number 5, pp 441 – 452.

Blais, J. F., Shen, S., Meunier, N. and Tyagi, R. D. (1976): Comparison of Natural Adsorbent for Metal Removal from Acidic Effluent, Environmental Technology Volume 24, Number 2, pp 205 – 215.

Blanachard, G., Maunaye, M. and Martin, G. (1984): Removal of Heavy Metals from Water by means of Natural Zeolites, Water Research, Volume 18, Number 12, pp 1501 – 1507.

Bloom, P. R. and McBride, M. B. (1979): Metal Ion Binding and Exchange with Hydrogen Ions in Acid-Washed Peat, Soil Science Society of America Journal, Volume 43, Issue 4, pp 687 – 692.

Bohlin, E., Hämäläinen, M. and Sunden, T. (1989): Botanical and Chemical Characterization of Peat Using Multivariate Methods, Journal of Soil Science, Volume 147, Number 4, pp 252 – 263.

Bowders, J. J., Daniel, D. E., Broderick, G. P. And Lijestrand, H. M. (1985): Methods for Testing the Compatibility of Clay Liners with Landfill Leachate, ASTM Special Technical Publication, pp 230 – 250.

Box, G. E. P., Hunter, W. G. and Hunter, J. S. (2005): Statistics for Experimenters: An Introduction to Design, Data Analysis and Model Building, John Wiley and Sons, 2nd Edition, pp 510 – 534.

Bozkhurt, S., Lucisano, M., Moreno, L and Neretnieks, I. (2001): Peat as a Potential Analogue for the Long - Term Evolution in Landfills, Earth - Science Reviews, Volume 53, Issue 1- 2, pp 95 - 147.

Bozzola, J. F. (2007): Conventional Specimen Preparations Techniques for Scanning Electron Microscopy of Biological Specimens In Kuo, J. (Ed): Electron Microscopy: Methods and Protocols, Methods in Molecular Biology 369, Humana Press Inc. USA, pp 449 – 466.

Brigatti, M. F., Campana, G., Medici, L. and Poppi, L. (1996): The Influence of Layer Charge on Zn^{2+} and Pb^{2+} Sorption by Smectites, Clay Minerals, Volume 31, Number 4, pp 477 – 483.

Brown, P. A., Gill, S. A. and Allen, S. J. (2000): Metal Removal from Wastewater Using Peat (Review Paper), Water Research, Volume 34, Number 16, pp 3907 – 3916.

Bunzl, K. (1974): Kinetics of Ion Exchange in Soil Organic Matter – II. Ion Exchange during Continuous Addition of Pb^{2+} ions to Humic Acid and Peat. Journal of Soil Science, Volume 25, Number 3, pp 343 – 356.

Campbell, D. R., Lavoie, C. and Rochefort, L. (2002): Wind Erosion and Surface Stability in Abandoned Milled Peatlands, Canadian Journal of Soil Science, Volume 82, Number 1, pp 85 – 95.

Canadian Mining (2008): www.theallineed.com/chemistry/06081812.htm accessed, 26th November, 2008.

CDC, (2008): Center for Disease Control and Prevention, www.cdc.gov/ accessed 10th February, 2008.

Chen, X.-H., Gosset, T. and Thévenot, D. R. (1990): Batch Copper Ion Binding and Exchange Properties of Peat, Water Research, Volume 24, Number 12, pp 1463 – 1471.

Chen, Z., Xing, B. and McGill, W. B. (1999). A unified sorption variable for environmental applications of the Freundlich isotherm, Journal of Environmental Quality, Volume 28, Number 5, pp 1422–1428.

Chiou, C. T. (2002): Partition and Adsorption of Organic Contaminants in Environmental Systems, John Wiley and Sons Inc., p 56.

Coates, J. (2000): Interpretation of Infrared Spectra, A Practical Approach, in Meyers, R. A. (Ed.) Encyclopaedia of Analytical Chemistry, John Wiley & Sons Ltd., Chichester, UK, pp 10815 - 10837.

Cooney, D. O. (1999): Adsorption Design for Wastewater Treatment, Lewis Publishers, US, pp 43 – 51.

Couillard, D. (1994): The use of Peat in Wastewater Treatment, Water Research, Volume 28, Number 6, pp 1261 – 1274.

Couillard, Y., Courcelles, M., Cattaneo, A. and Wunsam, S. (2004): A Test of Integrity of Metal Records in Sediment Cores Based on the Documented History of Metal Contamination in Lac Dufault (Québec, Canada), Journal of Paleolimnology, Volume 32, Issue 2, pp 149 – 162.

Coupal, B. and Lalancette, J.-M. (1976): The Treatment of Wastewaters With peat Moss, Water Research, Volume 10, Issue 12, pp 1071 – 1076.

Crist, R. H., Martin, J. R., Chonko, J. and Crist, D. R. (1996): Uptake of Metals on Peat Moss: An ion Exchange Process, Environmental Science and Technology Volume 30, Number 8, pp 2456 – 2461.

Crum, H. A. and Planisek, S. (2004): A Focus on Peatlands and Peat Mosses, University of Michigan Press, pp 180 – 182.

Czitrom, V. (1999): One Factor at a Time versus Designed Experiments, the American Statistician, Volume 53, pp 126 – 131.

Çiftçi, H., Ölçücü, A. and Çiftçi, T. (2007): The Determination of Nickel in Some Plants with Reversed-Phase High Performance Liquid Chromatography (HPLC), International Journal of Science and Technology, Volume 2, Number 2, pp 105 – 108.

Dachnowski, A. (1912): Peat Deposits of Ohio: their origin, formation and uses, Geological Survey of Ohio, Bulletin 16, Columbus (Ohio), pp 8-9.

Daigle, Jean-Yves and Gautreau-Daigle, H. (2001): Canadian Peat Harvesting and the Environment, second edition, Sustaining Wetlands Paper Series, Issues Paper Number 1.

De Zuane, J. (1997): Handbook of Drinking Water Quality, Second Edition, John Wiley and Sons, pp 102 - 103.

Dickerson, B. W. and Brooks, R. M. (1950): Neutralization of Acid Wastes, Industrial and Engineering Chemistry, Volume 42, Number 4, pp 599 – 605.

Dissanayake, C. B. and Weerasooriya, S. V. R. (1981): Peat as a Metal-Trapping Material in Purification of Industrial Effluents, International Journal of Environmental Studies, Volume 17, Number 3, pp 233 – 238.

Drury, W. J. (1999): Treatment of Acid Mine Drainage with Anaerobic Solid-Substrate Reactors, Water Environment Research, Volume 71, Number 6, pp 1244 – 1250.

Duer, M. J. (2004): Introduction to Solid – State NMR Spectroscopy, Blackwell Publishing Ltd., pp 56 -58.

Durig, D. T., Esterle, J. S., Dickson, T. J. and Durig, J. R. (1988): An Investigation of the Chemical Variability of Woody Peat by FT-IR Spectroscopy, Applied Spectroscopy, Volume 42, Number 7, pp 1239 - 1244.

Eccles, H. (1999): Treatment of Metal Contaminated Wastes: Why Select a Biological Process? Trends in Biotechnology, Volume 17, Issue 12, pp 462 – 465.

Eckenfelder, W. W. (2000): Industrial Water Pollution Control, McGraw-Hill Series in Water Resources and Environmental Engineering, 3rd Ed. Pp 581 – 585.

Egerton, R. F. (2005): Physical Principles of Electron Microscopy: An Introduction to TEM, SEM and AEM, Springer USA, pp 17 - 19, 143-150.

Egger, P., Lapakko, K., and Otterson, P. (1980) Trace Metal Uptake By Peat: Interaction of a White Cedar Bog and Mining Stockpile Leachate, Proceedings of the 6th International Peat Congress, Duluth Arena- Auditorium, Duluth, Minnesota, USA, pp 542 – 547.

Evangelou, V. P. (1998): Environmental Soil and Water Chemistry – Principles and Applications, John Wiley and Sons, Inc., p 167.

Evans, L. J. (1989): Chemistry of Metal Retention by Soils, Environmental Science Technology, Volume 23, Number 9, pp 1046 – 1056.

FAO (2008): Food and Agricultural Organization, www.fao.org accessed, 20th November, 2008.

Fong, S. S., and Mohamed M., (2007): Chemical Characterization of Humic Substances Occurring in the Peats of Sarawak, Malaysia. Organic Geochemistry, Volume 38, Issue 6, pp 967 – 976.

Forsberg, S., and Aldén, L. (1989): Dewatering of Peat: Characterization of Colloidal and Subcolloidal Particles in Peat, Colloids and Surfaces, Volume 34, Number 4, pp 335 – 343.

Fox, P. J. and Edil, T. B. (1996): Effect of Stress and Temperature on Secondary Compression of Peat, Canadian Geotechnical Journal, Volume 33, Issue 3, pp 405 - 415.

Frausto da Silva, J. J. R. (1983): The Chelation Effect Redefined, Journal of Chemical Education, Volume 60, Issue 5, pp 390 – 392.

Goel, J., Kadirvelu, K., Rajagopal, C. And Garg V. K. (2005): Removal of Lead (II) by Adsorption using treated Granular Activated Carbon: Batch and Column Studies, Journal of Hazardous Materials, Volume B125, Issue 1 – 3, pp 211 – 220.

Gondar, D., Lopez, R., Fiol, S., Antelo, J. M. and Arce, F. (2005): Characterization and Acid-Base Properties of Fulvic and Humic Acids isolated from two Horizons of an Ombrotrophic Peat Bog, Geoderma, Volume 126, Issues 3 – 4, pp 367 – 374.

Gosset, T., Trancart, J. L. and Thevenot, D. R. (1986): Batch Metal Removal by Peat Kinetics and Thermodynamics, Water Research, Volume 20, Number 1, pp 21 – 26.

Griffin, R. A., and Roy, W. R. (1985): Interaction of Organic Solvents with Saturated Soil-Water Systems: Environmental Institute for Waste Management Studies, Open Report 3, University of Alabama, p 86.

Griffiths, P. R. and de Haseth, J. A. (1986): Fourier Transform Infrared Spectrometry, 2nd Edition, Wiley-Interscience Publication, pp 19 - 75.

Hashem, A., Abdel-Halim, E. S., El-Tahlawfy, Kh. F. and Hebeish A. (2005): Enhancement of the Adsorption of the Adsorption of Co(II) and Ni (II) onto Peanut Hulls through Esterification using Citric Acid, Adsorption Science and Technology, Volume 23, Issue 5, pp 367 – 380.

Helfferich, F. (1962): Ion Exchange, McGraw-Hill Book Company, New York, pp 5 - 9.

Henry, M., Jolivet, J. P. and Livage, J. (1992): Aqueous Chemistry of Metal Cations: Hydroysis, Condensation and Complexation, Structure and Bonding, Volume 77/1992, pp 153 – 206.

Higgins, T. H. and Sater, V. E. (1984): Combined Removal of Cr Cd and Ni from Wastes, Environmental Progress, Volume 3, Number 1, pp 12–25.

Ho, Y. S. and McKay, G. (1999): Competitive Sorption of Copper and Nickel Ions from Aqueous Solution Using Peat, Adsorption, Volume 5, Number 4, pp 409–417.

Ho, Y. S., Wase, D. A. J. and Forster, C. F. (1995): Batch Nickel Removal from Aqueous Solution by Sphagnum Moss Peat, Water Research, Volume 29, Issue 5, pp 1327–1332.

Ho, Y. S., Wase, D. A. J. and Forster, C. F. (1996): Kinetics Studies of Competitive Heavy Metals Adsorption by Sphagnum Moss Peat, Environmental Technology, Volume 17, Issue 1, pp 71 – 77.

Huang, S-D., Huang, M-K., Gua, J-Y., Wu, T-P, and Huang, J-Y. (1988): Simultaneous Removal of Heavy Metal Ions from Wastewater by Foam Separation Techniques, Separation Science and Technology, Volume 23, Number 3 and 5, pp 489–505.

Huang, Y-C. and Koseoglu, S. S. (1993): Separation of Heavy Metals from Industrial Waste Streams by Membrane Separation Technology, Waste Management, Volume 13, Issues 5 – 7, pp 481 – 501.

Hutchins, R. (1973): New Method Simplifies Design of Activated Carbon Systems, Chemical Engineering, Volume 80, Issue 19, pp 133 – 138.

IARC (1990): Chromium, Nickel and Welding, International Agency for Research on Cancer Monographs on the Evaluation of Carcinogenic Risk of Chemicals to Humans, Volume 49, Lyon, France, pp 677.

Irish Peatland Conservation Council (1998): www.ipcc.ie accessed, 20th October, 2007.

Ismail, A. A., El-Midany, A. A., Ibrahim, I. A. and Matsunaga, H. (2008): Heavy Metal Removal using SiO_2-TiO_2 Binary Oxide: Experimental Design Approach, Adsorption, Volume 14, Number 1, pp 21–29.

Jaeger, L., and Erdöes, E. A. (1956): A General Formula of Multi-component Adsorption, Collection of Czechoslovakia Chemical Communication, Volume 24, p 2851.

Jha, I. N., Iyengar, L. and Prbhakara Rao, A. V. S. (1988): Removal of Cadmium Using Chitosan, Journal of Environmental Engineering, Volume 114, Issue 4, pp 926 – 974.

Jones, C. J. (2001): d- and f- Block Chemistry, RSC-Publishers, pp 71 – 96.

Kadlec, R. H., and Keoleian, G.A., (1986): Metal Ion Exchange on Peat, In Fuchsman C. H., (Ed): Peat and Water: Aspects of Water Retention and Dewatering, Elsevier Applied Science Publishers Ltd, pp 61- 93.

Kalmykova, Y., Strömvall, A-M. and Steenari, B-M. (2008): Adsorption of Cd, Cu, Ni, Pb and Zn on Sphagnum Peat from Solutions with Low Metal Concentrations, Journal of Hazardous Materials, Volume 152, Issue 2, pp 885 – 981.

Kapoor, A., Ritter, J. A. and Yang, R. T. (1989): On the Dubinin-Radushkevich Equation of Adsorption in Microporous Solids in the Henry's Law Region, Langmuir, Volume 5, Issue 4, pp 1118 – 1121.

Kerr, W. A. (1905): Peat and its Products; an Illustrated Treatise on Peat and its Products as a National Source of Wealth, Begg, Kennedy and Elder Publication, Glasgow, pp 1–15.

Kertman, S., Kertman, G. and Chibrikova, Z. (1993): Peat as a Heavy-Metal Sorbent, Russian Journal of Applied Chemistry, Volume 66, Number 2, pp 382 – 383.

Koretsky, C. (2000): The significance of Surface Complexation Reactions in Hydrologic Systems: A Geochemist's Perspective, Journal of Hydrology, Volume 230, Number 3, Elsevier, pp 127 – 171.

Kumar, U. and Bandyopadhyay, M. (2006): Sorption of Cadmium from Aqueous Solution using Pretreated Rice Husk, Bioresource Technology, Volume 97, Issue 1, pp 104 – 109.

Kurniawan, T. A., Chan, G. Y. S., Lo, W. H. and Babel, S. (2005): Comparisons of Low Cost Adsorbents for Treating Wastewaters Laden with Heavy Metals, Science Total Environment, Volume. 366, Issue 2-3, pp 409 – 426.

Kuziemska, I. and Quant, B. (1998): Peat as a Sorbent for Heavy Metal Removal from Water and Wastewater, The Proceedings of Green, the International Symposium on Geotechnics Related to Environment, Volume 2, pp 308 – 312.

Lagergren, S. (1898): Zur Theories der Sogenannten Adsorption Gelöster Stoffe, Journal Kungliga Svenska Vetenskapsakademiens, Handlingar, Volume 24, pp 1 – 39.

Lange, N. A. and Speight, J. G. (2005): Lange's handbook of Chemistry, 16th Ed., McGraw-Hill, Inc.

Lee, S-H. and Yang, J-W. (1997): Removal of Copper in Aqueous Solution by Apple Wastes, Separation Science and Technology, Volume. 32, Issue 8, pp 1371 – 1387.

Leslie, M. E. (1974): Peat: New Medium for Treating Dye House Effluent, American Dyestuff Reporter, Volume 63, pp 15 - 18.

Li, H., Parent, L. E., Karam, A. and Tremblay, C. (2004): Potential of Sphagnum Peat for improving Soil Organic Matter, Water Holding Capacity, Bulk Density and Potato Yield in a Sandy Soil, Plant and Soil Volume 265, Number 1 – 2, pp 355 - 365.

Malkoc, E., Nuhoglu, Y. and Dundar, M. (2006): Adsorption of Chromium(VI) on Pomace – An Olive Oil Industry Waste: Batch and Column Studies, Journal of Hazardous Materials B138, Issue 1 – 2, pp 142 – 151.

Mao, J-D., Hu, W-G, Schmidt-Rohr, K., Davies, G., Ghabbour, E. A. and Xing, B. (2000): Quantitative Characterization of Humic Substances by Solid-State Carbon-13 NMR, Soil Science Society of America Journal, Volume 64, Number 3, pp 873-884.

Marañón, E. and Sastre, H. (1991): Heavy Metak Removal in Packed Beds Using Apple Wastes, Bioresource Technology, Volume 38, Issue 1, pp 39 - 43.

Marshall, T. J., Holmes, J. W. and Rose C. W. (1996): Soil Physics, Cambridge University Press, pp 350 – 352.

Matis, K. A., Zouboulis, A. I., Lazaridi, N. K. and Hancock, I. C. (2003): Sorptive Flotation for Metal ions Recovery, International Journal of Mineral Processing, Volume 70, Issue 1 - 4, pp 99 – 108.

McKay, G. and Bino, M. J. (1990): Fixed-Bed Adsorption for the Removal of Pollutants from Water, Environmental Pollution, Volume 66, Issue 1, pp 33 – 53.

McKay, G. and Ng, J. Y. C. (2002): Sorbents for Chemical Spill Treatment In Fingas, M. F. (Ed): The Handbook of Hazardous Materials Spills Technology, McGraw-Hill Publishing, pp 15.34 – 15.35.

McKay, G., Porter, J. F. and Prasad G. R. (1999): The Removal of Dye Colours from Aqueous Solutions by Adsorption on Low-Cost Materials, Water, Air and Soil Pollution, Volume 114, Number 3 – 4, pp 423 – 438.

Meites, L. (1963): Handbook of Analytical Chemistry, McGraw Hill Book Company, New York, pp 1 – 13.

MMLERs, (2007): Metal Mining Liquid Effluent Regulations Act, Government of Canada.

Montgomery, D. C. and Runger, G. C. (2003): Applied Statistics and Probability for Engineers, 3rd Edition, John Wiley and Sons, Inc., USA, pp 506 – 524.

Morel, F. M. M. and Hering, J. G. (1983): Principles and Applications of Aquatic Chemistry, Wiley Inter-Science, pp 319 – 420.

Mulligan, C. N., Yong, R. N. and Gibbs, B. F. (2001): Remediation Technologies for Metal-Contaminated Soils and Groundwater: an Evaluation, Engineering Geology, Volume 60, Issues 1 - 4, pp 193–207.

Myers, R. H. and Montgmery, D. C. (2002): Response Surface Methodology: Process and Products Optimization Using Designed Experiments, 2nd Edition, Wiley-Interscience, pp 56 – 70.

Naja, G. and Volesky, B. (2006): Behaviour of a Mass Transfer Zone in a Biosorption Column, Environmental Science Technology, Volume 40, Number 12, pp 3996 – 4003.

Naumova, L., Gorlenko, N. and Otmakhova, Z. (1995): Peat as a Natural Sorbent for Recovery and Utilization of Metals from Wastewater, Russian Journal of Applied Chemistry, Volume 68, Number 9, pp 1273 – 1276.

Ngah, W. S. W. and Hanafiah, M. A. K. M. (2008): Removal of Heavy Metal ions from Wastewater by Chemically Modified Plant Wastes as Adsorbent: A Review, Bioresource Technology, Volume 99, Issue 10, pp 3935–3948.

Niemeyer, J., Chen, Y. and Bollag J.-M. (1992): Characterization of Humic Acids, Composts, and Peat by Diffuse Reflectance Fourier-Transform Infrared Spectroscopy, Soil Science Society of America Journal, Volume 56, Number 1, pp 135-140.

Nordén, B., Bohlin, E., Nilsson, M., Albano, Å. and Röckner, C. (1992): Characterization of Particle Size Fractions of Peat. An Integrated Biological, Chemical, and Spectroscopic Approach, Soil Science, Volume 153, Number 5, pp 382–396.

Ontario Fact Sheet (2001), Ministry of Environment Programs and Initiatives, March 2001.

Orem, W. H., Neuzil, S. G., Lerch, H. E. and Cecil, C. B. (1996): Experimental early-stage coalification of a peat sample and a peatified wood sample from Indonesia, Organic Geochemistry, Volume 24, Number 2, pp 111-125.

Papadama, T., Xekoukoulotakis, N. P., Poulios I. And Mantzavinos D. (2007): Photocatalytic Transformation of acid Orange 20 and Cr (VI) in aqueous TiO_2 Suspensions, Journal of Photochemistry and Photobiology A: Chemistry, Volume 186, Issues 2-3, pp 308 – 315.

Parker, R. and Dumaresq, C. (2002): Effluent Characterization, Water Quality Monitoring and Sediment Monitoring in the Metal Mining EEM Program, Water Quality Research Journal of Canada, Volume 37, Number 1, pp 219 – 228.

Patterson, J. W. (1989): Industrial Wastes Reduction, Environmental Science and Technology, Volume 23, Issue 9, pp 1032 – 1038.

Pavlovic, J., Stopic, S., Friedrich, B. and Kamberovic, Ž. (2007): Selective Removal of Heavy Metals from Metal-Bearing Wastewater in a Cascade Line Reactor, Environmental Science and Pollution Research, Volume 14, Number 7, pp 518 – 522.

Pecharsky, V. K. and Zavalij, P. Y. (2003): Fundamentals of Powder Diffraction and Structural Characterization of Materials, Kluwer Academic Publishers, pp 99 – 188.

Pérez, J. I., Hontoria, E., Zamorano, M. and Gómez, M. A. (2005): Wastewater Treatment Using Fibrist and Saprist Peat: A Comparative Study, Journal of Environmental Science and Health, Part A, Volume 40, Issue 5, pp 1021 – 1032.

Personal Communication (2008): Dansons Inc. 14648 – 138 Avenue, Edmonton, AB T5L 4J4.

Personal Communication (2010): Sales Representatives of L. Shawer Inc., P. O. Box Olds, AB, T4H 1P8.

Pollett, F. C. and Wells, E. D. (1977): Peatlands of Newfoundland – an Overview. In the Diversity of Peat, St. John's, Newfoundland, Newfoundland and Labrador Peat Association, pp 1–16.

Poots, V. J. P., McKay, G. and Healy, J. J. (1978): Removal of Basic Dye from Effluent using Wood as an Adsorbent, Journal of the Water Pollution Control Federation, Volume 50, Number 5, pp 926 – 935.

Preston, C. M., Axelson, D. E., Lévesque, M., Mathur, S. P., Dinel, H., Dudley, R. L. (1989). Carbon -13 NMR and Chemical Characterization of Particle-Size Separates of Peats Differing in Degree of Decomposition, Organic Geochemistry, Volume 14, Number 4, pp 393 – 403.

Puustjärvi, V. and Robertson, A. (1975): Physical and Chemical Properties of Horticultural Peat, In Robinson D. W. and Lamb J. G. D. (Eds): Peat in Horticulture, Academic Press, London UK, pp 32–38.

Qdais, H. A. and Moussa, H. (2004): Removal of Heavy Metals from Wastewater by Membrane Processes: a Comparative Study, Desalination, Volume 164, Issue 2, pp 105 – 110.

Qin, F. and Wen, B. (2007): Single and Multi Component Adsorption of Pb, Cu and Cd on Peat, Bulletin of Environmental Contamination and Toxicology, Volume 78, Number 3-4, pp 265 – 269.

Qin, F., Wen B., Shan, X.-Q., Xie, Y.-N., Liu, T., Zhang, S.-Z. and Khan, S. U. (2006): Mechanisms of Competitive Adsorption of Pb, Cu and Cd on Peat. Environmental Pollution, Volume 144, Issue 2, pp 669–680.

Reinbold, K. A., Hassett, J. J., Means, J. C. And Banwart, W. L. (1979): Adsorption of Energy-Related Organic Pollutants: A Literature Review: US Environmental Protection Agency, Athens, GA, EPA – 600/3 – 79 – 086 (NTIS: PB 80 – 105 – 117).

Ringqvist, L. and Holmgren, A. (1998): Treatment of Wastewater with Peat/Mineral Filters, the Spirit of Peatlands, Proceedings of the International Peat Symposium, Jyvaskyla, Finland, pp 111–114.

Ringqvist, L., Holmgren, A. and Öborn, I. (2002): Poorly Humified Peat as an Adsorbent for Metals in Wastewater, Water Research Volume 36, Issue 9, pp 2394–2404.

Ritchie, A. G. (1977): Alternative to the Elovich Equation for the Kinetics of Adsorption of Gases on Solids, Journal of the Chemical Society-Faraday Transactions 1, Volume 73, Part 10, pp 1650 – 1653.

Romao, L. P. C., Lead, J. R., Rocha, J. C., de Oliveira, L. C., Rosa, A. H., Mendonça, A. G. R. and Ribeiro, A. de Souza (2007): Structure and Properties of Brazilian Peat: Analysis by Spectroscopy and Microscopy, Journal of Brazilian Chemical Society, Volume 18, Number 4, pp 714–720.

Rubio, J. and Tessle, F. (1997): Removal of Heavy Metal Ions by Adsorptive Particulate Flotation, Mineral Engineering, Volume 10, Number 7, pp 671–679.

Ruthven, D. M. (1984): Principles of Adsorption and Adsorption Processes, John Wiley and Sons Inc., pp 431 – 434.

Saravanane, R., Sundararajan, T. and Sivamurthy Reddy, S. (2001): Chemically Modified Low Cost Treatment for Heavy Metal Effluent Management, Environmental Management and Health, Volume 12, Issue 2, pp 215 – 224.

Sawyer, C. N., McCarty, L. and Parkin, G. F. (1994): Chemistry for Environmental Engineering 4th Edition, McGraw Hill Series in Water and Environmental Engineering, New York, pp 97-98.

Schwarzenbach, R. P., Gschwend, P. M. and Imboden, D. M. (2003): Environmental Organic Chemistry, 2nd Edition, John Wiley and Sons Inc., New Jersey, pp 388 – 440.

Sciban, M., Klasnja, M. and Skrbic, B. (2006): Modified Hardwood Sawdust as Adsorbent of Heavy Metal ions from Water, Wood Science Technology, Volume 40, Issue 3, pp 217 – 227.

Shackelford, C. D. (1993): Contaminant Transport: In Daniel, E. D. (Ed): Geotechnical Practice for Waste Disposal, Springer, pp 46 -49.

Sharma, D. C. and Forster, C. F. (1993): Removal of Hexavalent Chromium using Sphagnum Peat Moss, Water Research, Volume 27, Number 7, pp 1210 – 1208.

Sharma, D. C. and Forster, C. F. (1995): Column Studies into the Adsorption of Chromium (VI) using Sphagnum Peat Moss, Bioresource Technology, Volume 52, Issue 3, pp 261 – 267.

Sheldrick, B. H. (Ed) (1984): Analytical Methods Manual 1984, Research Branch, Agriculture Canada, LRRA Contribution Number 84-30 6/1 - 3.

Smith, B. C. (1996): Fundamentals of Fourier Transform Infrared Spectroscopy, CRC Press, pp 7 – 10.

Smuts, W. J. (1996): Peat and Related Biofuels as an Alternative Energy Supply for Certain Developing Communities, Geology for Development within a Sustainable Environment, pp 471 – 484.

Sparks, D. L. (2003): Environmental Soil Chemistry, Academic Press Amsterdam, pp 101 – 108.

Spedding, P. J. (1988): Peat – Review, Fuel, Volume 67, Issue 7, pp 883–900.

Sposito, G. (1984): The Surface Chemistry of Soils, Oxford University Press New York, pp 210 – 215.

Stat-Ease, Inc: www.statease.com

Stefan, R. (2008): The Nickel Processing Plant, Long Harbour, Presented at Mineral Resources Review, 2008, www.vinl.valeinco.com/PresentationDetails.asp?id=40 accessed 27th November, 2008.

Summa, V. and Tateo, F. (1999): Geochemistry of two Peats Suitable for Medical Uses and their Behaviour During Leaching, Applied Clay Science, Volume 15, Number 5-6, pp 477 - 489.

Sze, M. F. F., Lee, V. K. C. and McKay, G. (2008): Simplified Fixed Bed Column Model for Adsorption of Organic Pollutants using Tapered Activated Carbon Columns, Desalination, Volume 218, Issues 1 – 3, pp 323 – 333.

Tan, W., Ooi, S. and Lee, C. (1993): Removal of Chromium (VI) from Solution by Coconut Husk and Palm Pressed Fibers, Environmental Technology, Volume 14, Number 3, pp 277–282.

Taylor, A. (2007): The Use of Stainless and Other High Performance Alloys in Hydrometallurgical Process Plants for the Recovery of Metals, ASSDA 8th National Stainless Steel Conference, Gold Coast, Queensland, Australia.

Teng, Q. (2005): Structural Biology: Practical NMR Applications, Springer, pp 1 – 55.

Thomas, R. (2004): Practical Guide to ICP-MS, Mercel-Dekker Publications, pp 5 – 30.

Türkman, A., Aslan, S. and Ege, l. (2004): Treatment of Metal Containing Wastewaters by Natural Zeolites, Fresenius Environmental Bulletin, Volume 13, Number 6, pp 574 –580.

Twardowska, I. and Kyziol, J. (2003): Sorption of Metals onto Natural Organic Matter as a Function of Complexation and Adsorbent-Adsorbate Contact Mode, Environment International, Volume 28, Number 8, pp 783 – 791.

Typliski, R. V. and Labarre, G. J. (1980): Wastewater Treatment at Hudson Bay Mining and Smelting Co., Limited, Environmental Control CIM Bulletin.

USEPA (1982): Development Document for Effluent Limitations Guidelines and Standards for the Metal Finishing (Proposed), Point Source Category, EPA 440/1 - 82/091 – b.

USEPA (2009): List of Contaminants and their MCLs Levels, United States Environmental Pollution Agency, EPA 816 – F – 009 - 004.

USGS (2006a): US Geological Survey, 2006 Minerals Yearbook, Zeolites, pp 83.1 – 2.

USGS (2006b): US Geological Survey, 2006 Minerals Yearbook: Clay and Shale, 18.4-5.

USGS (2006c): US Geological Survey, 2006 Minerals Yearbook: Peat, pp 54.1 – 2.

USGS (2008): US Geological Survey, Mineral Commodity Summaries, p 115 www.minerals.usgs.gov/minerals/pubs/mcs/2008/mcs2008.pdf accessed 28th November, 2008.

USGS (2010): US Geological Survey, Mineral Commodity Summary, Jan. 2010.

Vale (2007): www.vinl.valeinco.com (Formerly, Voisey's Bay Nickel Company Limited) accessed 26th October, 2007.

Viraraghavan, T. and Dronamraju, M. M. (1993): Removal of Copper, Nickel and Zinc from Wastewater by Adsorption using Peat, Journal of Environmental Science and Health A, Volume 28 Issue 6, pp 1261 - 1276.

Voice, T. C. And Weber, W. J. (1983): Sorption of Hydrophobic Compounds by Sediments, Soils and Suspended Solids - I. Theory and Background, Water Research, Volume 17, Number 10, pp 1433 – 1441.

Voisey's Bay (2007): Environmental Impact Statement: Long Harbour Commercial Nickel Processing Plant, Executive Summary, Voisey's Bay Nickel Company Limited.

Volesky, B., Weber, J. and Park, J. M. (2003): Continuous – Flow Metal Biosorption in a Regenerable Sargassum Column, Water Research, Volume 37, Number 2, pp 297 – 306.

Waddle, R. J., (2004): The Mineral Industry in Newfoundland and Labrador: Its Development and Economic Contributions. Government of NL, Department of Natural Resources, Geological Survey.

Walker G. M. and Weatherley, L. R. (1997): Adsorption of Acid Dyes on to Granular Activated Carbon in Fixed Beds, Water Resaerch, Volume 31, Number 8, pp 2093 – 2101.

Wang, L. K., Vaccari, D. A., Li, Y. and Shammas, N. K. (2004): Chemical Precipitation In Wang, L. K., Hung, Y.-T. and Shammas, N. K. (Eds): Physicochemical Treatment Processes, Environmental Engineering, Volume 3, Humana Press, NJ, pp 141 - 197.

Wang, L., Wang, N., Zhu, L., Yu, H. and Tang H. (2008): Photocatalytic Reduction of Cr(VI) over Different TiO_2 Photocatalysts and the Effects of Dissolved Organic Species, Journal of Hazardous Materials, Volume 152, Issue 1, pp 93 – 99.

Warith, M. A., (1996): Evaluation and Design of Peat Filter to Attenuate Landfill Leachate, Water Quality Research Journal of Canada, Volume 31, Number 1, pp 65 – 83.

WHO (2006): World Health Organization Guidelines for Drinking Water Quality, Volume 1, pp 194.

Yong, R. N., Mohamed, A. M. O. and Warkentin, B. P. (1992): Principles of Contaminant Transport in Soils, Development in Geotechnical Engineering, 73, Elsevier Amsterdam p 207.

Zagorodni, A. A. (2007): Ion Exchange Materials: Properties and Applications, Elsevier publications, Netherlands pp 17 - 18, p 223.

Zamlow, M., Eichbaum, B., Sandgren, K. and Shanks, D. (1990): Removal of Heavy Metals and Other Cations from Wastewater Using Zeolites, Separation Science, Volume 25, Number 13 – 15, pp 1555 – 1569.

Zarraa, M. A. (1995): Study on the Removal of Chromium (VI) from Wastes Solutions by Adsorption on to Sawdust in Stirred Vessels, Adsorption Science and Technology, Volume 12, Issue 2, pp 129 – 138.

Zhipei, Z., Junlu, Y., Zengnui, W. and Piya, C. (1984): A Preliminary Study of the Removal of Pb^{2+}, Cd^{2+}, Zn^{2+}, Ni^{2+} and Cr^{6+} from Wastewaters with Several Chinese Peats, Proceedings of the 7th International Peat Congress, Dublin, pp 18 – 23.

Zhou, P., Huang, J.-C., Li, A. W. F. and Wei, S. (1999): Heavy Metal Removal from Wastewater in Fluidized Bed Reactor, Water Research, Volume 33, Number 8, pp 1918 – 1924.

Zhou, D., Zhang, L., Zhou, J. And Guo, S. (2004): Cellulose/Chitin Beads for Adsorption of Heavy Metals in aqueous Solution, Water Research, Volume 38, Number 11, pp 2643 – 2650.

Zouboulis, A. I. And Matis, K. A. (1997): Removal of Metals ions from Dilute Solutions by Sorptive Flotation, Critical Reviews in Environmental Science and Technology, Vol. 27, Issue 3, pp 195 – 235.

Appendix A1

The derivation of pseudo-second order kinetic equation (Ho et al., 1995) for an adsorption reaction follows the Langmuir equation and essentially assumed that chemisorption is the main route of metal uptake on the adsorbent surface. The rate of pseudo-second order reaction may be dependent on the quantity of metal ion q_t, at any time t, and the quantity at equilibrium, q_e, a function of temperature of the system, initial metal concentration, the adsorbent dose and the interaction between the metal and adsorbent.

If the sorption of Metal M on peat surface P can be represented as:

$$2P + M^{2+} = MP_2 \qquad (1)$$

or

$$2HP + M^{2+} = MP_2 + 2H^+ \qquad (2)$$

Then the rate expression can be given as:

$$\frac{d(P)_t}{dt} = k\left[(P)_0 - (P)_t\right]^2 \qquad (3)$$

or

$$\frac{d(HP)_t}{dt} = k\left[(HP)_0 - (HP)_t\right]^2 \qquad (4)$$

Where P and HP are the polar sites on the peat surface, and $(P)_h$, $(HP)_h$ are occupied active sites on the peat, $(P)_o$ and $(HP)_o$ are the equilibrium available sites. Equation 4 can then be reduced to quantity adsorbed if assumed to be equivalent to the occupied sites.

$$\frac{dq_t}{dt} = k[q_e - q_t]^2 \qquad (5)$$

Where k is the rate constant in (g/mg hr), q_e is the amount of metal adsorbed at equilibrium in (mg/g) and q_t the amount of metal adsorbed at any time t. Equation 5 is re-arranged to Equation 6 by separating variables.

$$\frac{dq_t}{[q_e - q_t]^2} = kdt \qquad (6)$$

Integratung equation 6 with boundary conditions set at t = 0 to t = t and q_t = 0 to q_t = q_t.

$$\frac{1}{(q_e - q_t)} = \frac{1}{q_e} + kdt \qquad (7)$$

Equation 7 is referred to as the integrated rate law of the pseudo-second order reaction. This equation can further be re-arranged and the linearized as in equation 8 used in the study.

$$\frac{t}{q_t} = \frac{1}{kq_e^2} + \frac{1}{q_e}t \qquad (8)$$

Appendix A2

Breakthrough curves are temporal variation in the concentration of a solute at different effluent end of the column of porous materials and can be measured by using laboratory column by:

1. Establishing steady-state fluid flow conditions.

2. Continuously introducing at the influent end of the column a liquid containing a solute at concentration Co and;

3. Monitoring the solute concentration at the effluent end

In this approach, the effect of retardation is considered and the abscissa for the breakthrough curves has been defined in terms of pore volumes instead of time. One pore volume is the volume of water that completely will fill the void in along a column length. The number of pore volume of flow (U) is equal to the cumulative volume of flow through the sample divided by the volume of void space in the material.

$$ U \quad = \quad \frac{v_s n A t}{L A n} $$

Where, L is the length of the column, A is the cross-sectional area, t is the time, v_s is the seepage velocity of pore fluid, n is the porosity.

When the relative concentration (C/C_0) is plotted against U, an S shaped curve is obtained and various transit points can be identified corresponding to the behaviour of the contaminant along the column during adsorption (Bowder et al., 1985; Marshall et al., 1996).

Appendix B1

Response   1 % Ni Removed
ANOVA for Response Surface Reduced Quadratic Model
Analysis of variance table [Partial sum of squares - Type III]

Source	Sum of Squares	df	Mean Square	F Value	p-value Prob > F	
Model	21878.95	7	3125.56	49.76	< 0.0001	significant
A-Conc	616.91	1	616.91	9.82	0.0050	
B-Peat dose	2204.86	1	2204.86	35.10	< 0.0001	
D-pH	9413.60	1	9413.60	149.86	< 0.0001	
AB	402.80	1	402.80	6.41	0.0194	
BD	694.32	1	694.32	11.05	0.0032	
B^2	499.77	1	499.77	7.96	0.0102	
D^2	8449.80	1	8449.80	34.52	< 0.0001	
Residual	1319.13	2	162.82			
Lack of Fit	1096.59	17	64.51	1.16	0.4939	not significant
Pure Error	222.54	4	55.64			
Cor Total	23198.08	28				

Std. Dev.	7.93	R-Squared	0.9431	
Mean	73.50	Adj R-Squared	0.9242	
C.V. %	10.78	Pred R-Squared	0.8217	
PRESS	4137.13	Adeq Precision	19.969	

Final Equation in Terms of Actual Factors:

%Metal Removed = +0.85363 -0.24348 * Conc +2.11096 * Peat dose +33.28979 * pH
+7.04211E-003 * Conc * Peat dose -0.19812 * Peat dose * pH
-0.023572 * Peat dose^2 -2.85628 * pH^2

183

The Diagnostic Plots

1.
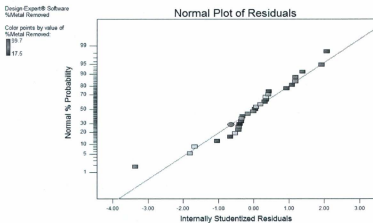
Figure IIA.1: Normal probability plot of the studentized residuals to check for normalty of residuals
Residuals randomly scattered. Check is OK!

2.
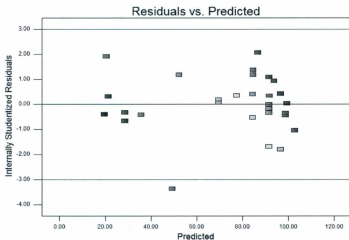
Figure IIA.2: Studentized residuals versus predicted values to check for constant error
Residuals have no unique shape especially funnel shape. Check is OK!

3.
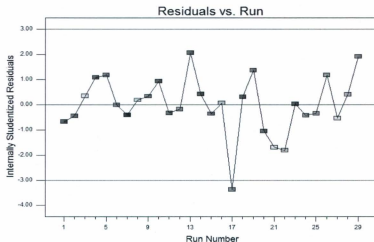
Figure IIA.3: Externally Studentized Residuals versus Run
No significant outliers of influence. Check OK!

4.
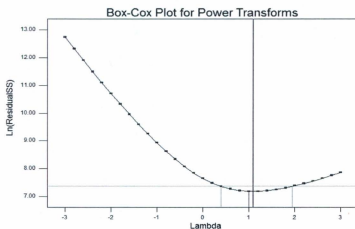
Figure IIA.4: Box-Cox plot for power transformations

Box-Cox plot suggested no power transformation. Check OK!

185

Appendix B2

Response   1 % Co Removed
   ANOVA for Response Surface Reduced Quadratic Model
Analysis of variance table [Partial sum of squares - Type III]

Source	Sum of Squares	df	Mean Square	F Value	p-value Prob > F	
Model	11917.20	8	1489.65	388.90	< 0.0001	significant
A-Conc	372.97	1	372.97	97.37	< 0.0001	
B-Peat dose	7777.52	1	7777.52	2030.47	< 0.0001	
D-pH	726.96	1	726.96	189.79	< 0.0001	
AD	25.50	1	25.50	6.66	0.0179	
BD	44.89	1	44.89	11.72	0.0027	
A^2	24.45	1	24.45	6.38	0.0201	
B^2	2357.14	1	2357.14	615.37	< 0.0001	
D^2	216.19	1	216.19	56.44	< 0.0001	
Residual	76.61	20	3.83			
Lack of Fit	72.08	16	4.50	3.98	0.0955	not significant
Pure Error	4.53	4	1.13			
Cor Total	11993.81	28				

Std. Dev.	1.96	R-Squared	0.9936
Mean	75.82	Adj R-Squared	0.9911
C.V. %	2.58	Pred R-Squared	0.9811
PRESS	226.30	Adeq Precision	62.414

Final Equation in Terms of Actual Factors:

% Co Removed = +50.05389 -0.22159 * Conc +3.84514 * Peat dose -3.93667 * pH
   +9.61905E-003 * Conc * pH -0.050376 * Peat dose * pH
   +3.38919E-004 * Conc^2 -0.051852 * Peat dose^2 +0.46277 * pH^2

The Diagnostic plots

1.
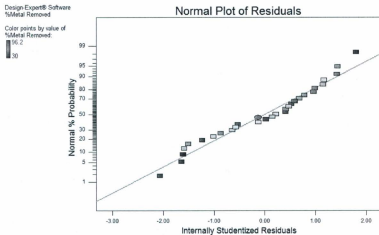
Figure IIB.1: Normal probability plot of the studentized residuals to check for normalty of residuals

Residuals randomly scattered. Check is OK!

2.
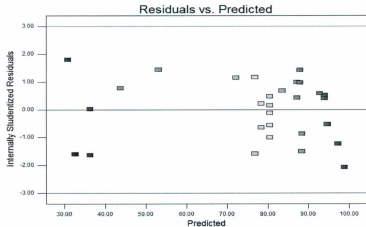
Figure IIB.2: Studentized residuals versus predicted values to check for constant error

Residuals have no unique shape especially funnel shape. Check is OK!

3.
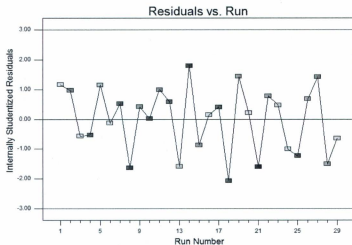
Figure IIB.3: Externally Studentized Residuals versus Run

No significant outliers of influence. Check OK!

4.
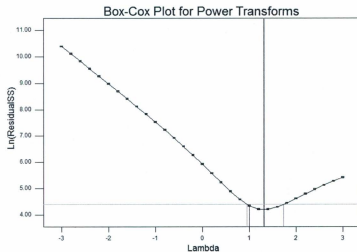
Figure IIB.4: Box-Cox plot for power transformations

Box-Cox plot suggested no power transformation. Check OK!

Appendix C

Table C1: Average Ni^{2+} concentration (mg/L) measured during kinetic study at pH 3

Time (hr)	Conc. 25 mg/L Peat dose (g/L)				Conc. 50 mg/L Peat dose (g/L)				Conc. 125 mg/L Peat dose (g/L)				Conc. 200 mg/L Peat dose (g/L)			
	2	10	21	40	2	10	21	40	2	10	21	40	2	10	21	40
0.5	24.90	7.80	4.00	2.06	49.8	18.42	10.32	5.16	113.72	71.40	49.11	23.93	199.00	117.60	91.70	53.06
1	24.86	7.50	3.23	1.69	47.44	22.34	9.80	4.00	116.90	71.60	46.04	22.42	196.40	112.80	83.70	46.03
1.5	23.87	7.46	3.03	1.62	48.60	19.18	8.16	4.43	109.12	70.80	44.23	22.11	197.20	113.60	86.30	50.06
2	24.86	7.12	2.75	1.60	49.60	20.07	8.23	4.21	106.76	72.70	43.95	21.76	196.00	114.00	88.60	47.23
3	24.90	6.75	2.72	1.44	49.40	20.02	8.10	3.89	110.80	68.10	42.72	20.13	196.50	113.20	84.90	45.04
4	23.54	6.84	2.85	1.63	49.70	20.04	8.67	3.66	112.88	67.40	42.27	21.22	195.80	109.80	84.40	47.85
5	24.06	6.70	2.50	1.50	49.80	20.08	8.47	3.84	109.30	67.50	40.88	20.10	195.20	103.20	83.60	43.22
6	23.86	6.59	2.50	1.46	49.90	17.25	7.63	3.76	112.08	70.70	40.44	20.90	194.80	107.80	80.50	45.98
8	21.77	6.81	2.60	1.46	46.80	19.35	7.63	3.68	109.20	63.50	42.09	20.83	194.80	105.00	74.80	41.15
10	23.82	6.09	2.59	1.64	49.66	17.26	8.24	3.94	104.60	63.50	42.99	20.25	194.60	103.40	74.80	45.30
12	23.4	6.70	2.50	1.60	46.80	17.30	7.71	3.71	104.80	64.10	41.01	20.23	195.10	104.20	75.00	45.84

Table C2: Average Ni^{2+} concentration measured (mg/L) during kinetic study at pH 5.5

Time (hr)	Conc. 25 mg/L Peat dose (g/L)				Conc. 50 mg/L Peat dose (g/L)				Conc. 125 mg/L Peat dose (g/L)				Conc. 200 mg/L Peat dose (g/L)			
	2	10	21	40	2	10	21	40	2	10	21	40	2	10	21	40
0.5	7.80	3.10	1.70	2.0	24.50	12.10	4.40	3.40	83.20	52.70	41.60	17.40	181.10	110.90	66.90	35.50
1	6.50	2.80	2.20	0.70	22.80	9.80	4.60	2.80	83.50	51.10	29.30	15.80	181.40	106.70	68.60	36.60
1.5	5.90	2.60	1.30	0.70	22.20	10.20	4.90	2.60	84.40	50.90	30.20	16.30	182.60	107.40	64.90	36.90
2	5.30	2.30	1.20	1.10	22.20	10.50	4.90	2.30	83.30	48.90	30.70	15.40	178.60	102.30	63.00	37.10
3	5.30	2.60	1.20	1.00	22.60	9.80	4.50	1.80	86.90	47.30	30.60	13.20	176.20	105.10	67.10	36.10
4	5.70	2.30	1.20	0.90	22.00	8.50	4.10	1.80	84.40	47.60	28.50	14.20	174.60	105.70	67.40	35.00
5	5.50	2.30	1.30	1.10	21.30	7.10	4.70	2.00	83.50	45.70	29.10	14.50	172.80	105.60	62.00	35.90
6	5.10	2.50	1.20	1.10	19.70	8.70	4.60	2.10	82.90	46.70	27.60	15.00	173.00	96.50	59.20	35.80
8	5.20	2.50	1.20	1.00	21.60	7.90	4.70	1.90	82.40	46.50	27.80	14.60	168.20	102.20	58.50	36.80
10	5.20	2.60	1.40	0.90	21.50	8.30	4.70	2.00	82.80	48.00	28.20	14.40	165.90	97.70	59.30	35.50
12	5.20	2.60	1.30	1.00	21.00	7.60	4.60	1.90	83.10	47.20	28.00	14.00	166.40	98.20	59.70	35.80

Table C3: Average Ni^{2+} concentration (mg/L) measured during kinetic study at pH 8

Time (hr)	Conc. 25 mg/L Peat dose (g/L)				Conc. 50 mg/L Peat dose (g/L)				Conc. 125 mg/L Peat dose (g/L)				Conc. 200 mg/L Peat dose (g/L)			
	2	10	21	40	2	10	21	40	2	10	21	40	2	10	21	40
0.5	8.60	6.30	3.00	2.40	30.10	22.60	10.00	6.20	89.40	71.00	52.00	29.60	187.00	124.10	80.50	51.80
1	8.46	6.35	2.80	2.20	28.50	21.80	8.50	5.60	88.00	70.20	50.85	28.00	186.00	120.70	78.20	50.50
1.5	8.51	6.28	2.42	1.80	28.35	19.55	6.10	4.37	88.50	68.40	51.20	26.50	184.60	118.30	76.70	49.00
2	8.19	6.00	2.45	1.88	27.20	17.40	6.70	5.15	87.25	67.50	48.60	22.40	184.70	116.90	74.30	48.60
3	8.10	5.25	2.80	1.85	26.50	18.15	7.20	5.48	87.10	64.90	46.52	17.50	182.10	112.50	72.50	47.0
4	7.90	5.47	2.71	1.94	24.30	18.90	7.50	5.62	86.00	62.00	43.70	18.10	178.40	110.60	70.90	47.70
5	7.81	5.71	2.55	1.90	25.70	17.95	7.64	5.20	84.70	59.50	44.80	18.70	176.50	107.00	70.10	48.10
6	7.72	5.50	2.50	1.97	25.10	17.65	7.05	4.90	85.75	60.40	44.95	17.70	174.30	102.00	71.00	47.50
8	7.78	5.42	2.49	1.88	24.90	17.50	7.20	4.80	84.80	59.90	44.20	17.90	170.20	95.40	71.40	48.00
10	7.76	5.36	2.45	1.88	24.70	17.80	7.00	4.85	85.90	59.70	43.80	18.00	172.00	96.80	70.50	48.20
12	7.91	5.40	2.47	1.90	24.40	17.48	6.80	4.91	85.10	59.80	43.85	17.80	171.80	95.70	70.30	47.60

Table C4: Average Ni^{2+} concentration (mg/L) measured during kinetic study at pH 10

Time (hr)	Conc. 25 mg/L Peat dose (g/L)				Conc. 50 mg/L Peat dose (g/L)				Conc. 125 mg/L Peat dose (g/L)				Conc. 200 mg/L Peat dose (g/L)			
	2	10	21	40	2	10	21	40	2	10	21	40	2	10	21	40
0.5	14.30	14.30	14.00	13.60	41.80	38.70	36.90	34.90	107.50	100.00	94.20	79.00	176.40	167.00	160.8	149.8
1	14.30	14.10	14.20	13.40	42.00	38.30	36.80	35.10	106.40	98.30	90.80	78.80	176.00	166.50	160.5	150.1
1.5	14.40	14.20	13.70	13.60	41.90	38.10	37.00	34.90	107.10	97.00	92.10	78.50	176.10	167.20	159.2	148.3
2	14.40	13.70	13.60	13.50	41.80	38.00	36.80	34.30	106.20	97.10	92.40	76.30	175.40	167.00	160.0	148.1
3	14.10	13.60	13.60	13.30	41.40	37.30	36.10	34.30	104.00	96.70	89.80	76.80	175.20	166.80	159.2	147.2
4	14.20	13.80	13.50	13.30	40.40	37.20	36.40	34.50	102.50	96.40	89.20	76.30	174.00	166.40	158.7	147.9
5	14.30	14.10	14.00	13.40	40.10	37.40	36.20	34.30	103.40	97.20	89.00	76.10	174.10	166.20	158.4	147.2
6	14.20	14.10	14.00	13.30	41.00	37.40	36.30	34.60	102.50	96.20	90.10	76.40	174.00	165.10	158.6	147.8
8	14.40	14.10	13.80	13.30	40.80	37.30	36.10	34.40	102.80	96.40	90.00	76.60	173.90	164.50	158.4	147.5
10	14.40	13.90	13.80	13.40	40.60	37.20	36.10	34.40	102.10	96.20	89.80	76.40	173.80	166.10	158.4	147.5
12	14.30	13.80	13.70	13.40	40.36	37.30	36.20	34.50	102.60	96.50	89.40	76.50	173.90	164.80	158.6	147.4

Table C5: Average Co^{2+} concentration (mg/L) measured during kinetic study at pH 3

Time (hr)	Conc. 25 mg/L Peat dose (g/L)				Conc. 50 mg/L Peat dose (g/L)				Conc. 125 mg/L Peat dose (g/L)				Conc. 200 mg/L Peat dose (g/L)			
	2	10	21	40	2	10	21	40	2	10	21	40	2	10	21	40
0.5	20.30	9.40	4.80	3.40	46.90	23.70	10.80	7.10		70.20	38.50	25.80			71.30	53.50
1	19.50	8.00	4.20	3.10	44.40	20.70	9.60	6.30		68.50	36.70	21.80			68.10	49.30
1.5	18.40	8.90	4.40	3.00	42.60	21.20	9.60	5.50		70.10	37.00	22.40			71.70	49.30
2	18.50	7.90	4.10	3.00	42.90	21.50	9.90	5.90		69.90	37.10	23.90			72.40	49.90
3	19.10	8.40	4.40	3.10	43.80	21.80	9.80	6.50		70.40	36.90	23.50			68.90	52.40
4	18.80	8.00	4.20	3.00	43.70	21.30	10.40	6.50		70.50	37.00	23.60			68.90	49.40
5	19.40	8.10	4.10	3.20	43.70	21.10	10.20	5.50		68.90	37.30	24.40			70.70	51.70
6	18.50	8.00	4.10	3.20	42.90	22.40	9.60	6.20		71.20	36.70	24.20			7.00	47.50
8	21.40	9.00	4.30	3.10	43.20	22.20	10.20	6.70		72.20	38.30	24.40			71.20	50.30
10	21.70	9.10	4.20	3.10	44.90	22.30	10.60	7.00		71.90	39.80	23.70			71.50	49.90
12	19.60	8.20	4.20	3.20	44.60	22.80	9.80	7.10		71.80	38.50	24.00			70.30	49.80

Table C6: Average Co^{2+} concentration (mg/L) measured during kinetic study at pH 5.5

Time (hr)	Conc. 25 mg/L Peat dose (g/L)				Conc. 50 mg/L Peat dose (g/L)				Conc. 125 mg/L Peat dose (g/L)				Conc. 200 mg/L Peat dose (g/L)			
	2	10	21	40	2	10	21	40	2	10	21	40	2	10	21	40
0.5	8.40	4.40	2.50	2.00	30.30	14.50	7.20	5.10	91.00	67.50	36.50	22.10			73.30	55.20
1	8.20	4.00	2.00	1.60	29.10	13.60	6.40	4.10	89.30	64.30	31.30	19.40			69.10	47.10
1.5	7.90	3.80	2.50	1.60	27.30	13.40	6.40	4.60	89.40	63.30	33.80	21.20			70.70	48.50
2	8.30	4.00	2.01	1.70	28.10	13.70	6.40	4.30	89.00	61.00	32.50	20.50			69.20	47.30
3	8.30	4.00	2.30	1.60	27.60	13.50	6.60	4.30	88.60	62.40	32.30	19.80			69.20	47.40
4	8.30	3.80	2.00	1.60	28.50	13.80	6.60	4.40	88.90	63.00	31.90	19.70			70.20	48.70
5	8.00	4.10	2.20	1.80	29.30	13.30	6.90	4.55	87.50	63.10	31.90	19.90			69.90	49.20
6	8.40	4.05	2.36	2.00	28.80	14.20	6.50	5.10	89.10	62.60	32.10	20.90			70.40	49.40
8	8.60	3.90	2.20	1.90	27.90	13.60	6.65	4.65	87.30	62.40	31.60	20.90			69.30	49.30
10	7.90	3.90	2.24	2.00	27.80	13.80	6.54	4.42	88.10	62.80	32.00	19.80			69.70	49.30
12	8.00	4.00	2.10	1.80	28.30	13.60	6.50	4.25	87.90	61.70	31.70	19.60			69.30	48.80

Table C7: Average Co^{2+} concentration (mg/L) measured during kinetic study at pH 8

Time (hr)	Conc. 25 mg/L Peat dose (g/L)				Conc. 50 mg/L Peat dose (g/L)				Conc. 125 mg/L Peat dose (g/L)				Conc. 200 mg/L Peat dose (g/L)			
	2	10	21	40	2	10	21	40	2	10	21	40	2	10	21	40
0.5	6.80	3.90	2.18	1.86	26.00	10.6	4.71	3.06	82.40	50.70	31.00	14.90	75.00	69.40	54.60	31.80
1	6.60	3.56	1.74	1.58	25.10	9.57	3.15	2.18	76.20	41.10	24.36	9.25	66.58	59.80	49.40	20.55
1.5	6.15	3.20	1.81	1.21	22.30	8.25	3.40	2.25	76.80	43.50	26.52	11.10	67.80	63.00	51.85	25.30
2	6.27	3.28	1.83	1.26	24.20	8.63	3.70	2.28	77.60	44.00	26.78	11.20	68.50	63.50	52.00	26.00
3	6.30	3.41	1.76	1.35	22.90	8.74	3.54	2.32	77.10	44.80	26.30	10.60	68.53	63.10	51.66	25.31
4	6.35	3.41	1.75	1.33	22.40	8.49	3.39	2.36	77.50	43.20	26.00	10.80	67.36	62.05	51.30	24.60
5	6.25	3.27	1.74	1.29	22.80	8.49	3.19	2.28	77.29	43.00	25.50	10.30	67.60	62.18	50.80	23.90
6	6.19	3.20	1.74	1.29	23.10	8.33	3.17	2.19	77.35	43.20	25.32	9.35	67.15	61.50	50.65	22.18
8	6.21	3.24	1.77	1.25	23.10	8.36	3.21	2.20	76.84	42.80	24.90	9.31	66.82	60.25	50.10	21.50
10	6.18	3.25	1.76	1.22	22.70	8.28	3.25	2.25	76.41	42.30	24.58	9.26	66.60	59.80	49.80	20.90
12	6.16	3.22	1.76	1.22	22.50	8.26	3.20	2.21	76.25	42.10	24.40	9.28	66.75	60.10	49.49	20.58

Table C8: Average Co^{2+} concentration (mg/L) measured during kinetic study at pH 10

Time (hr)	Conc. 25 mg/L Peat dose (g/L)				Conc. 50 mg/L Peat dose (g/L)				Conc. 125 mg/L Peat dose (g/L)				Conc. 200 mg/L Peat dose (g/L)			
	2	10	21	40	2	10	21	40	2	10	21	40	2	10	21	40
0.5	23.80	19.80	14.20	6.40	48.50	45.10	38.00	25.80	124.00	122.50	118.60	105.00	198.70	196.10	188.9	170
1	24.00	19.20	13.10	6.30	48.50	44.90	38.20	24.60	124.10	122.80	116.00	104.00	198.20	195.60	188.3	170.2
1.5	23.60	18.10	12.40	6.40	48.10	44.80	37.80	23.50	123.40	122.80	113.50	103.00	196.80	193.90	187.2	170.1
2	23.10	18.60	8.20	6.20	47.20	44.50	36.50	21.20	122.80	122.00	112.90	102.00	197.50	193.80	186.7	168.8
3	22.90	17.10	10.50	5.60	47.40	44.20	35.20	20.80	122.80	121.50	112.80	101.00	197.60	193.00	186.7	168.5
4	22.40	17.60	9.80	6.00	48.10	43.10	36.40	19.60	123.40	119.20	110.90	98.10	197.50	192.50	185.1	164.5
5	22.60	18.10	8.80	5.80	47.80	43.70	36.00	20.20	123.10	118.20	111.80	99.80	197.20	192.40	183.2	162.5
6	22.40	17.90	8.60	5.60	47.90	43.80	35.50	19.80	122.80	119.00	111.40	98.20	196.90	191.00	183.9	162.5
8	22.80	17.60	8.40	5.80	47.50	43.70	35.20	19.80	122.90	118.50	110.90	98.50	196.80	191.20	183.9	162.8
10	22.60	17.80	8.40	5.60	47.30	43.40	35.80	19.90	122.90	118.20	111.20	98.60	196.80	191.10	183.7	162.9
12	22.50	17.30	8.20	5.70	47.40	43.20	35.40	19.70	122.80	118.40	111.20	98.30	196.80	191.30	184.0	162.5

Appendix D

Table D1: Average adsorbed Ni^{2+} at various peat doses at pH 3 during batch kinetic test

Time (hr)	Conc. 25 mg/L				Conc. 50 mg/L				Conc. 125 mg/L				Conc. 200 mg/L			
	q_1	q_2	q_3	q_4	q_1	q_2	q_3	q_4	q_1	q_2	q_3	q_4	q_1	q_2	q_3	q_4
0.5	0.025	1.720	1.000	0.574	0.050	3.158	1.890	1.121	2.820	5.360	3.614	2.527	0.250	8.240	5.157	3.674
1	0.035	1.750	1.037	0.583	0.640	2.766	1.914	1.150	2.025	5.340	3.760	2.565	0.900	8.720	5.538	3.849
1.5	0.283	1.754	1.046	0.585	0.530	3.082	1.992	1.139	3.970	5.420	3.846	2.572	0.700	8.640	5.414	3.749
2	0.035	1.788	1.060	0.585	0.100	2.993	1.989	1.145	4.560	5.230	3.860	2.581	1.000	8.600	5.305	3.819
3	0.025	1.825	1.061	0.589	0.150	2.998	1.995	1.153	3.560	5.770	3.918	2.622	0.875	8.680	5.481	3.874
4	0.365	1.816	1.055	0.585	0.075	2.996	1.968	1.159	3.030	5.760	3.980	2.595	1.050	9.020	5.505	3.804
5	0.235	1.830	1.071	0.588	0.050	2.992	1.978	1.154	3.925	5.750	4.006	2.623	1.200	9.680	5.543	3.920
6	0.285	1.841	1.071	0.585	0.025	3.275	2.018	1.156	3.230	5.430	4.027	2.603	1.300	9.220	5.690	3.851
8	0.808	1.819	1.067	0.589	0.800	3.065	2.018	1.158	3.950	6.150	3.948	2.604	1.300	9.160	5.962	3.971
10	0.295	1.891	1.067	0.584	0.085	3.274	1.989	1.152	5.100	6.150	3.905	2.619	1.350	9.660	5.962	3.868
12	0.400	1.830	1.071	0.585	0.800	3.270	2.014	1.157	5.050	6.090	4.000	2.619	1.225	9.580	5.952	3.854

Where q_1, q_2, q_3 and q_4, in mg/g, are the peat doses at 2, 10, 21 and 40 g/L

Table D2: Average adsorbed Ni^{2+} at various peat doses at pH 5.5 during batch kinetic test

Time (hr)	Conc. 25 mg/L				Conc. 50 mg/L				Conc. 125 mg/L				Conc. 200 mg/L			
	q_1	q_2	q_3	q_4	q_1	q_2	q_3	q_4	q_1	q_2	q_3	q_4	q_1	q_2	q_3	q_4
0.5	4.300	2.190	1.110	0.575	6.375	3.790	2.171	1.165	10.450	7.230	3.971	2.690	4.725	8.910	6.338	4.113
1	4.625	2.220	1.086	0.608	6.800	4.020	2.162	1.180	10.375	7.390	4.557	2.730	4.650	9.330	6.257	4.085
1.5	4.775	2.240	1.129	0.608	6.950	3.980	2.148	1.185	10.150	7.410	4.514	2.718	4.350	9.260	6.433	4.078
2	4.925	2.270	1.133	0.598	6.950	3.950	2.148	1.193	10.425	7.610	4.490	2.740	5.350	9.770	6.524	4.073
3	4.925	2.240	1.133	0.600	6.850	4.020	2.167	1.205	9.525	7.770	4.495	2.795	9.450	9.620	6.329	4.098
4	4.825	2.270	1.133	0.603	7.000	4.150	2.186	1.205	10.250	7.740	4.595	2.770	6.350	9.430	6.314	4.125
5	4.875	2.270	1.129	0.598	7.175	4.290	2.157	1.200	10.375	7.930	4.567	2.763	6.400	9.440	6.571	4.103
6	4.975	2.250	1.133	0.598	7.575	4.130	2.162	1.198	10.525	7.830	4.638	2.750	6.750	10.350	6.705	4.105
8	4.950	2.250	1.133	0.600	7.100	4.210	2.157	1.203	10.650	7.850	4.629	2.760	7.950	9.780	6.738	4.080
10	4.950	2.240	1.124	0.603	7.125	4.170	2.157	1.200	10.550	7.700	4.610	2.765	8.525	10.230	6.700	4.113
12	4.950	2.240	1.129	0.598	7.250	4.240	2.162	1.203	10.475	7.780	4.619	2.775	8.400	10.180	6.681	4.105

Table D3: Average adsorbed Ni^{2+} at various peat doses at pH 8 during batch kinetic test

Time (hr)	Conc. 25 mg/L				Conc. 50 mg/L				Conc. 125 mg/L				Conc. 200 mg/L			
	q_1	q_2	q_3	q_4	q_1	q_2	q_3	q_4	q_1	q_2	q_3	q_4	q_1	q_2	q_3	q_4
0.5	4.100	1.870	1.048	0.565	4.975	2.740	1.905	1.095	8.900	5.400	3.476	2.385	3.250	7.590	5.690	3.705
1	4.135	1.870	1.057	0.570	5.375	2.820	1.976	1.110	9.250	5.480	3.531	2.425	3.500	7.930	5.800	3.738
1.5	4.123	1.870	1.075	0.580	5.413	3.045	2.090	1.141	9.125	5.670	3.514	2.463	3.850	8.170	5.871	3.775
2	4.203	1.900	1.074	0.578	5.700	3.260	2.062	1.121	9.438	5.750	3.638	2.565	3.825	8.310	5.986	3.785
3	4.225	1.980	1.057	0.579	5.875	3.185	2.038	1.113	9.475	6.010	3.737	2.688	4.475	8.750	6.071	3.825
4	4.275	1.950	1.061	0.577	6.425	3.110	2.024	1.110	9.750	6.300	3.871	2.673	5.400	8.940	6.148	3.808
5	4.298	1.930	1.069	0.578	6.075	3.205	2.017	1.120	10.08	6.550	3.819	2.658	5.875	9.300	6.186	3.798
6	4.320	1.950	1.071	0.576	6.225	3.235	2.045	1.128	9.813	6.460	3.812	2.683	6.425	9.800	6.143	3.813
8	4.305	1.960	1.072	0.578	6.275	3.250	2.038	1.130	10.05	6.510	3.848	2.678	7.450	10.460	6.124	3.800
10	4.310	1.960	1.074	0.578	6.325	3.220	2.048	1.129	9.775	6.530	3.867	2.675	7.000	10.320	6.167	3.795
12	4.273	1.960	1.073	0.578	6.400	3.252	2.057	1.127	9.975	6.520	3.864	2.680	7.050	10.430	6.176	3.810

Table D4: Average adsorbed Ni^{2+} at various peat doses at pH 10 during batch kinetic test

Time (hr)	Conc. 25 mg/L				Conc. 50 mg/L				Conc. 125 mg/L				Conc. 200 mg/L			
	q_1	q_2	q_3	q_4	q_1	q_2	q_3	q_4	q_1	q_2	q_3	q_4	q_1	q_2	q_3	q_4
0.5	2.675	1.070	0.524	0.285	2.050	1.130	0.624	0.378	4.375	2.490	1.467	1.150	5.900	3.300	1.867	1.255
1	2.675	1.090	0.517	0.290	2.000	1.170	0.629	0.373	4.650	2.670	1.629	1.155	6.000	3.350	1.881	1.248
1.5	2.650	1.080	0.536	0.285	2.025	1.190	0.619	0.378	4.475	2.800	1.567	1.163	5.975	3.280	1.943	1.293
2	2.650	1.130	0.543	0.288	2.050	1.200	0.629	0.393	4.700	2.790	1.552	1.218	6.150	3.300	1.905	1.298
3	2.725	1.140	0.542	0.293	2.150	1.270	0.662	0.380	5.250	2.830	1.676	1.205	6.200	3.320	1.943	1.320
4	2.700	1.120	0.548	0.293	2.400	1.280	0.648	0.388	5.625	2.860	1.705	1.218	6.500	3.360	1.967	1.303
5	2.688	1.090	0.523	0.285	2.475	1.260	0.660	0.393	5.400	2.780	1.714	1.213	6.475	3.380	1.981	1.320
6	2.700	1.100	0.526	0.290	2.250	1.260	0.652	0.385	5.625	2.880	1.662	1.215	6.500	3.490	1.971	1.305
8	2.660	1.090	0.532	0.293	2.300	1.270	0.662	0.390	5.550	2.860	1.667	1.210	6.525	3.550	1.981	1.305
10	2.650	1.110	0.532	0.290	2.350	1.280	0.662	0.390	5.725	2.880	1.676	1.215	6.550	3.390	1.981	1.313
12	2.675	1.120	0.538	0.291	2.410	1.270	0.657	0.388	5.600	2.850	1.695	1.213	6.525	3.520	1.971	1.315

Table D5: Average adsorbed Co^{2+} at various peat doses at pH 3 during batch kinetic test

Time (hr)	Conc. 25 mg/L				Conc. 50 mg/L				Conc. 125 mg/L				Conc. 200 mg/L			
	q_1	q_2	q_3	q_4	q_1	q_2	q_3	q_4	q_1	q_2	q_3	q_4	q_1	q_2	q_3	q_4
0.5	1.175	1.560	0.962	0.540	0.775	2.630	1.867	1.073		5.480	4.119	2.480			6.129	3.663
1	1.375	1.700	0.990	0.548	1.400	2.930	1.924	1.093		5.650	4.205	2.580			6.281	3.768
1.5	1.650	1.610	0.981	0.550	1.850	2.880	1.924	1.113		5.490	4.190	2.565			6.110	3.768
2	1.625	1.710	0.995	0.550	1.775	2.850	1.910	1.103		5.510	4.186	2.528			6.076	3.753
3	1.475	1.660	0.981	0.548	1.550	2.820	1.914	1.088		5.460	4.195	2.538			6.243	3.690
4	1.550	1.700	0.990	0.550	1.575	2.870	1.886	1.088		5.450	4.190	2.535			6.243	3.765
5	1.400	1.690	0.995	0.545	1.575	2.890	1.895	1.113		5.610	4.176	2.515			6.157	3.708
6	1.625	1.700	0.995	0.545	1.775	2.760	1.924	1.095		5.380	4.205	2.520			6.190	3.813
8	0.900	1.600	0.986	0.548	1.700	2.780	1.895	1.083		5.280	4.129	2.515			6.133	3.743
10	0.825	1.590	0.990	0.548	1.275	2.770	1.876	1.075		5.310	4.057	2.533			6.119	3.753
12	1.350	1.680	0.990	0.545	1.350	2.720	1.914	1.073		5.320	4.119	2.525			6.176	3.755

Table D6: Average adsorbed Co^{2+} at various peat doses at pH 5.5 during batch kinetic test

Time (hr)	Conc. 25 mg/L				Conc. 50 mg/L				Conc. 125 mg/L				Conc. 200 mg/L			
	q_1	q_2	q_3	q_4	q_1	q_2	q_3	q_4	q_1	q_2	q_3	q_4	q_1	q_2	q_3	q_4
0.5	4.150	2.06	1.071	0.575	4.925	3.550	2.038	1.123	8.500	5.750	4.214	2.573			6.033	3.620
1	4.200	2.100	1.095	0.585	5.225	3.640	2.076	1.148	8.925	6.070	4.462	2.640			6.233	3.823
1.5	4.275	2.120	1.071	0.585	5.675	3.660	2.057	1.135	8.900	6.170	4.343	2.595			6.157	3.788
2	4.175	2.100	1.095	0.583	5.475	3.630	2.076	1.143	9.000	6.400	4.405	2.613			6.229	3.818
3	4.200	2.100	1.081	0.585	5.600	3.650	2.067	1.143	9.100	6.260	4.414	2.630			6.229	3.815
4	4.175	2.120	1.095	0.585	5.375	3.620	2.067	1.140	9.025	6.200	4.433	2.633			6.181	3.783
5	4.250	2.090	1.086	0.585	5.175	3.600	2.052	1.136	9.375	6.190	4.433	2.628			6.195	3.770
6	4.150	2.100	1.078	0.575	5.300	3.580	2.071	1.123	8.975	6.240	4.424	2.603			6.171	3.765
8	4.100	2.110	1.086	0.578	5.525	3.640	2.064	1.134	9.425	6.260	4.448	2.603			6.224	3.773
10	4.275	2.110	1.084	0.575	5.550	3.620	2.070	1.140	9.225	6.220	4.429	2.630			6.205	3.768
12	4.250	2.100	1.09	0.580	5.425	3.640	2.071	1.144	9.275	6.330	4.443	2.635			6.224	3.780

Table D7: Adsorbed Co^{2+} at various peat doses at pH 8 during batch kinetic test

| Time (hr)	Conc. 25 mg/L				Conc. 50 mg/L				Conc. 125 mg/L				Conc. 200 mg/L			
	q_1	q_2	q_3	q_4	q_1	q_2	q_3	q_4	q_1	q_2	q_3	q_4	q_1	q_2	q_3	q_4
0.5	4.550	2.110	1.087	0.579	6.000	3.940	2.157	1.174	10.650	7.430	4.476	2.753	31.250	13.060	6.924	4.205
1	4.600	2.140	1.108	0.586	6.225	4.043	2.231	1.196	12.200	8.395	4.792	2.894	33.355	14.020	7.171	4.486
1.5	4.713	2.180	1.104	0.595	6.925	4.175	2.219	1.194	12.050	8.150	4.690	2.848	33.050	13.700	7.055	4.368
2	4.683	2.170	1.103	0.594	6.450	4.137	2.205	1.193	11.850	8.100	4.677	2.845	32.875	13.650	7.048	4.350
3	4.675	2.160	1.107	0.591	6.775	4.126	2.212	1.192	11.975	8.018	4.700	2.859	32.868	13.690	7.064	4.367
4	4.663	2.160	1.107	0.592	6.900	4.151	2.220	1.191	11.875	8.183	4.714	2.855	33.160	13.800	7.081	4.385
5	4.688	2.170	1.108	0.593	6.800	4.151	2.229	1.193	11.928	8.200	4.738	2.868	33.100	13.780	7.105	4.403
6	4.703	2.180	1.108	0.593	6.725	4.167	2.230	1.195	11.913	8.179	4.747	2.891	33.213	13.850	7.112	4.446
8	4.698	2.180	1.106	0.594	6.725	4.164	2.228	1.195	12.040	8.220	4.767	2.892	33.295	13.980	7.138	4.463
10	4.705	2.180	1.107	0.595	6.825	4.172	2.226	1.194	12.148	8.275	4.781	2.894	33.350	14.020	7.152	4.478
12	4.710	2.180	1.107	0.595	6.875	4.174	2.229	1.195	12.188	8.290	4.790	2.893	33.313	13.990	7.167	4.486

Table D8: Adsorbed Co^{2+} at various peat doses at pH 10 during batch kinetic test

Time (hr)	Conc. 25 mg/L				Conc. 50 mg/L				Conc. 125 mg/L				Conc. 200 mg/L			
	q_1	q_2	q_3	q_4	q_1	q_2	q_3	q_4	q_1	q_2	q_3	q_4	q_1	q_2	q_3	q_4
0.5	0.300	0.520	0.514	0.465	0.375	0.490	0.571	0.605	0.25	0.250	0.305	0.500	0.325	0.390	0.529	0.750
1	0.250	0.580	0.567	0.468	0.375	0.510	0.562	0.635	0.225	0.220	0.429	0.530	0.450	0.440	0.557	0.745
1.5	0.350	0.690	0.600	0.465	0.475	0.520	0.581	0.663	0.400	0.220	0.548	0.550	0.700	0.610	0.610	0.748
2	0.475	0.640	0.800	0.470	0.700	0.550	0.643	0.720	0.550	0.300	0.576	0.588	0.625	0.620	0.633	0.780
3	0.525	0.790	0.690	0.485	0.650	0.580	0.705	0.730	0.550	0.530	0.581	0.605	0.600	0.700	0.633	0.788
4	0.650	0.740	0.724	0.475	0.475	0.690	0.648	0.760	0.400	0.580	0.671	0.673	0.625	0.750	0.710	0.888
5	0.600	0.690	0.771	0.480	0.550	0.630	0.667	0.745	0.475	0.680	0.629	0.630	0.700	0.760	0.800	0.930
6	0.650	0.710	0.781	0.485	0.525	0.620	0.690	0.755	0.550	0.600	0.648	0.670	0.775	0.900	0.767	0.938
8	0.550	0.740	0.790	0.480	0.625	0.630	0.705	0.755	0.525	0.650	0.671	0.663	0.800	0.880	0.767	0.930
10	0.600	0.720	0.790	0.485	0.675	0.660	0.676	0.753	0.525	0.680	0.657	0.660	0.800	0.890	0.776	0.928
12	0.625	0.770	0.800	0.483	0.650	0.680	0.695	0.758	0.550	0.660	0.657	0.668	0.800	0.870	0.762	0.938
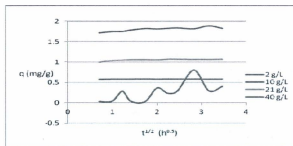
Plot E1: q (mg/g) vs $t^{0.5}(h^{0.5})$ at 25 mg/L Ni^{2+} at pH 3
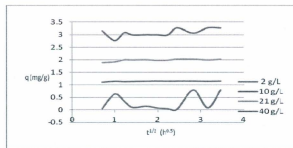
Plot E2: q (mg/g) vs $t^{0.5}(h^{0.5})$ at 50 mg/L Ni^{2+} at pH 3

Plot E3: q (mg/g) vs $t^{0.5}(h^{0.5})$ at 125 mg/L Ni^{2+} at pH 3

Plot E4: q (mg/g) vs $t^{0.5}(h^{0.5})$ at 200 mg/L Ni^{2+} at pH 3

Plot E5: q (mg/g) vs $t^{0.5}$($h^{0.5}$) at 25 mg/L Ni^{2+} at pH 5.5

Plot E6: q (mg/g) vs $t^{0.5}$($h^{0.5}$) at 50 mg/L Ni^{2+} at pH 5.5

Plot E7: q (mg/g) vs $t^{0.5}$($h^{0.5}$) at 125 mg/L Ni^{2+} at pH 5.5

Plot E8: q (mg/g) vs $t^{0.5}$($h^{0.5}$) at 200 mg/L Ni^{2+} at pH 5.5

Plot E9: q (mg/g) vs $t^{0.5}(h^{0.5})$ at 25 mg/L Ni^{2+} at pH 8

Plot E10: q (mg/g) vs $t^{0.5}(h^{0.5})$ at 50 mg/L Ni^{2+} at pH 8

Plot E11: q (mg/g) vs $t^{0.5}(h^{0.5})$ at 125 mg/L Ni^{2+} at pH 8

Plot E12: q (mg/g) vs $t^{0.5}(h^{0.5})$ at 200 mg/L Ni^{2+} at pH 8
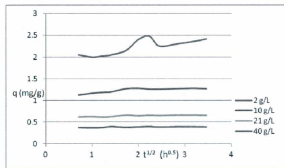
Plot E13: q (mg/g) vs $t^{0.5}(h^{0.5})$ at 25 mg/L Ni^{2+} at pH 10
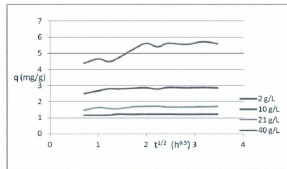
Plot E14: q (mg/g) vs $t^{0.5}(h^{0.5})$ at 50 mg/L Ni^{2+} at pH 10
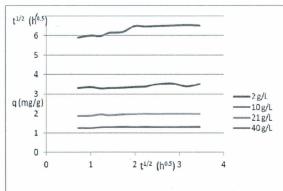
Plot E15: q (mg/g) vs $t^{0.5}(h^{0.5})$ at 125 mg/L Ni^{2+} at pH 10
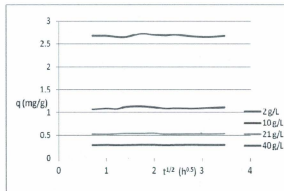
Plot E16: q (mg/g) vs $t^{0.5}(h^{0.5})$ at 200 mg/L Ni^{2+} at pH 10
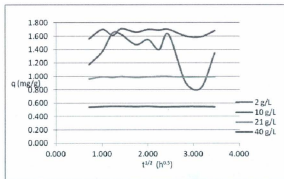
Plot E17: q (mg/g) vs $t^{0.5}$ ($h^{0.5}$) at 25 mg/L Co^{2+} at pH 3
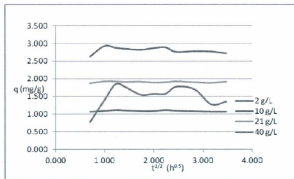
Plot E18: q (mg/g) vs $t^{0.5}$ ($h^{0.5}$) at 50 mg/L Co^{2+} at pH 3
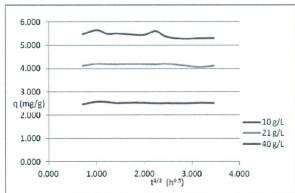
Plot E19: q (mg/g) vs $t^{0.5}$ ($h^{0.5}$) at 125 mg/L Co^{2+} at pH 3
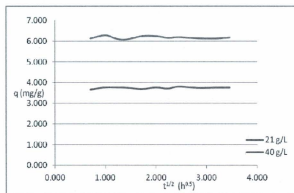
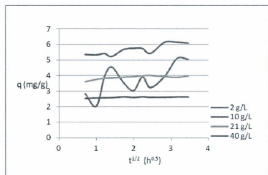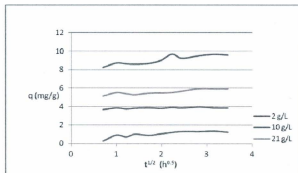Plot E20: q (mg/g) vs $t^{0.5}$ ($h^{0.5}$) at 200 mg/L Co^{2+} at pH 3
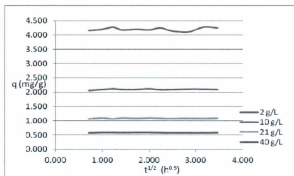
Plot E21: q (mg/g) vs $t^{0.5}(h^{0.5})$ at 25 mg/L Co^{2+} at pH 5.5
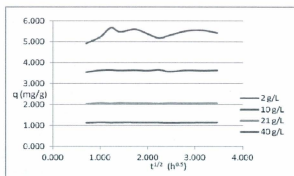
Plot E22: q (mg/g) vs $t^{0.5}(h^{0.5})$ at 50 mg/L Co^{2+} at pH 5.5
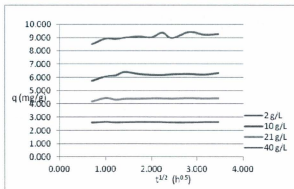
Plot E23: q (mg/g) vs $t^{0.5}(h^{0.5})$ at 125 mg/L Co^{2+} at pH 5.5
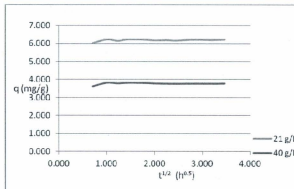
Plot E24: q (mg/g) vs $t^{0.5}(h^{0.5})$ at 200 mg/L Co^{2+} at pH 5.5
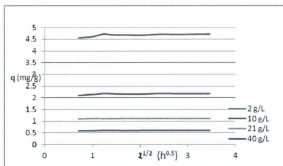
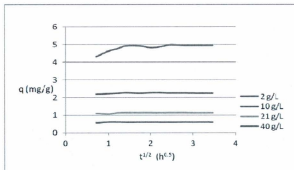Plot E25: q (mg/g) vs $t^{0.5}$($h^{0.5}$) at 25 mg/L Co^{2+} at pH 8
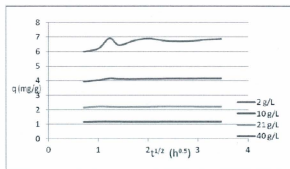
Plot E26: q (mg/g) vs $t^{0.5}$($h^{0.5}$) at 50 mg/L Co^{2+} at pH 8
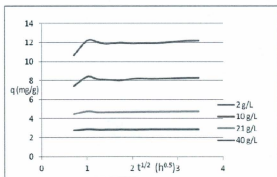
Plot E27: q (mg/g) vs $t^{0.5}$($h^{0.5}$) at 125 mg/L Co^{2+} at pH 8
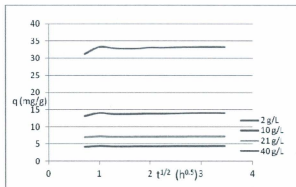
Plot E28: q (mg/g) vs $t^{0.5}$($h^{0.5}$) at 200 mg/L Co^{2+} at pH 8
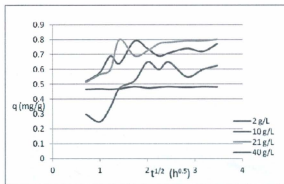
Plot E29: q (mg/g) vs $t^{0.5}(h^{0.5})$ at 25 mg/L Co^{2+} at pH 10
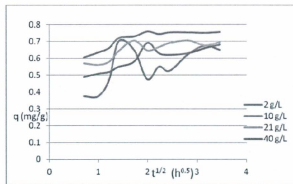
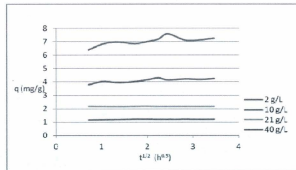Plot E30: q (mg/g) vs $t^{0.5}(h^{0.5})$ at 50 mg/L Co^{2+} at pH 10
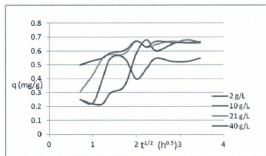
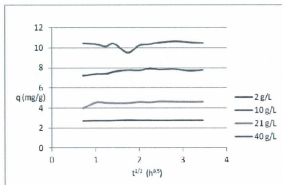Plot E31: q (mg/g) vs $t^{0.5}(h^{0.5})$ at 125 mg/L Co^{2+} at pH 10

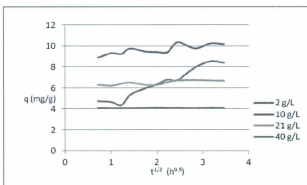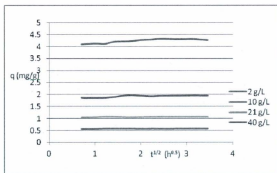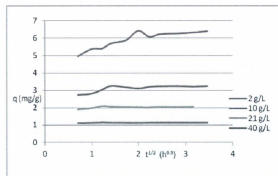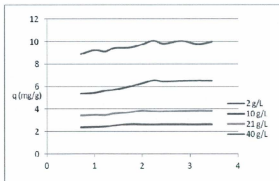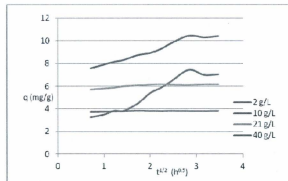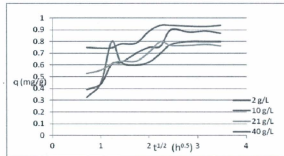Plot E32: q (mg/g) vs $t^{0.5}(h^{0.5})$ at 200 mg/L Co^{2+} at pH 10

Appendix F

Table F1: Average final concentration of Ni^{2+} measured during 24 hours Adsorption

pH	Initial Ni Conc. (mg/L)	Conc. (mg/L) at various peat doses (g/L)			
		2	10	21	40
10	200	173.6	165.8	157.8	146.9
	125	102.5	96.2	89	76.3
	50	34.0	31.0	26.0	22.0
	25	14.2	14.3	14.2	14.1
	12.5	11.1	11.0	10.3	9.8
8	200	171.8	126.4	59.8	50.8
	125	71.9	63.3	27.0	24.0
	50	24.2	20.0	8.3	6.9
	25	9.2	7.5	3.0	2.5
	12.5	3.9	2.5	1.25	0.9
5.5	200	169.4	94.8	39.3	24
	125	50.0	40.3	18.5	11.2
	50	16.0	12.5	12.0	6.0
	25	5.3	2.0	0.7	0.4
	12.5	3.8	1.2	0.5	0.3
3	200	127.1	67	32.9	18.4
	125	54.6	29.6	16.2	7.4
	50	9.8	4.3	2.0	1.0
	25	1.1	0.5	0.2	0.1
	12.5	0.9	0.4	0.2	0.1

Table F2: Average final concentration of Co^{2+} measured during 24 hours Adsorption

pH	Initial Ni Conc. (mg/L)	Conc. (mg/L) at various peat doses (g/L)			
		2	10	21	40
10	200	196.7	191	185.4	182
	125	122.8	120.7	110.6	98.6
	50	47.1	43.5	30.2	19.2
	25	22.4	16.2	6.6	5.2
	12.5	11.9	8.1	3.5	3.4
8	200	176.4	139.2	79	71.4
	125	100.5	69	42.5	38.6
	50	39.8	25.3	14.6	13.3
	25	19.8	9.5	3.8	4.7
	12.5	9.8	4.5	1.7	1.7
5.5	200	170.0	108.0	51.0	38.5
	125	94.0	52.0	41.0	29.2
	50	38.2	21.2	10.4	6.8
	25	19.7	4.7	2.1	1.5
	12.5	9.2	4.3	1.2	0.7
3	200	145	94.6	80.4	49
	125	70.1	38.8	23.1	14.0
	50	24.5	11.1	6.7	3.5
	25	3.5	1.7	1.1	0.7
	12.5	2.5	1.2	0.5	0.2

Table F3: Competitive Sorption of Cd^{2+}, Co^{2+}, Ni^{2+}, Pb^{2+} and Zn^{2+} at pH 5.5

Peat dose (g/L)	Initial Conc. (mg/L)	Final Conc. (mg/L)					Adsorbed metal, q (mg/g)				
		Cd	Co	Ni	Pb	Zn	Cd	Co	Ni	Pb	Zn
2	200	196	198	189	6.8	197	1	0.5	2.75	48.3	0.75
	100	91	97	76	2.5	98	2.25	0.75	6	24.375	0.5
	50	27	36	26	0.5	30	5.75	3.5	6	12.375	5
	25	8	11	8	0.1	10	4.25	3.5	4.25	6.225	3.75
	12.5	1.6	2.9	2	0	2	2.725	2.4	2.625	3.125	2.625
10	200	181	188	166	3.6	185	1.9	1.2	3.4	19.64	1.5
	100	53	66	46	0.7	61	4.7	3.4	5.4	9.93	3.9
	50	14	19	14	0.2	17	3.6	3.1	3.6	4.98	3.3
	25	3	5	3	0	4.2	2.2	2	2.2	2.5	2.08
	12.5	0.6	1.3	0.9	0	1.1	1.19	1.12	1.16	1.25	1.14
21	200	117	134	89	1.3	125	3.952	3.143	5.286	9.462	3.571
	100	26	38	22	0.5	32	3.524	2.952	3.714	4.738	3.238
	50	6	9	6	0.2	7.2	2.095	1.952	2.095	2.371	2.038
	25	1.2	2	1.5	0	1.7	1.133	1.095	1.119	1.190	1.110
	12.5	0.3	0.7	0.4	0	0.5	0.581	0.562	0.576	0.595	0.571
40	200	69	84	49	0.8	75	3.275	2.900	3.775	4.980	3.125
	100	15	19	12	0.5	16.4	2.125	2.025	2.200	2.488	2.090
	50	8	11	8	0.1	9.6	1.050	0.975	1.050	1.248	1.010
	25	0.7	1.3	0.8	0	1.1	0.608	0.593	0.605	0.625	0.598
	12.5	0.2	0.4	0.3	0	0.3	0.308	0.303	0.305	0.313	0.305

Appendix G

Table G1: Initial Ni^{2+} adsorbed and percent desorbed after HCl was added at various peat doses

pH	Ci (mg/L)	C$_{adsorbed}$ (mg/L) 2g/L	10g/L	21g/L	40g/L	HCl (M)	% of C$_{desorbed}$ at 2 g/L peat dose C$_1$	C$_2$	C$_3$	C$_4$	C$_5$	% of C$_{desorbed}$ at 10 g/L peat dose C$_1$	C$_2$	C$_3$	C$_4$	C$_5$
10	12.5	0.6	4.4	9	9.1	0.1	17.2	23	42.7	55	68	28.4	31.8	48.1	71.4	73.8
	25	2.6	8.8	18.4	19.8	0.2	21	28.4	49.5	63.5	74.5	35.6	39.3	55.6	75	77.2
	50	2.9	6.5	19.8	30.8	0.5	30.5	34.8	56.7	78	83.7	39	44.6	72	80.3	80.4
	125	2.2	4.3	14.4	26.4	1	36.2	40.7	66	82	84.5	46.7	51	74.5	85.8	88.8
	200	3.3	9	14.6	18	2	42.6	50	72	82.8	85.2	50.1	55	74.8	86.1	90
8	12.5	2.7	8	10.8	10.8	0.1	12.9	16	37.3	43.7	49.1	12.5	25	50	125	200
	25	5.2	15.5	21.2	20.3	0.2	17.5	21.7	42	48.5	53.7	16.8	19.7	41	48.2	52.1
	50	10.2	24.7	35.6	36.7	0.5	20.2	32.4	46.8	57.5	60.2	21.7	24.9	45.4	53.5	58.6
	125	24.5	56	82.5	86.4	1	27.6	35.5	53.8	63.8	68.5	29.5	36.2	50.6	62.8	69.7
	200	24.6	60.8	121	128.6	2	31.3	40.8	60.5	69.1	75	35	41.8	56.9	67.1	73.9
5.5	12.5	3.3	8.2	11.3	11.8	0.1	4	9.5	13.8	15.8	17.5	12.6	16.3	23.4	26.4	28.5
	25	5.3	20.3	22.9	23.5	0.2	7.4	14.7	17.2	20.5	21.2	17.2	20.5	28.6	29.7	30.3
	50	11.8	28.8	39.6	43.2	0.5	11.5	17.4	21.2	23.1	27.3	22	27.4	33.9	36.3	36.7
	125	31	73	80	95.8	1	14.2	19.3	24.5	26	29.1	29.4	31.5	36.4	38.4	40.1
	200	30	92	149	161.5	2	17.3	21.8	27.5	29.1	32.4	35	38.2	40.5	42.1	44.6

where C1, C2, C3, C4 and C5 are the metal concentrations at 12.5, 25, 50, 125 and 200 mg/L respectively.

Table G1 (contd).

pH	Ci (mg/L)	$C_{adsorbed}$ (mg/L)				HCl (M)	% of $C_{desorbed}$ at 21 g/L peat dose					% of $C_{desorbed}$ at 40 g/L peat dose				
		2g/L	10g/L	21g/l	40g/l		C_1	C_2	C_3	C_4	C_5	C_1	C_2	C_3	C_4	C_5
10	12.5	0.6	4.4	9	9.1	0.1	50.4	56.2	64	70.6	50.4	60.1	63.8	68.6	74	77.3
	25	2.6	8.8	18.4	19.8	0.2	68.7	73.7	77.8	79.2	68.7	69.6	75.5	79.9	83.7	86.5
	50	2.9	6.5	19.8	30.8	0.5	75.3	79.5	85.4	87.1	75.3	78.5	81	87.2	90.5	93.5
	125	2.2	4.3	14.4	26.4	1	80	87	89.2	92.4	80	82.4	88.6	94.2	95.4	96.9
	200	3.3	9	14.6	18	2	84.7	89.5	94.1	95.8	84.7	87	92	96.1	96.8	97.5
8	12.5	2.7	8	10.8	10.8	0.1	43.6	47	52.4	60.6	62.1	48.9	51.6	56.5	63.7	66.5
	25	5.2	15.5	21.2	20.3	0.2	51.8	54.2	58.1	65.7	68.7	54.3	59.5	63.1	68.5	74.2
	50	10.2	24.7	35.6	36.7	0.5	62.3	65.4	69.7	74.5	76.9	64.5	67.6	70.4	78.9	80.7
	125	24.5	56	82.5	86.4	1	67.1	70.5	73.5	77.5	82.6	68.5	71.2	75.8	80.6	84
	200	24.6	60.8	121	128.6	2	70.2	76.8	79.1	84.8	87	73.2	78.7	82.5	85.1	88.2
5.5	12.5	3.3	8.2	11.3	11.8	0.1	28.1	30.5	33.9	32.4	36.5	35.7	38	40.1	42.7	44.8
	25	5.3	20.3	22.9	23.5	0.2	32.4	35.7	37.5	38.5	40.5	39.4	42.9	43.5	46.5	47.3
	50	11.8	28.8	39.6	43.2	0.5	37.6	39.1	40.2	42.8	46.7	42.5	46.1	46.9	48.2	49.4
	125	31	73	80	95.8	1	40.2	42.3	44.6	46.5	48.1	45.8	47.5	49.4	50.7	51
	200	30	92	149	161.5	2	45.2	47.7	49.5	50.1	51	50.4	52.4	53.6	54.5	55.2

where C_1, C_2, C_3, C_4 and C_5 are the metal concentrations at 12.5, 25, 50, 125 and 200 mg/L respectively.

Table G2: Initial Co^{2+} adsorbed and percent desorbed after HCl was added at various peat doses

pH	Ci (mg/L)	C$_{adsorbed}$ (mg/L)				HCl (M)	% of C$_{desorbed}$ at 2 g/L peat dose					% of C$_{desorbed}$ at 10 g/L peat dose				
		2g/L	10g/L	21g/L	40g/L		C$_1$	C$_2$	C$_3$	C$_4$	C$_5$	C$_1$	C$_2$	C$_3$	C$_4$	C$_5$
	12.5	0.6	4.4	9	9.1	0.1	14.3	18.2	21	27.3	29.5	19	23.1	29.9	35.8	45
	25	2.6	8.8	18.4	19.8	0.2	17.5	20.8	24.5	29.1	33.9	22.5	29.2	34.6	39.4	48.5
10	50	2.9	6.5	19.8	30.8	0.5	20.1	23.7	28.4	33.8	37.1	27.3	33.7	39.1	43.5	55
	125	2.2	4.3	14.4	26.4	1	24.3	29	31.8	38.4	42.3	29.5	38.4	43.5	53	60.3
	200	3.3	9	14.6	18	2	28.5	32.5	35.1	45.6	48.5	34.2	45.7	52.1	61.2	67
	C$_i$ (mg/L)	C$_{adsorbed}$ (mg/L)				HCl (M)	% of C$_{desorbed}$ at 21 g/L peat dose					% of C$_{desorbed}$ at 40 g/L peat dose				
		2g/L	10g/L	21g/L	40g/L		C$_1$	C$_2$	C$_3$	C$_4$	C$_5$	C$_1$	C$_2$	C$_3$	C$_4$	C$_5$
	12.5	0.6	4.4	9	9.1	0.1	31.8	39.2	44.5	49	52.3	38.5	43.8	49.6	54.2	58.5
	25	2.6	8.8	18.4	19.8	0.2	38.5	43.6	49.2	55.2	58.5	42.8	50.1	55.4	59.2	63
10	50	2.9	6.5	19.8	30.8	0.5	44.9	48.5	56.3	63.9	68.3	50.6	62.5	66.7	65.4	69.1
	125	2.2	4.3	14.4	26.4	1	51.7	57.3	64.3	68.1	72.3	61.7	67.2	71	72.5	75.7
	200	3.3	9	14.6	18	2	60.4	66	70.1	73.4	75.8	67.1	70.9	77.3	80.1	83.5

where C_1, C_2, C_3, C_4 and C_5 are the metal concentrations at 12.5, 25, 50, 125 and 200 mg/L respectively.

Appendix H

Table H1: Average column effluent concentrations at flow rate 1.0 L/h for the determination of Ni^{2+} breakthrough point.

Vol. (L)	C (mg/L)	C/Co	Vol. (L)	C (mg/L)	C/Co	Vol. (L)	C (mg/L)	C/Co	Vol. (L)	C (mg/L)	C/Co
1	4.37	0.0437	28	29.19	0.2919	55	34.58	0.3458	82	41.95	0.4195
2	8.71	0.0871	29	26.4	0.264	56	34.85	0.3485	83	36.42	0.3642
3	13.45	0.1345	30	29.49	0.2949	57	35.5	0.355	84	39.24	0.3924
4	16.32	0.1632	31	29.48	0.2948	58	35.13	0.3513	85	38.88	0.3888
5	18.51	0.1851	32	29.87	0.2987	59	33.29	0.3329	86	36.76	0.3676
6	20.25	0.2025	33	31.95	0.3195	60	33.62	0.3362	87	38.48	0.3848
7	23.31	0.2331	34	33.31	0.3331	61	34.71	0.3471	88	38.2	0.382
8	24.08	0.2408	35	33.55	0.3355	62	35.92	0.3592	89	39.19	0.3919
9	25.39	0.2539	36	36.88	0.3688	63	35.54	0.3554	90	39.39	0.3939
10	26.79	0.2679	37	34.13	0.3413	64	33.1	0.331	91	38.11	0.3811
11	17.81	0.1781	38	33.05	0.3305	65	33.77	0.3377	92	38.23	0.3823
12	19.69	0.1969	39	30.85	0.3085	66	35.74	0.3574	93	44.16	0.4416
13	22	0.22	40	34.72	0.3472	67	34.37	0.3437	94	43.07	0.4307
14	23.89	0.2389	41	36.12	0.3612	68	36.01	0.3601	95	42.1	0.421
15	25.34	0.2534	42	33.23	0.3323	69	35.08	0.3508	96	42.93	0.4293
16	25.63	0.2563	43	31.47	0.3147	70	36.07	0.3607	97	43.89	0.4389
17	25.52	0.2552	44	34.98	0.3498	71	36.86	0.3686	98	45.19	0.4519
18	26.46	0.2646	45	31.75	0.3175	72	37.68	0.3768	99	44.41	0.4441
19	27.61	0.2761	46	35.65	0.3565	73	36.15	0.3615	100	47.78	0.4778
20	24.22	0.2422	47	36.57	0.3657	74	35.87	0.3587	101	44.91	0.4491
21	22.24	0.2224	48	33.54	0.3354	75	37.29	0.3729	102	40.78	0.4078
22	23.79	0.2379	49	29.61	0.2961	76	36.26	0.3626	103	40.01	0.4001
23	24.92	0.2492	50	34.27	0.3427	77	39.1	0.391	104	40.51	0.4051
24	24.4	0.244	51	35.37	0.3537	78	40.25	0.4025	105	42.04	0.4204
25	27.35	0.2735	52	35.78	0.3578	79	41.4	0.414	106	41.62	0.4162
26	28.46	0.2846	53	35.14	0.3514	80	38.84	0.3884	107	40.44	0.4044
27	30.63	0.3063	54	36.13	0.3613	81	39.04	0.3904	108	40.1	0.401

Table H1 (contd.)

Vol. (L)	C (mg/L)	C/Co	Vol. (L)	C (mg/L)	C/Co
109	43.51	0.4351	136	44.2	0.442
110	42.5	0.425	137	40.8	0.408
111	43.47	0.4347	138	40.7	0.407
112	43.48	0.4348	139	42.7	0.427
113	42.8	0.428	140	39.2	0.392
114	42.46	0.4246	141	42.5	0.425
115	45.5	0.455	142	41.2	0.412
116	42.8	0.428	143	52.8	0.528
117	44.2	0.442	144	51.8	0.518
118	42.1	0.421	145	48.6	0.486
119	40.3	0.403	146	50.5	0.505
120	41.3	0.413	147	49.05	0.4905
121	40.5	0.405	148	49.43	0.4943
122	44	0.44	149	51.53	0.5153
123	40.5	0.405	150	49.78	0.4978
124	39.1	0.391	151	48.27	0.4827
125	38.2	0.382	152	49.03	0.4903
126	41.6	0.416	153	50.8	0.508
127	41.7	0.417	154	51.84	0.5184
128	42.8	0.428	155	53.8	0.538
129	39.2	0.392	156	53.4	0.534
130	40.5	0.405			
131	42.9	0.429			
132	42	0.42			
133	39.1	0.391			
134	41.1	0.411			
135	51.4	0.514			

Table H2: Average column effluent concentrations at flow rate 2.0 L/h for the determination of Ni^{2+} breakthrough point.

| Vol.(L)	C (mg/L)	C/Co	Vol. (L)	C (mg/L)	C/Co	Vol. (L)	C (mg/L)	C/Co
0	0	0	28	13.2	0.132	56	39.1	0.391
1	5.7	0.057	29	13.7	0.137	57	42.3	0.423
2	6.1	0.061	30	13.7	0.137	58	42.1	0.421
3	5.9	0.059	31	15.6	0.156	59	42.6	0.426
4	5.8	0.058	32	15.9	0.159	60	45.8	0.458
5	6.6	0.066	33	16.3	0.163	61	47.5	0.475
6	6.9	0.069	34	16.5	0.165	62	49.2	0.492
7	7.5	0.075	35	16.9	0.169	63	50.2	0.502
8	6.8	0.068	36	15.4	0.154	64	50.7	0.507
9	6.8	0.068	37	15.4	0.154	65	51.4	0.514
10	7.3	0.073	38	15.7	0.157			
11	7.8	0.078	39	15.9	0.159			
12	8.6	0.086	40	15.9	0.159			
13	7.9	0.079	41	17.4	0.174			
14	7.8	0.078	42	17.9	0.179			
15	7.6	0.076	43	19.6	0.196			
16	8.8	0.088	44	21.8	0.218			
17	9.4	0.094	45	23.1	0.231			
18	9.1	0.091	46	25.6	0.256			
19	10.3	0.103	47	25.4	0.254			
20	10.6	0.106	48	25.1	0.251			
21	11.7	0.117	49	28.6	0.286			
22	10.5	0.105	50	29.1	0.291			
23	10.4	0.104	51	30.5	0.305			
24	10.7	0.107	52	31.8	0.318			
25	11.5	0.115	53	33.5	0.335			
26	11.8	0.118	54	35.7	0.357			
27	12.6	0.126	55	37.9	0.379			

Table H3: Average column effluent concentrations at flow rate 1.0 L/h

for the determination of Co^{2+} breakthrough point.

| Vol. (L)	C (mg/L)	C/Co	Vol. (L)	C (mg/L)	C/Co
0	0	0	28	28.4	0.284
1	1.6	0.016	29	29.7	0.297
2	1.9	0.019	30	32.7	0.327
3	2.3	0.023	31	33.5	0.335
4	3.2	0.032	32	34.8	0.348
5	4.1	0.041	33	35.4	0.354
6	5.7	0.057	34	40	0.4
7	6.3	0.063	35	40.4	0.404
8	7.1	0.071	36	41.4	0.414
9	7.9	0.079	37	43.7	0.437
10	9.8	0.098	38	44.3	0.443
11	10.3	0.103	39	45.9	0.459
12	10.9	0.109	40	46.2	0.462
13	11.4	0.114	41	46.8	0.468
14	13.5	0.135	42	47.5	0.475
15	14.7	0.147	43	47.8	0.478
16	14.9	0.149	44	48.4	0.484
17	15.6	0.156	45	48.9	0.489
18	15.9	0.159	46	49.5	0.495
19	16.1	0.161	47	49.7	0.497
20	18.6	0.186	48	50.6	0.506
21	19.3	0.193	49	51.1	0.511
22	21.2	0.212	50	51.7	0.517
23	22.8	0.228	51	52.8	0.528
24	24.5	0.245	52	54.3	0.543
25	26.1	0.261	53	55.8	0.558
26	26.8	0.268	54	59.2	0.592
27	27.9	0.279			

Table H4: Average column effluent concentrations at flow rate 2.0 L/h
for the determination of Co^{2+} breakthrough point (contd.)

| Vol. (L)	C (mg/L)	C/Co
0	0	0
1	0.91	0.0091
2	1.8	0.018
3	2.6	0.026
4	2.9	0.029
5	3.5	0.035
6	4.2	0.042
7	5.4	0.054
8	5.7	0.057
9	6.3	0.063
10	9.1	0.091
11	9.4	0.094
12	9.1	0.091
13	11.8	0.118
14	13.7	0.137
15	16.3	0.163
16	18.6	0.186
17	21.5	0.215
18	21.8	0.218
19	25.9	0.259
20	34.1	0.341
21	35.3	0.353
22	41.4	0.414
23	47.1	0.471
24	48.5	0.485
25	50.6	0.506
26	51.5	0.515
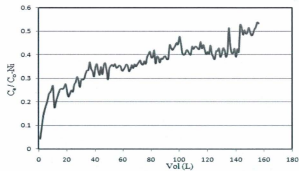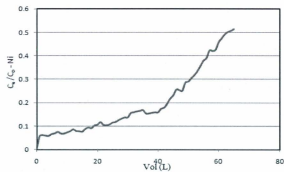
Plot I1 & I2: Breakthrough curves for Ni adsorption at pH 5.5, conc., 100 mg/L, 22°C and at a flow rate of 1.0 & 2.0 L/h.
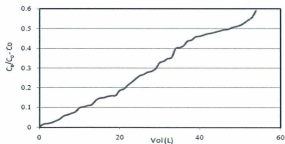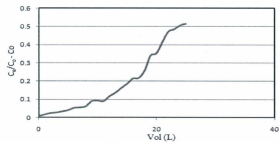
Plot I3 & I4: Breakthrough curves for Co adsorption at pH 5.5, conc., 100 mg/L, 22°C and at a flow rate of 1.0 & 2.0 L/h.

Appendix J

Table J: Ratios of metal concentration to initial influent concentration at specified column depth

Column Height, H (cm)	Ni Conc. (mg/L)	Co Conc. (mg/L)	C/Co-Ni	C/Co-Co
0	25.85	24.78	0.2585	0.2478
2	22.4	19.97	0.224	0.1997
4	21.7	19.63	0.217	0.1963
6	21.2	19.52	0.212	0.1952
8	21	19.35	0.21	0.1935
10	19.08	18.44	0.1908	0.1844
12	18.34	17.05	0.1834	0.1705

Appendix K

Table K: Breakthroughs at flow rate of 1.0 for Ni^{2+} and Co^{2+} at different column heights

Height of Column (cm)	Ni Breakthrough t_{50} (h)	Co Breakthrough t_{50} (h)
5.5	68	26
12.5	153	51
26.5	390	185

Appendix L

Table L1: Concentrations of blank test for kinetics study at pH 5.5

Time (h)	Ni conc. (mg/L)				Co conc. (mg/L)			
	25	50	125	200	25	50	125	200
0.5	24.9	49.7	125	200	25.1	50	125	200
1	25.1	50	125	200	25.1	49.7	125	200
1.5	25.1	50	124.8	200	25	50	125	200
2	25	50	124.8	200	24.9	50	124.8	200
3	24.9	50	125	200	24.8	49.5	125	200
4	25	49.5	124.9	200	25	50.1	125	200
5	25	50	124.9	200	25	50	125.8	200
6	24.8	50	125	200	25	50	125	200
8	25	50	125	200	25.1	50	125	200
10	24.9	50	125	200	25	49.5	125	200
12	25	50	125	200	25	50.1	125	200

Table L2: Concentration of blanks for equilibrium adsorption study at pH 5.5 after 24 hrs

Initial conc. (mg/L)	Ni conc. (mg/L)	Co conc. (mg/L)
200	200	200
125	124.9	124.8
50	49.8	50
25	24.8	25.1
12.5	12.6	12.6

Table L3: Concentrations of blanks fixed bed column at pH 5.5 for 100 mg/L initial metal conc.

Vol. (L)	1	2	3	4	5	6	7	8	9	10
Ni-conc. at exit (mg/L)	98	98.5	98	98	99	99.5	98	99	98.5	98.5
Co-conc. at exit (mg/L)	99	100	99.5	99	99	99	100	100	100	100